Study on Electro-Optic Modulators Using Planar Antennas for Wireless Microwave-Lightwave Signal Conversion

A dissertation submitted to
THE GRADUATE SCHOOL OF ENGINEERING SCIENCE
OSAKA UNIVERSITY
in partial fulfillment of the requirements for the degree of
DOCTOR OF PHILOSOPHY IN ENGINEERING

BY

YUSUF NUR WIJAYANTO

SEPTEMBER 2013

Abstract

In the wireless communication, demand for high quality multimedia services through mobile devices increases continuously. It is shown by increasing the global data traffic every year. Currently, the wireless communication with data rate of about a hundred Mbps is developed such as in WiMAX, LTE, and WiFi standards. Capacity enhancement is still required for anticipating the large data traffic and bottleneck in the future. The capacity enhancement can be obtained by using high frequency operation to the microwave, millimeter-wave, or sub-millimeter-wave bands. However, the wireless signals with high frequency operation have large transmission losses in the air, so that the coverage area becomes small to the pico/ femto cells. The coverage areas can be expanded by installing many pico/ femto cells, where each cell is connected to other cells through optical fiber cables with lightwave as the carrier. Thus, broadband wireless communication can be realized by utilizing the radio-over-fiber (ROF) technology.

In the ROF technology, converters between wireless microwave/ millimeter-wave/ sub-millimeter-wave and lightwave signals are required as the key devices. Lightwave to wireless microwave/ millimeter-wave signal converters are typically composed of a high-speed photo-detector and antenna. These converters for high frequency operation have been developed. On the other hand, the converters from wireless microwave/ millimeter-wave/ sub-millimeter-wave to lightwave signals can be composed of an antenna and optical modulator. The wireless microwave-lightwave signal converters in microwave band operation have been developed. The converters have drawback for high frequency operation such as millimeter-wave/ sub-millimeter-wave losses, substrate resonant mode, precise tuning requirement, and so on.

Electro-optic (EO) modulators are promising for conversion from microwave/ millimeter-wave/ sub-millimeter-wave to lightwave signals with their advantages such as high speed operation, large bandwidth, and good linearity. Optical modulation through the Pockels effect of an EO crystal can be obtained by applying microwave/ millimeter-wave/ sub-millimeter-wave electric fields to the crystal.

This dissertation covers a study on EO modulators using planar antennas for wireless microwave/ millimeter-wave-lightwave signal conversion. The devices with fusion and integrated structures are presented. New EO modulators based on fusion structures using patch antennas embedded with narrow gaps is proposed. Then, an integrated EO modulator using planar Yagi antennas coupled to resonant electrodes are also discussed. Arrays of the EO modulators using planar antennas are presented for modulation efficiency improvement and wireless beamforming receiving.

Optical modulators using an EO crystal suspended to a low-*k* dielectric substrate for further modulation efficiency improvement, high operational frequency, and substrate resonant mode elimination are also proposed.

This dissertation is constructed as following:

Firstly, I present fundamental of planar antennas and EO modulators for wireless microwave/ millimeter-wave-lightwave signal conversion. A wireless microwave/ millimeter-wave signal is received by the planar antennas and converted to lightwave signals by EO modulators through the Pockels effects of an EO crystal. Planar antennas and EO modulators can be arranged discretely. The discrete structures have large losses at high frequency operation along the connection cable. Microwave/ millimeter-wave losses can be minimized using integrated structures. In order to achieve effective modulation, precise tuning between the planar structures is required. I concern to the new invention using fusion structures, very low microwave/ millimeter-wave losses can be obtained with no precise tuning requirement, since there are only planar antennas on the substrate.

Secondly, new invented EO modulators using a patch antenna embedded with a single narrow gap are proposed for wireless microwave-lightwave signal conversion. A patch antenna is fabricated on an EO crystal substrate. A micrometer-order narrow gap is set in the center of the patch. The antenna characteristics of the proposed devices are similar to the standard patch antenna with no gap. When wireless microwave signal irradiated to the devices, displacement current is induced across the gap for current flow continuity. Displacement current and strong microwave electric field is induced across the gap. I expected that the strong electric field can be used for EO modulation. The proposed devices have simpler and more compact structures and no required precise tuning. Very low microwave losses can be obtained since there are no other planar structures on the substrate except the antennas. In the experiment, prototype devices for the 26 GHz microwave bands were designed and fabricated. Basic operations of the proposed devices for wireless microwave-lightwave signal conversion were verified successfully. In summary, the basic operations of the new EO modulators using a patch antenna embedded with a narrow gap have been verified for direct wireless microwave-lightwave signal conversion. The proposed devices are operated effectively when the microwave polarization is perpendicular to the gap.

Thirdly, in order to enhance the device functionality for wireless microwave polarization identification, fusion EO modulators using a patch antenna embedded with double narrow gaps are proposed. First, an EO modulator using a patch antenna embedded with two parallel gaps is proposed. It is suggested for application to the Mach-Zehnder interferometer by using two induced displacement current across the gaps. Second, an EO modulator using a patch antenna embedded with two orthogonal gaps is also proposed. The characteristics of the wireless microwave signals such as amplitude, phase, and polarization can be measured and identified using this proposed device. In the experiment, the proposed devices for microwave bands of 26 GHz operational frequency were

designed and fabricated. Wireless microwave characteristics were measured by use of the proposed device through optical technology. In summary, the fusion EO modulator using patch antenna embedded with double narrow gaps can be used for enhancing device functionality.

Fourthly, I propose an integrated EO modulator using a planar Yagi antenna coupled to a resonant electrode. The proposed device is composed of optical waveguides, a planar Yagi antenna, a planar standing-wave resonant electrode, and a planar connection line. They are fabricated on an EO crystal as a substrate. By using the proposed device, high gain of the Yagi antenna and long interaction length of the resonant electrode can be utilized to improve modulation efficiency of wireless microwave/ millimeter-wave-lightwave signals. In order to achieve effective optical modulation, precise tuning of the planar structures, which are the antenna, resonant electrode, and connection line, is required for reducing the millimeter-wave losses. Design and analysis of the proposed device for the millimeter-wave bands is presented. In the calculation, modulation efficiency of the proposed device has larger about 10 dB than the fusion EO modulators using a patch antenna embedded with narrow gaps.

Fifthly, in order to improve modulation efficiency in further and enhancing device functionality, EO modulators using arrays of planar antennas are proposed. The modulation efficiency is proportional to the number of the antennas since effective EO modulation occurs at each antenna. In order to obtain effective EO modulation, transit time of lightwave propagating along optical waveguides must be considered. An new EO modulator using a quasi-phase-matching (QPM) array of gap-embedded patch antennas is proposed for further modulation efficiency improvement. Additional gap-embedded patch antennas are inserted between the conventional array structures. To compensate for the degradation of EO modulation, the gap position of the odd and even patch antennas are slightly shifted respect to the optical waveguide. The proposed QPM device has double modulation efficiency while maintaining the same device length with the no QPM devices (conventional array structures). An array structure can be used also for controlling wireless irradiation angle (beamforming). An EO modulator using a 2-D array of patch antennas embedded with orthogonal gaps is proposed. 1-D beamforming can be achieved by taking the modulated lightwave signal from each optical waveguide. Furthermore, by considering orthogonal modulated lightwave signals, 2-D beamforming is obtainable. When the irradiation angle direction of the wireless microwave signal is changed, degradation of EO modulation will occur. It can be solved using meandering gap structures. In the experiment, the proposed devices were designed and fabricated for microwave bands of 26 GHz operational frequency. Double modulation efficiency improvement using the QPM device was verified experimentally. Additionally, a ROF link using the fabricated devices is also demonstrated. 1-D and 2-D beamforming receivers can be realized using the proposed devices through optical technology.

Finally, in order to improve modulation efficiency furthermore and consider to the higher frequency operation, I propose new optical modulators using a thin EO waveguide suspended to planar

antennas on a low-*k* dielectric substrate. Antenna aperture becomes large due to the low value of the effective dielectric constant of the suspended structures. As a result, owing to larger receiving power and longer interaction length for EO modulation compared to the devices fabricated on an EO crystal substrate, the modulation efficiency can be improved. Additionally, since the thin EO crystal is used, substrate resonant mode effect can be eliminated. In the experiment, the proposed devices for millimeter-wave bands of 60 GHz operational frequency were fabricated. A thin EO crystal (~80 μm) was suspended on a low-*k* dielectric substrate. Measurements of modulation efficiency as functions of frequency, directivity, and polarization of the wireless millimeter-wave signal coincide well with the calculation results. Compared to the devices fabricated on EO crystal substrate, modulation efficiency improvement of about 20 dB is achieved using the proposed devices.

Based on the operations of the proposed devices for wireless microwave-lightwave signal conversion, the proposed devices can be used for realizing wireless broadband communication using ROF technology. Data rate of about 1 Gbps can be obtained using the scheme. Therefore, the demand to large data traffic of wireless communication in the future can be anticipated using the proposed devices with the ROF technology. The proposed devices can be used also for other applications such as electromagnetic compatibility measurement, sensing, and so on.

Table of Contents

Chapter 1 Introduction

1.1 Background

1.1.1 Wireless communication trends

The wireless communication has attracted much interest in past decade, owing to its high mobility. People can connect their mobile devices to a network by radio signals anywhere without cable connection.

Currently, the most useful frequency carrier bands for wireless communication is located in the frequency range of 0.3 – 3.5 GHz with the compact antenna size, low propagation loss, and good penetration through building [1]. This frequency carrier bands can be operated for wide coverage area such as in standards of three-generation (3G), worldwide interoperability for microwave access (WiMAX), long-term evolution (LTE), or so on, however they have moderate bandwidth and high power consumption. Wireless communication with small coverage area in the current frequency carrier bands are also used in wireless-fidelity (Wi-Fi) standard with low power consumption and high security. The various standards for wireless communication are shown in Figure 1-1. A 100 Mbps data rate and large coverage area can be obtained using the current wireless communication [2] [3] [4].

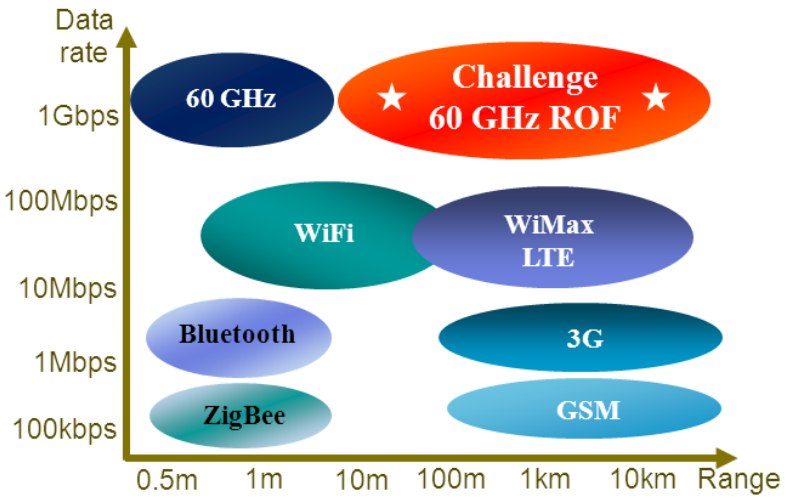

Figure 1-1 Development of wireless communication **[2] [3] [4]**.

The demand for wireless broadband services is growing rapidly due to the people requirements for high quality communication, video, and data transfer using mobile devices. During

2010 to 2013, wireless data traffic grew by over two-times, and this increase is predicted to continue for several years later [5]. The global wireless data traffic growth reported by the Cisco is shown Figure 1-2 [6]. We can see that in the 2017 the data traffic increases over five-times than current data traffic status.

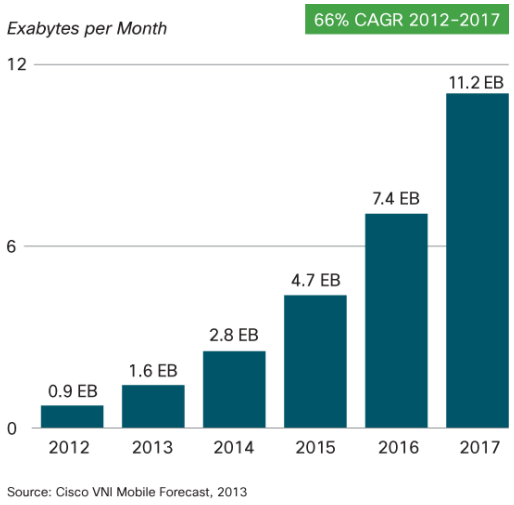

Figure 1-2 Global wireless data traffic growth **[6]**.

In order to anticipate the bottleneck in the future, transmission capacity for the wireless communication must be improved. Now, many researchers concern to solve this issue. One promising technique to improve transmission capacity is by increasing operational carrier frequency of the wireless communication to the millimeter-wave bands such as 60 GHz operational frequency [7].

1.1.2 60 GHz wireless communication

The millimeter wave bands of 60 GHz is of increasing interest to service providers and systems designers because of the wide bandwidths available for carrying data at the frequency range [8] [9]. Since 60 GHz millimeter-wave bands have large bandwidth, transmission capacity of wireless communication can be increased. The 60 GHz millimeter-wave band receives much attention because it can provide wide bandwidth as well as high directivity. Generally, about 7 GHz bandwidths are allocated for license free operation, where the center spectrum is about 60 GHz [10]. In Japan, 9 GHz bandwidth from 57 to 66 GHz is allocated for the millimeter-wave band with license free operation.

The wireless communication with 60 GHz millimeter-wave bands have several advantages such as large bandwidth, low power consumption, high security, and so on [11]. However, they have big drawback, which is high transmission loss in the air as shown in Figure 1-3 [12] [13]. Wireless communication with short coverage area can be realized due the high transmission loss in the air. The

femto/ pico cells with 60 GHz operational frequency have high data rate of about 1 Gbps and small coverage area of about 10 m as shown in Figure 1-1.

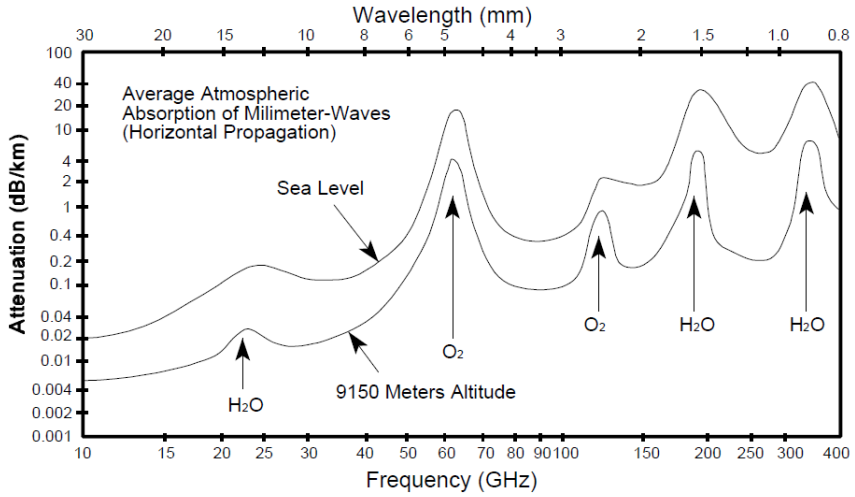

Figure 1-3 Attenuation of the microwave/ millimeter/ sub-millimeter-waves in the air **[14]**.

In order to coverage large areas, large numbers of antenna base stations should be installed since the short coverage wireless communication is realized using each base station. Therefore, much consideration should be given to linking the pico/ femto cell wireless networks to broadband wire-line networks. They can be connected using metal coaxial cable [15]. By increasing the base station numbers, the cost for realizing the 60 GHz wireless communication becomes expensive since many antennas, signal generators, amplifiers, and other microwave equipment are required at each base station.

The microwave equipment can be installed at the center station only for reducing the cost. The microwave signals are transferred to each base station. Since the 60 GHz operational frequency is used as the carrier, the propagation loss is large along the metal coaxial cables. Optical fibers with extremely propagation loss are promising for transferring the 60 GHz millimeter-wave signal with a lightwave as the carrier [15]. The propagation loss of a single mode silica optical fiber is 0.2 dB/km at 1.55 μm lightwave wavelength [16]. Additionally, the optical fiber has large throughput about 10 Gbps and low latency about 10 ms [12].

1.1.3 Radio-over-fiber technology

Wireless network with 60 GHz millimeter-wave band has large bandwidth and small coverage area [9]. In the other, optical fiber networks have mature technology with low propagation loss, large bandwidth, and high speed data transfer. Therefore, the optical fiber fed to wireless networks is attractive solution to expand coverage area of the wireless millimeter-wave communication [17] [18].

This technology is called radio-over-fiber (ROF) technology. The broadband wireless communication with high date rates and expanded coverage areas using the ROF technology can be obtained.

The wireless millimeter-wave communication using ROF technology can be illustrated typically in Figure 1-4. The wireless millimeter-wave network in the pico/ femto cells are connected each other using optical fibers. The millimeter-wave signals are transferred to other pico/ femto cells through optical fibers with a lightwave as the carrier. The ROF technology has large bandwidth, low propagation loss, good mobility, low induction, low power consumption, high security, and so on [19].

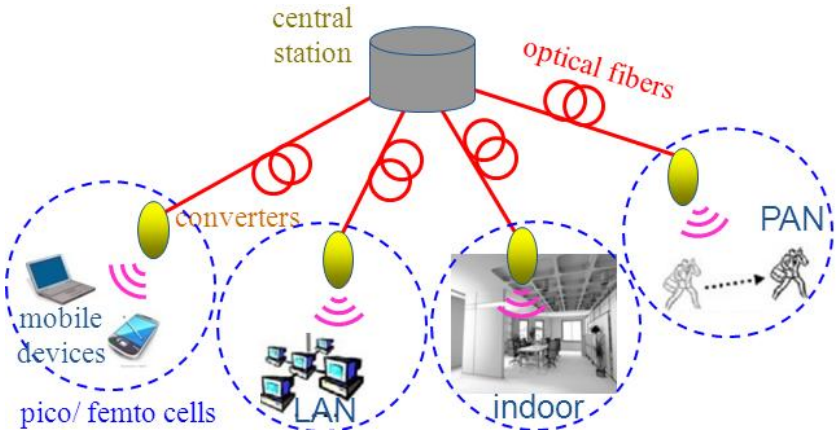

Figure 1-4 Schematic of the pico/ femto cells wireless communication using ROF technology.

By adopting the ROF technology in the wireless communication with 60 GHz millimeter-wave band, large bandwidth and coverage area expansion can be obtained. Therefore, the new challenged broadband wireless communication with data rate about 1 Gbps and coverage area expansion can be realized as shown in Figure 1-1.

1.1.4 Converters between microwave and lightwave signals

The ROF technology is operated in two domains: one is for microwave domain and the other is lightwave domain [20] [21] [22]. Since the microwave and lightwave signals are used simultaneously in the ROF technology, converters between them are required as the key devices. They have two types: one is a converter from lightwave to microwave signals and the other is a converter from microwave to lightwave signals.

In the wireless communication with the ROF technology, the converter from lightwave to microwave signals can be composed of a high speed photo-detector and antenna as shown in Figure 1-5 (a) [23] [19]. A modulated lightwave signal is detected and converted to a microwave signal using the photo-detector. Then, the converted microwave signal is transmitted to the air using the antenna. Many researchers develop the converter for high frequency operation [24]. Currently, this converter

has a mature and advanced technology, where high performance photo-detector using uni-travelling-carrier photo-diode (UTC-PD) has been development for high frequency operation [25] [26] [27]. By combining the UTC-PD with antenna, the lightwave to wireless microwave signal conversion can be achieved. Figure 1-5 (b) shows the typical of an UTC PD integrated with an antenna [28].

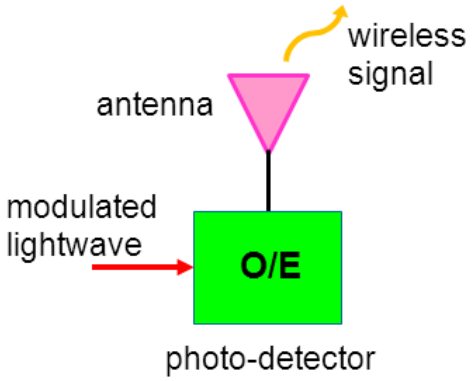

(a)

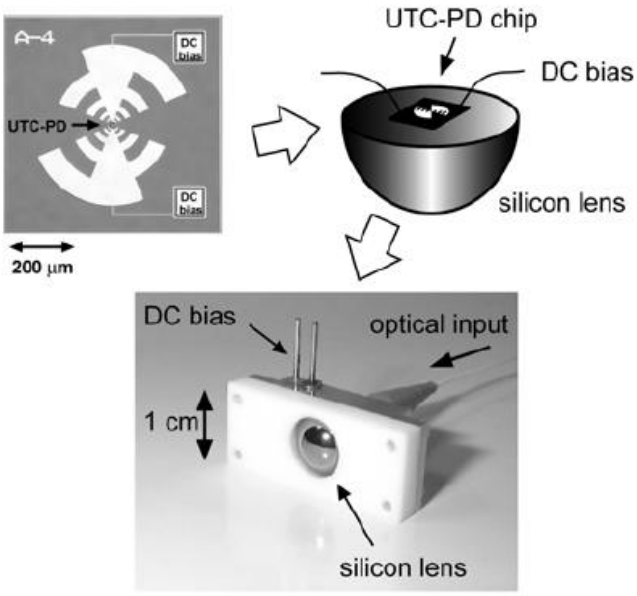

(b)

Figure 1-5 (a) Schematic of a converter from lightwave to wireless microwave signals. (b) Example of an UTC-PD combined with an antenna **[28]**.

In contrary, the converter from microwave to lightwave signals can be composed of an antenna and an optical modulator as shown in Figure 1-6 (a) [29] [30]. A wireless microwave signal is received using the antenna. Then, the received microwave signal is converted to a lightwave signal using the optical modulator. Several optical modulators have been proposed and reported their performance [31] [32] [33]. The optical modulator can be achieved through electro-absorption, electro-refraction, photo-elastic, and so on [34]. Considering for operating in the high frequency, an

electro-optic (EO) modulator using electro-refraction effects is one candidate with their advantages such as high speed operation, large bandwidth, and good linearity [35]. Currently, the EO modulators have advanced performance based on phase, intensity, polarization, and so on. By combining the antenna and EO modulator, the wireless microwave to lightwave signal conversion can be achieved [36]. Figure 1-6 (b) shows the examples of antennas combined with EO modulators [30] [37]. The converters were proposed and demonstrated experimentally for microwave bands.

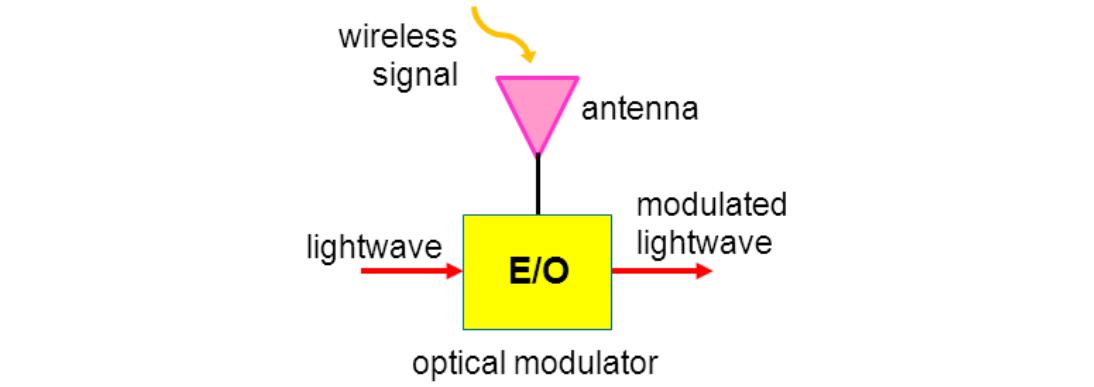

(a)

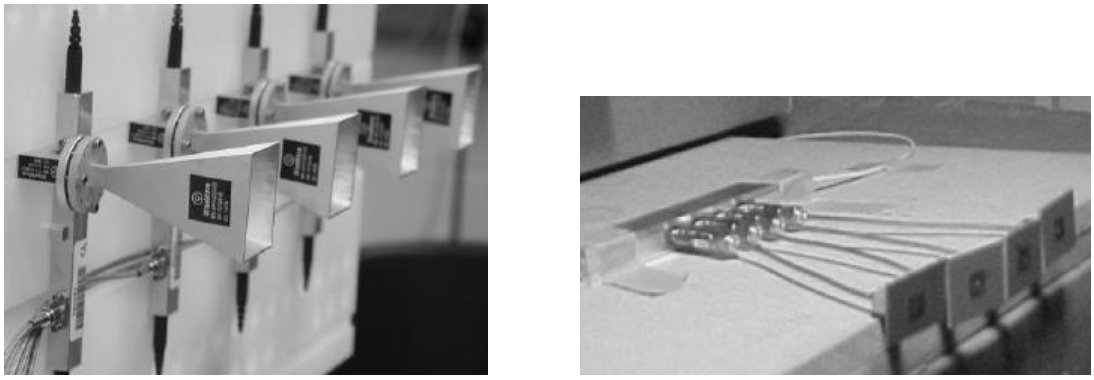

(b)

Figure 1-6 (a) Schematic of a converter from wireless microwave to lightwave signals. (b) Examples of antennas combined with EO modulators **[30] [37]**.

The key devices in the ROF technology for converting between the wireless microwave and lightwave signals were discussed. The converters from lightwave to wireless microwave signals have advanced technology for high frequency operation up to terra-hertz bands [28]. In contrary, the converters from wireless microwave to lightwave signals were reported for microwave bands [30]. In order to improve the operational frequency, the losses might be induced due to the coupling between the antenna and EO modulator [38]. The remaining problems in the wireless microwave-lightwave signal converters can be solved by EO modulators integrated with planar antennas in simple and compact structures. These devices will be discussed in this dissertation.

1.2 Objective of this research

In this section, the goals of the research are stated. I study EO modulators using planar antennas for wireless microwave-lightwave signal conversion. The devices are operated for high frequency operation through the ROF technology with low microwave loss and no external power supply. Efforts to enhance the device functionality and improve device performances are also discussed.

New EO modulators using a planar antenna with fusion and integrated structures are described in follows:

1. A new fusion EO modulator using a patch antenna embedded with a single narrow gap is proposed. By utilizing displacement current and electric field across the gap in the proposed device, optical modulation through the Pockels effects can be obtained. Verification of the basic operations for direct wireless microwave-lightwave signal conversion was experimentally done.
2. In order to enhance the fusion device functionality, fusion EO modulators using a patch antenna embedded with double narrow gaps are proposed. Optical intensity modulators with the Mach-Zehnder interferometer can be realized using a fusion EO modulator using a patch antenna embedded with parallel narrow gaps. Wireless microwave signals with two orthogonal linear polarizations can be received and converted directly, simultaneously, and independently by a fusion EO modulator using a patch antenna embedded with orthogonal narrow gaps.
3. By considering the antenna gain, an integrated EO modulator using a planar Yagi antenna coupled to a resonant electrode is proposed. The gain of the Yagi antenna is larger than the patch antenna. Interaction length between microwave and lightwave electric fields for EO modulation is longer than the fusion EO modulators for the single structure. As a result, modulation efficiency improvement can be obtained. The precise tuning is required for minimizing the microwave losses.

Furthermore, the objective of this research includes the efforts to improve device performance and enhance device functionality. The efforts are described in follows:

1. EO modulators using arrays of planar antennas for improving modulation efficiency are proposed. The transit time of lightwave propagating in the optical waveguide and passing through each planar antenna should be considered for effective optical modulation. The modulation efficiency improvement is proportional to number of the planar antennas. A new EO modulator using a quasi-phase-matching (QPM) array of patch antennas embedded with a narrow gap is proposed for further efficiency improvement with more compact device structure. A ROF link is demonstrated using the proposed device. A new

EO modulator using a 2-D array of patch antennas embedded with orthogonal meandering gaps is also proposed. 1-D and 2-D beamforming receiving of wireless microwave signal can be achieved using the proposed device.

2. In order to improve in further the modulation efficiency and operate in the high frequency operation, new optical modulators using a thin EO waveguide suspended to planar antennas on a low-*k* dielectric substrate are proposed. Large antenna size can be obtained due to low effective dielectric constant. As a result, modulation efficiency become large since antenna aperture and interaction length is larger and longer, respectively. Additionally, substrate resonant modes can be eliminated since a thin EO crystal is used.

Those are the main objectives of this research. The current research progress and future research prospect are also presented. The applications of the proposed devices through the ROF technology are also discussed such as for broadband wireless communication, low induction electromagnetic compatibility measurement, high resolution automotive radar, and so on.

1.3 Organization of this dissertation

This dissertation begins by an introduction, which explains the background and objective of this research. Then, the main issues of this dissertation are explained by six chapters. Finally, this dissertation closes with conclusions of this research. The relationship between the chapters in this dissertation is shown schematically by Figure 1-7. The brief contents of the main chapters in this dissertation are given as following:

Chapter 2 Wireless microwave-lightwave signal conversion using planar antennas with EO modulators

This chapter shows the fundamental of planar antennas and EO modulators. Their characteristics and advantages are discussed separately. By combining the planar antennas and EO modulators, wireless microwave-lightwave signal conversion can be obtained. Various combinations of them and their advantages are discussed such as discrete structures and integrated structures. Furthermore, new fusion structures are also presented. In the discrete structures, the planar antennas and EO modulators are fabricated on different substrate and connected using microwave connection lines. In the integrated structures, the planar antennas and EO modulators are fabricated on the same substrate, where a connection line is still required between them. In the fusion structures, a planar structure can be functioned for wireless microwave signal receiving and EO modulation with no additional connection line.

Chapter 3 EO modulators using a patch antenna embedded with a single narrow gap

In this chapter, new EO modulators using a patch antenna embedded with a narrow gap are proposed for wireless microwave-lightwave signal conversion. The proposed devices are composed of a patch antenna only with no other planar structure on the substrate. A narrow gap is introduced at the center of the patch antenna. Displacement current and electric field are induced across the gap and can be used for optical modulation through the Pockels effects of an EO crystal. The proposed devices have simple and compact structure and can be operated with low microwave loss and no external power supply. The verification of their basic operation for direct wireless microwave-lightwave signal conversion is presented.

Chapter 4 EO modulators using a patch antenna embedded with double narrow gaps

In order to enhance the functionality of the new fusion devices, EO modulators using a patch antenna embedded with double narrow gaps are proposed and discussed in this chapter. By using the proposed device, wireless microwave signals can be received and converted to two lightwave signals simultaneously and independently. In here, two device configurations are presented. Firstly, I propose an EO modulator using a patch antenna embedded with two parallel narrow gaps. The proposed device can be used for a Mach-Zehnder interferometer. Secondly, I propose an EO modulator using a patch antenna embedded with two orthogonal narrow gaps. By analyzing the two modulated lightwave signals, wireless microwave signal with two orthogonal polarizations can be received and converted directly to lightwave signals. Furthermore, the proposed device can be used for receiving a circular polarization of wireless microwave signals. The polarization of the wireless microwave signals can be identified using the proposed device through optical technology.

Chapter 5 EO modulator using a planar Yagi antenna coupled to a resonant electrode

Purpose of this chapter is to present an EO modulator using a planar Yagi antenna coupled to a resonant electrode. Since the Yagi antenna has higher antenna gain than the patch antenna, I expect that modulation efficiency improvement can be achieved. In order to achieve effective optical modulation, precise tuning between the planar structures, which are the planar Yagi antenna, resonant electrode, and connection line, is required and rather difficult to obtain. The calculation of the modulation efficiency improvement was done.

Chapter 6 EO modulators using arrays of planar antennas

In this chapter, efforts to improve the device performances and enhance device functionality are discussed by EO modulators using arrays of planar antennas. By utilizing array structures, the modulation efficiency can be improved proportional to number of the planar antennas since the transit

time of lightwave passing through each antenna is considered for effective optical modulation. In order to improve modulation efficiency furthermore, I propose an EO modulator using a QPM array of patch antennas embedded with a narrow gap. The proposed device has twice antennas with the same device length compared to the conventional array devices. As a result, double modulation efficiency improvement can be obtained with more compact device structures. Since the array structure affects to the wireless irradiation angle (beamforming), an EO modulator using a 2-D array of patch antennas embedded with orthogonal gaps is presented. I proposed new technique using meandering gaps for beamforming receiver. The meandering gaps are used to compensate for the degradation of optical modulation in certain beamforming. By analyzing two orthogonal modulated lightwave signals, 1-D and 2-D beamforming of wireless microwave signal can be obtained.

Chapter 7 Optical modulators using EO waveguides suspended to planar antennas on low-*k* dielectric substrate

New optical modulators using thin EO waveguides suspended to planar antennas on a low-*k* dielectric substrate are proposed. Large antenna size can be obtained using the proposed devices, since the effective dielectric constant is low. As a result, large antenna aperture and long interaction length can be obtained for enhancing modulation efficiency. Additionally, by using a thin EO crystal, the substrate resonant mode can be eliminated. The proposed devices are promising for high frequency operation. Millimeter-wave optical modulators using a thin EO waveguide suspended to patch antennas embedded with a narrow gap on a low-*k* dielectric substrate are presented.

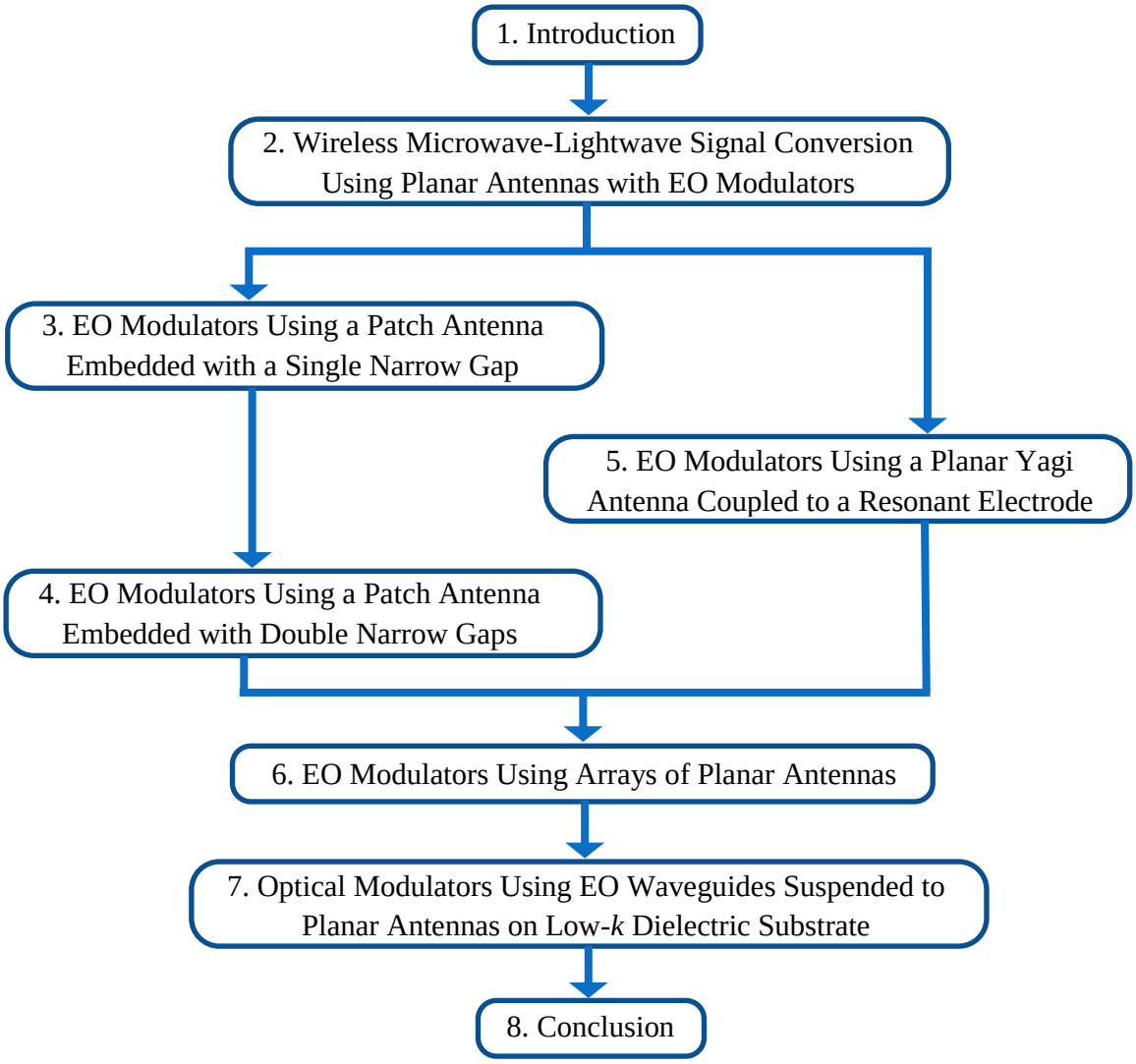

Figure 1-7 Structure of this dissertation.

Chapter 2 Wireless Microwave-Lightwave Signal Conversion Using Planar Antennas with Electro-Optic Modulators

2.1 Introduction

In the radio-over-fiber (ROF) technology, the wireless microwave signals can be converted to the lightwave signals. Then, the converted/ modulated lightwave signals are propagated through optical waveguides such as silica optical fibers [1] [21]. Since microwave and lightwave signals are used simultaneously, converters between microwave and lightwave signals are required. There are two types, which are converters from lightwave to wireless microwave signals and converters from wireless microwave to lightwave signals [39].

The converters from lightwave to wireless microwave signals can be composed of a high speed photo detector and antenna [23] [19]. A modulated lightwave signal is detected and converted to a microwave signal using the photo-detector. Then, the converted microwave signal is transmitted to the air using the antenna. These converters have a mature and advanced technology, where high performance photo-detector using uni-travelling-carrier photodiode (UTC-PD) has been development for high frequency operation [25] [26] [27].

In this dissertation, the converters from wireless to lightwave signals are discussed. They can be composed of an antenna and optical modulator as shown in Figure 2-1. In the schematic shows that the wireless microwave signal can be detected and converted to the lightwave signal. Furthermore, the converted signal is propagated into a silica optical fiber.

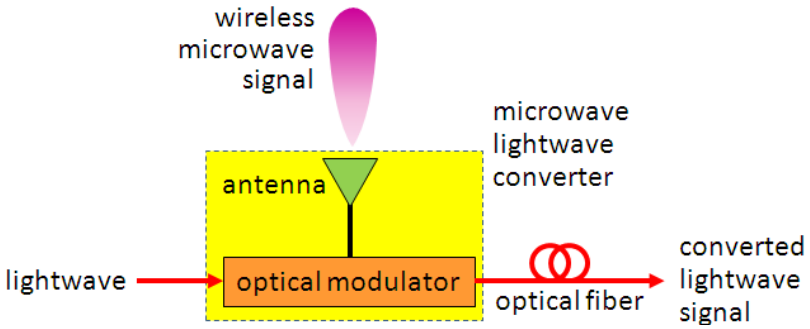

Figure 2-1 Basic schematic of the microwave-lightwave signal converter in the ROF technology.

Several microwave antennas are possible for constructing the microwave-lightwave signal converters. In this thesis, I concern on planar antennas with their advantages such as simple and

compact structure, low profile, lightweight, and easy fabrication [40] [41]. The planar antennas have several types such as dipole, square patch, circular patch, and so on.

Several optical modulators can be used for converting from microwave to lightwave signals [42]. Electro-optic (EO) modulators is promissing candidate due to their advantages such as high speed operation, large bandwidth, and good linearity. The EO modulators are operated by using EO effect of an EO crystal such as $LiNbO_3$, $LiTaO_3$, KTP, and so on. EO polymers with single polarized molecules are also applicable for the substrate. Several types of the EO modulators such as bulk and guided-wave types were developed and reported [43] [44].

The fundementals of the planar antennas and EO modulators are discussed in this chapter. Several device configurations for realizing wireless microwave-lightwave signal conversion such as discrete, integrated, and new fusion structures are presented also in here. The features and characteristics for each configurations of the wireless microwave-lightwave signal conversion are discussed.

2.2 Planar antennas

Antennas are an important device for detecting wireless microwave signals. Several types of antennas were established such as parabolic reflectors, horn antennas, dipole antennas, and so on. Each type of the antennas has their own features for certain applications. The antennas are widely used in the world for wireless communication, electromagnetic sensing, or other applications [40] [45].

One type of antennas is planar antennas. The planar antennas have a lot of popularity based on their applications, which have some merits and de-merits as any others. The merits of these antennas have some similarities as of the conventional microwave antennas such as a broader range of frequency up to 100 GHz. In wireless communication, these are widely used in the mobile devices such as mobile phones, notebook, tablet, and so on. The merit of the planar antennas are low weight, low volume and thin profile configurations which can be made conformal, low fabrication cost, readily available to mass production, linear and circular polarizations are possible, easily integrated with microwave integrated circuits, and capable of dual and triple frequency operations. However, the de-merit of the planar antennas compared with conventional antennas are low efficiency, lower gain, low power handling capacity, excitation of surface waves, difficult polarization purity, and complex feed structures for high performance arrays.

2.2.1 Antenna types

There are several types of planar antennas which are classified based on their physical parameters. There different types of antennas have many different shapes and dimensions as show in

Figure 2-2. The basic categories of these planar antennas can be classified into four, which are patch antennas, planar dipole antennas, printed slot antennas, and planar travelling wave antennas. Yagi and log periodic antennas are available in the planar structures.

A planar antenna is a thin planar metal electrode on one side of a dielectric substrate and the other side having a plane to the ground metal electrode. The planar antenna is made of a conducting material Cu (Copper), Au (Gold), or Al (Aluminum).

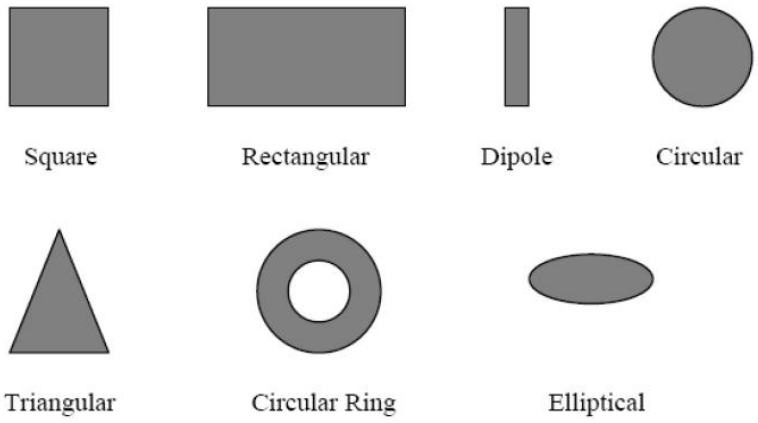

Figure 2-2 Typical shapes of antenna using planar elements **[46]**.

2.2.2 Resonant frequency

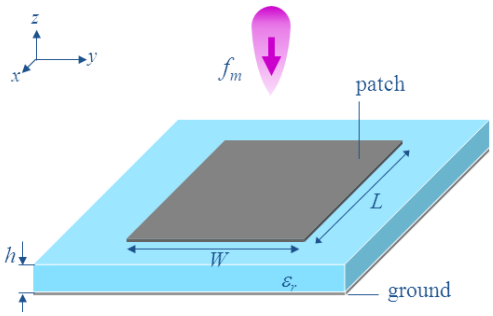

Figure 2-3 Basic structure of the planar antennas with a rectangular shape.

The resonant frequency of the planar antennas is determined by the size of the planar metal electrode. The basic parameter of the planar is a strip conductor as shown in Figure 2-3 with length, L, and width, W, on a dielectric substrate with constant, ε_r, and thickness, h. The planar antenna is designed so that it can operate at the resonance frequency of microwave signals, where the resonant frequency can be determined by tuning the length of the antennas. The length of the antennas depends on the effective dielectric of the substrate, ε_{eff}, height of the dielectric substrate, and the antenna width. The length of the planar antenna can be calculated using the following equation [40]

$$L = \frac{c}{2f_m\sqrt{\varepsilon_{eff}}} \tag{2-1}$$

where f_m is the frequency of the designed microwave signal and c is the speed of the light in the vacuum.

There are many methods to analyze planar antennas. The most popular is a transmission line method, where the patch is a transmission line or a part of a transmission line is assumed. The second method is a cavity model, where the patch is a dielectric-loaded cavity is assumed.

The transmission line method is the easiest way to study the planar antenna. In this method the transmission line model represents the planar patch antenna by two slots, separated by a low-impedance transmission line of length L. The method is good enough to design the antenna. The general model of the planar antennas is shown in Figure 2-4.

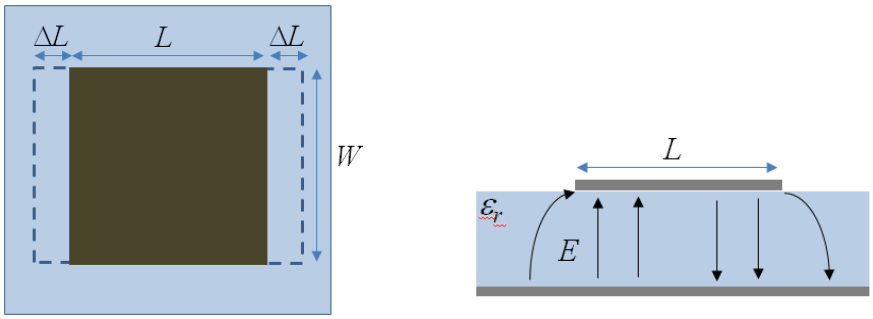

Figure 2-4 Transmission line model.

The first approximation, the thickness of the conductor, t, is assumed that forms the line has no effect on the calculations, because it is very thin comparing with the substrate, h ($h >> t$), so the empirical formulas that depend only on the line dimensions: the width, W, the length, L, the height, h, and the dielectric constant, ε_r, of the substrate [47]. The electric field lines in the antenna mostly exist in the substrate and evenly leak a little bit to the air. The transmission lines are not able to support the pure transverse electric magnetic (TEM) mode of transmission because the lines in the substrate and lines in the air have different phase velocities. In order to have a notice of wave propagation and the fringing in the line with the effective dielectric constant, ε_{eff}, it can be formulized as

$$\varepsilon_{eff} = \frac{\varepsilon_r + 1}{2} + \frac{\varepsilon_r - 1}{2}\left[1 + \frac{12h}{W}\right]^{0.5} \tag{2-2}$$

The value of ε_{reff} is slightly less than that of ε_r as that the fringing fields are not confined only in the substrate but some are out in the air.

The fringing fields along the width of the structure are taken as radiating slots and the patch of the antenna electrically seen to be a bit larger than usual design. So the dimensions are extended a little bit ΔL for a better performance, ΔL can be expressed by

$$\Delta L = 0.412h\frac{(\varepsilon_{eff}+0.3)\left(\frac{W}{h}+0.264\right)}{(\varepsilon_{eff}-0.258)\left(\frac{W}{h}+0.8\right)} \tag{2-3}$$

The effective length of patch antenna, L_{eff} is given by

$$L_{eff} = L + 2\Delta L \tag{2-4}$$

For the particular resonant frequency the effective length of the patch is calculated by

$$L_{eff} = \frac{c}{2f_m\sqrt{\varepsilon_{eff}}} \tag{2-5}$$

Considering the rectangular patch antenna the resonant frequency for the mode TM_{mn} is given by [48]

$$f_m = \frac{c}{2\sqrt{\varepsilon_{eff}}}\left[\left(\frac{m}{L}\right)^2+\left(\frac{n}{W}\right)^2\right] \tag{2-6}$$

where m and n are the operating modes of the patch antenna, along L and W, respectively. In order to avoid unwanted higher order mode effect, the width of the patch antenna is set below one wavelength of the wireless microwave signal. Furthermore for the effective receiving, the width of patch antenna should be set to

$$W = \frac{c}{2f_m}\sqrt{\frac{2}{\varepsilon_r+1}} \tag{2-7}$$

In the antenna analysis, the size of patch antenna can be estimated using transmission line model for designed frequency operation. The two edges of patch antenna are induced a strong electric field, and the highest current magnitude is induced at the center of patch antenna. Those are general characteristic of patch antenna along its length, which is illustrated in Figure 2-5.

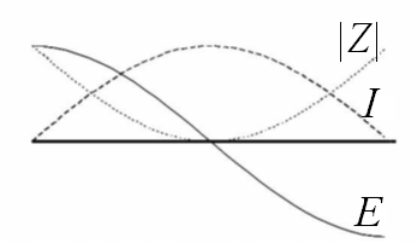

Figure 2-5 Characteristics of the patch antenna.

These planar antennas are narrow bandwidth about 10% of the designed microwave signal. A good performance from the planar antennas can be expected with a thick dielectric substrate with a low dielectric constant as this gives larger bandwidth, efficiency, and radiation [41]. These antennas with the low dielectric substrate are larger than expected in the construction. Small size with compact structure can be obtained using high dielectric substrate, which is less efficient, and having a narrow bandwidth. The planar antennas fabricated on a high dielectric substrate such as EO crystals such as $LiNbO_3$ or $LiTaO_3$ were reported [49].

The planar antennas are basically used for receiving wireless microwave signals. In order to realize wireless microwave-lightwave signal conversion, the planar antennas can be combined with optical modulators. The optical modulators by use of the Pockels effects will be discussed in the next section.

2.3 Electro-optic modulators

Ferroelectric optical materials such as $LiNbO_3$ and $LiTaO_3$ have a large electro-optic (EO) coefficient in first order (Pockels effects) [34]. They have fast response time of less than picosecond. By using the EO effect, the high speed optical modulators can be expected up to 100 GHz frequency [50] [51].

2.3.1 Linear electro-optic effect

Microwave-lightwave signal converters using planar antennas with EO modulators are studied in here. The EO modulators are fabricated on EO crystals such as $LiNbO_3$, $LiTaO_3$, polymer, or others.

The refraction index varies linearly with the applied electric field. It proportionally depends on the axis direction of the strongest the linear EO effects or the Pockels effects in the EO crystal. The resulting change of the refraction index in the optical path length of the light passing through the EO crystal is proportional to the electric field applied in the modulation electrodes [43]. As a result, a phase shift of the lightwave passed through the modulation electrode is induced.

The effects of an applied electric field on the propagation of the lightwave are defined by the change of the refraction indices [22] [52]. When field component E_k is applied, the change in an element can be expressed as

$$\Delta\left(\frac{1}{n^2}\right)_{ij} = \sum_{k}^{3} r_{ijk}\, E_k \tag{2-8}$$

where *i*, *j* each range over the three spatial coordinates and *k* is 1, 2, 3 denote *x*, *y*, *z*, respectively. There are six relevant indices of refraction from the index ellipsoid, three terms for the three principle directions (*x*, *y*, and *z*), and three cross terms. An electric field has *x*, *y*, and *z* components, so in general this effect is described with a 6x3 tensors. So that Eq. (2-8) may be written as [53]

$$\Delta\left(\frac{1}{n^2}\right)_{p} = \sum_{k}^{3} r_{pk}\, E_k \tag{2-9}$$

where *k* ranging from 1 to 3 and *p* from 1 to 6. In the non-EO crystals (centro-symmetric), all of the terms r_{pk} are zero. The most EO crystals have some degree of symmetry leading to many of the r_{pk} terms equaling zero [22] [54]. The EO coefficient is generally very small in pico-meter-order per volt.

The crystals are cut and used in an orientation to maximize the field projected onto the direction with the largest EO effect [55]. Clearly, it would be inefficient to rely on the r_{13} and r_{22} terms in $LiNbO_3$/ $LiTaO_3$ crystal. While the formalism to describe the EO effect is fairly complex, in practice there is only one scalar quantity used in the analysis of EO modulators, that is r_{33} (about 30 pm/V), which describes the effect of an applied electric field in the *z*-direction on an optical wave polarized in the *z*-direction. For the *z*-cut $LiNbO_3$/ $LiTaO_3$, the *z*-axis is normal to the surface of the crystal and the optical wave is transverse magnetic (TM) polarized and for the *x*-cut $LiNbO_3$/ $LiTaO_3$, the *x*-axis is normal to surface of the crystal and the optical field is transverse electric (TE) polarized.

2.3.2 Bulk EO modulator

The basic mechanism for EO modulators is a voltage-dependent phase shift. The optical and electrical fields must be oriented with respect to the crystal orientation with the highest EO effect [55]. The first EO phase modulators were built using bulk crystals, and used either a longitudinal or transverse orientation of the electric field with respect to the propagation direction of the optical wave.

The longitudinal method is not particularly desirable because the electric field direction and the optical path length are parallel. Thus, it increases the length of the crystal to increase the accumulated phase shift. It also decreases the electric field for the same voltage applied to the crystal ends. The net effect is no improvement in phase shift with increased crystal length. Furthermore, the electrodes needed to apply the electric field in this direction typically interfere with the optical pathway.

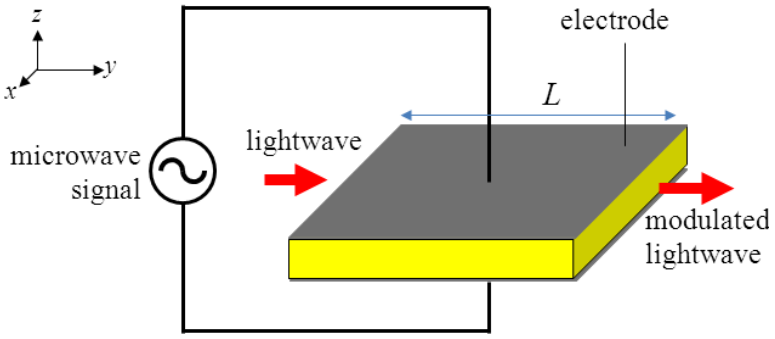

Figure 2-6 Structure of a bulk EO modulator.

The transverse mode of operation is more desirable, in that the field is applied normal to the direction of propagation, as shown in Figure 2-6. The optical phase shift or retardation can be increased by increasing the length of the crystal without changing the strength of the applied electric field. The other advantage is no interference between the electrode and lightwave. It takes a lot of voltage to obtain effective optical modulation in the bulk modulator.

By increasing electrode length and thin EO crystal, effective optical modulation can be easily obtained. It becomes more difficult to fabricate long and thin crystals. However, a more fundamental limitation occurs because of diffraction of the propagating light. If the transverse dimension is made very small, the light propagating through the crystal will spread more rapidly, and hit the sides of the crystal, thus being absorbed.

In order to obtain more effective optical modulation guided-wave EO modulator can be adopted. Very narrow gap width and long electrode can be realized easily since the device is planar structure. The EO guided-wave optical modulator will be discussed at following.

2.3.3 Guided-wave EO modulator

The limitations of the bulk EO modulator for obtaining effective optical modulation are short electrode length and wide electrode gap depends on the EO crystal thickness. In order to realize narrow gap width is rather difficult by fabricating a thin EO crystal. The limitations can be solved by using a guided-wave EO modulator. The guided-wave modulator is composed of a planar electrode fabricated on an EO crystal as shown in Figure 2-7, where an channel optical waveguide is located under the gap. Very narrow gap width can be realized for generating strong electric field between electrodes. The waveguide eliminates diffraction, so that the crystal length may be made as long as required to achieve the desired sensitivity, limited only by optical loss in the crystal. This device is suitable for wide range of applications.

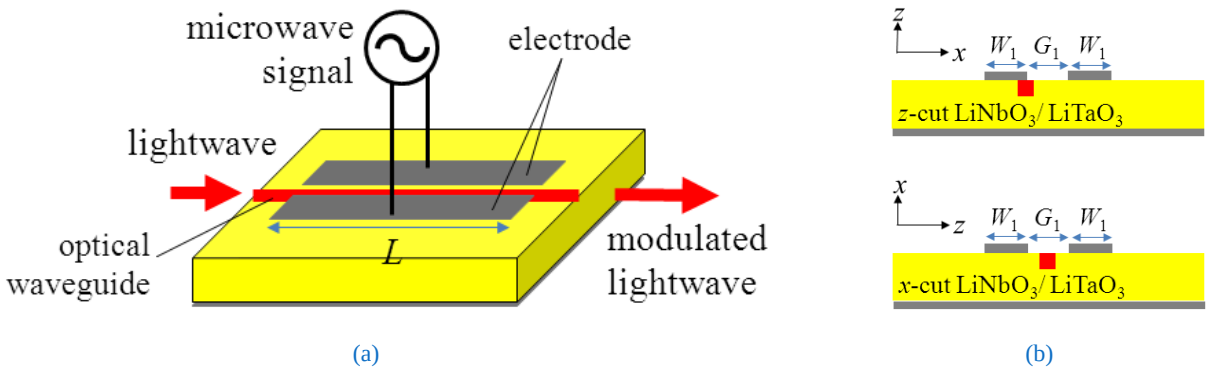

(a) (b)

Figure 2-7 Structure of a guided-wave EO modulators (a) whole view and (b) cross-sectional view of the device fabricated on a *z*-cut and *x*-cut $LiNbO_3$/ $LiTaO_3$ crystal.

The optical waveguide can be fabricated using an annealed proton exchange or titanium diffusion methods [56] [57] [58]. The electrode can be fabricated using a metal such as aluminum, gold, copper, or so on [44] [59].

A phase EO modulator is the simplest modulator to build. Figure 2-7 shows a guided-wave EO modulator fabricated on an EO crystal such as $LiNbO_3$ or $LiTaO_3$ crystals. There is a single channel optical waveguide parallel to the *y*-axis of the crystal. The electrodes are fabricated as strips of metal on the crystal surface. The gap between the waveguides is sized and positioned to maximize the electric field component along the direction of the crystal with the strongest EO coefficient. In case of *z*-cut EO crystal, light propagates along the *y*-direction, the *z*-direction is normal to the substrate, and the *x*-direction is along the surface, perpendicular to the direction of propagation. The electric field lines penetrate down into the EO crystal, continue perpendicular to the waveguide in the *z*-direction of the crystal, and then go back up to the opposite electrode.

Several types of guide-wave EO modulators are available such as lumped, travelling-wave, and resonant types with their features. The traveling-wave EO modulators have large bandwidth and

relatively low modulation efficiency. The resonant EO modulators have narrow bandwidth and relatively large modulation efficiency.

2.4 Wireless microwave-lightwave signal converters

In the previous sub-chapter, the fundamentals of planar antennas and EO modulators were discussed in detail. By combining the planar antennas and EO modulators, wireless microwave-lightwave signal conversion through EO modulation can be realized. The wireless microwave signals can be received using the planar antennas and then the microwave signals can be converted to lightwave signals using the EO modulators. Various configurations using the combination of the planar antennas and EO modulators can be formed. The configurations are discussed in here such as by discrete, integrated, and new fusion structures.

2.4.1 Discrete structure

In the discrete structure, the planar antenna and EO modulator are fabricated on difference substrate as shown in Figure 2-8. The planar antenna is fabricated on a low dielectric substrate for effective wireless microwave signal receiving and the EO modulator using a resonant electrode is fabricated on an EO crystal with high EO coefficient. A connector using a microwave coaxial cable is required to transferring the received microwave signal from the planar antenna to the resonant electrode. Several wireless microwave-lightwave signal converters using discrete structures were proposed and reported [29] [30].

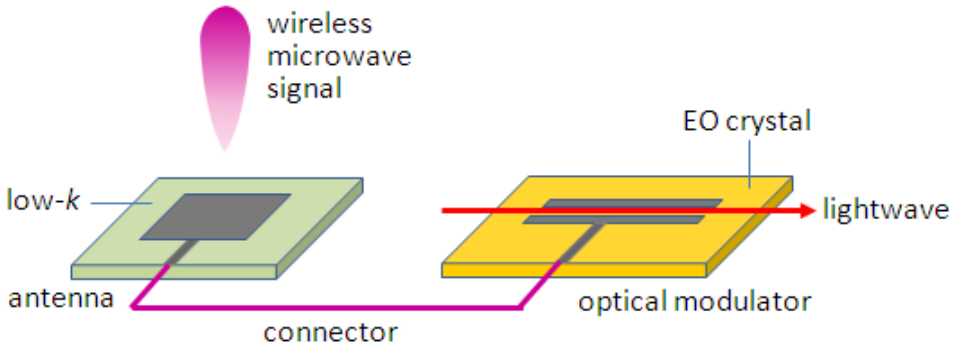

Figure 2-8 Structure of wireless microwave-lightwave signal converters with discrete structures.

High performance of the planar antenna and EO modulator can be obtained separately. In the discrete structures of the wireless microwave-lightwave signal converters, a connection line between the antennas and the EO modulators is used. The connection line is commonly using microwave coaxial cables or planar microwave waveguide. However, losses of the microwave signal might be

occurred in the coaxial cables due to high operational frequency such as over 30 GHz in millimeter-wave bands [38]. Some decay might be also induced in these discrete structures. In order to reduce the microwave signal losses, good matching condition is required between the antennas, connection line, and optical modulators. Additional microwave components such as amplifier can be used between the antennas and optical modulators.

2.4.2 Integrated structure

In order to minimize the loss and realize compact device, wireless microwave-lightwave signal converters with integrated structures can be adopted. The example of the integrated structure is shown in Figure 2-9, where the antenna and planar EO modulator are fabricated on the same substrate. A wireless microwave signal is received using the planar antenna, then the received microwave signal is transferred to the resonant electrode using the planar connection line, after that the transferred microwave signal is converted to a lightwave signal using the resonant electrode through EO modulation by the Pockels effects. Several wireless microwave-lightwave signal converters using integrated structures were proposed and reported [38] [59] [60].

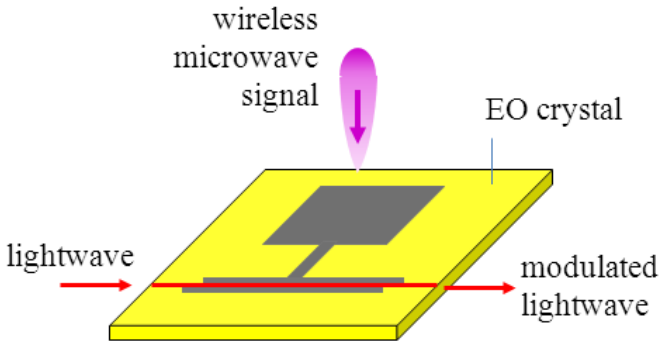

Figure 2-9 Structure of wireless microwave-lightwave signal converters with integrated structures.

The integrated converters from wireless microwave to lightwave signals have simple and compact structure with planar structure. Low microwave loss can be obtained using the integrated structures with short planar strip line as the connector. Additionally, the integrated converters can be operated passively with no external power supply. However, the precise tuning among the planar structures, which are the planar antenna, resonant electrode, and connector, is still required for effective optical modulation. The precise tuning is sometimes rather difficult to obtain.

2.4.3 Fusion structure

We have so far discussed two configurations of wireless microwave-lightwave signal converters based on planar antennas and EO modulators. The device configurations with discrete and integrated structures were presented with their features.

New wireless microwave-lightwave signal converters using fusion structures are proposed, where one structure/ component can be used for two functionalities to wireless microwave receiving and optical modulation. The new fusion converters are fabricated on an EO crystal as a substrate and composed of a patch antenna only with no other planar structure on the substrate. The basic structure of the fusion converters is shown in Figure 2-10. The new fusion converters will be discussed in detail in this dissertation with their hypothesis of the operational principle, analysis of the microwave characteristics and optical modulation, and verification of their basic operations. The effort for enhancing their functionality and improving their performances are also discussed.

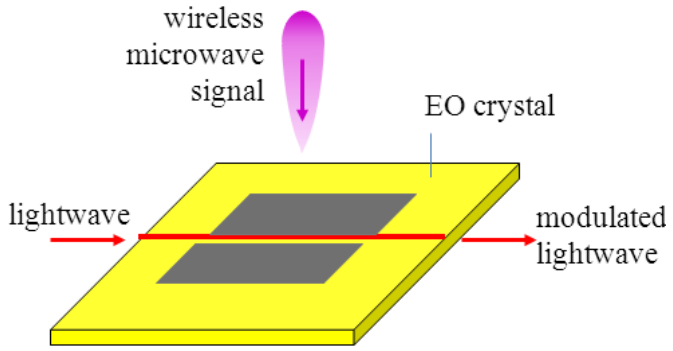

Figure 2-10 Structure of wireless microwave-lightwave signal converters with fusion structures.

Since there is no other planar structure on the substrate except the patch antenna, very low microwave loss can be achieved with more compact structure. The fusion converters can be operated passively with no external power supply. Furthermore, they are easy in design since no precise tuning requirements.

2.5 Summary

In this chapter, the fundamentals of planar antennas and EO modulators for wireless microwave-lightwave signal conversion were explained briefly. The planar antennas have simple compact structure, low profile, lightweight, and easy in fabrication. The guided-wave EO modulators were also discussed with a simple compact device in the planar structure. The optical modulation using the Pockels effects of the EO crystal was also described. Theses fundamentals of the planar

antennas and EO modulators are necessary for designing the wireless microwave-lightwave signal converters.

Wireless microwave-lightwave signal conversion can be achieved by combining the planar antennas and EO modulators. Various configurations were presented with discrete, integrated, and fusion structures. Their features were also discussed as summarized in Table 2-1. In this dissertation, new fusion structures of the wireless microwave-lightwave signal converters are proposed and discussed in detail. Additionally, an integrated wireless microwave-lightwave signal converter is also presented.

Table 2-1 Comparison of the converters from wireless microwave to lightwave signals.

Discrete structure	Integrated structure	Fusion structure
• Enlarge structure	• Compact structure	• Very compact structure
• Complex structure	• Simple structure	• Simple structure
• Require connection line	• Require connection line	• No require connection line
• Large microwave loss	• Low microwave loss	• Very low microwave loss
• Need precise tuning	• Need precise tuning	• No need precise tuning

Chapter 3 Electro-Optic Modulators Using a Patch Antenna Embedded with a Single Narrow Gap

3.1 Introduction

Radio-over-fiber (ROF) technology suitably supports for mobile communication systems in microwave/ millimeter-wave bands by compensating for large transmission losses of metallic cables [21]. In the ROF technology for communication systems, microwave signals are converted to lightwave signals and transferred through optical fibers with low transmission loss. Large transmission bandwidth and no induction are also advantages of the optical fibers [1]. In the ROF technology, microwave and lightwave signals are used simultaneously. In order to realize the ROF systems, converters between the microwave and lightwave signals are required.

A microwave generation for downlink in the ROF systems can be achieved by a high-speed photo-detector [61]. On the contrary for uplink conversion, the microwave signals can be directly converted into lightwave signals by use of high-speed optical modulation technology [62].

A converter from wireless microwave to lightwave signals can be composed of wireless microwave antennas and electro-optic (EO) modulators [29] [30]. Wireless microwave signals can be received by the antennas. The received signals are transferred to the EO modulators by a connection line such as coaxial cables. However, microwave signal distortion and decay might occur in the connection line for high-frequency operation.

In order to reduce the microwave signal distortion and realize a simple compact device, wireless microwave-lightwave signal conversion by EO modulators using integration of microwave antennas and resonant modulation electrodes have been developed. Several EO modulators using antenna-coupled resonant modulation electrodes were reported [36] [60] [63]. They were composed of planar antennas for wireless microwave signal receiver, resonant electrodes for optical modulation, and their connection lines on an EO crystal as a substrate. The antennas, resonant electrodes, and connection lines should be tuned precisely to obtain good resonance and impedance matching conditions for effective conversion. The microwave distortion might be still induced through the coupling of them.

In this chapter, new invention of EO modulators using a patch antenna embedded with a single narrow gap is presented for wireless microwave-lightwave signal conversion [64] [65]. The proposed devices are composed of an optical waveguide and patch antenna fabricated on an EO crystal such as $LiNbO_3$ or $LiTaO_3$. No other planar structure is fabricated on the substrate except the patch antenna. The patch antenna is designed for operation of the fundamental order mode in the microwave signals,

where the antenna length is set about a half wavelength of the designed microwave signal. A narrow gap in micrometer order is set at the center of the planar patch antenna. A microwave displacement current and electric field is induced across the gap simultaneously for current flow continuity of the standing wave current on the antenna surface. Optical modulation can be obtained by use of the induced electric field through the Pockels effects of the EO crystal substrate. Wireless microwave-lightwave signal conversion can be obtained by utilizing displacement current across the narrow gap.

The proposed EO modulators have simple and compact structures. They can be operated with low microwave loss and no external power supply. Precise tuning is not required in the proposed devices since only patch antenna and no other planar structure on the EO crystal substrate. The proposed devices are easy in design and fabrication. Basically, the proposed devices are used for wireless microwave-lightwave signal conversion and EO modulation by wireless microwave signals.

In the following sections, I will present the basic structure of the new fusion EO modulator using *z*-cut $LiTaO_3$ and *x*-cut $LiNbO_3$ crystals as the substrate. Its operational principles as the hypothesis are also discussed. The device analysis, fabrication, and measurement are presented for verifying the hypothesis of the new device proposal [64] [65]. The proposed device advantages/ disadvantages and applications to wireless microwave-lightwave signal conversion are also discussed.

3.2 *Z*-cut $LiTaO_3$ optical modulators using a patch antenna embedded with a narrow gap

3.2.1 Device structure

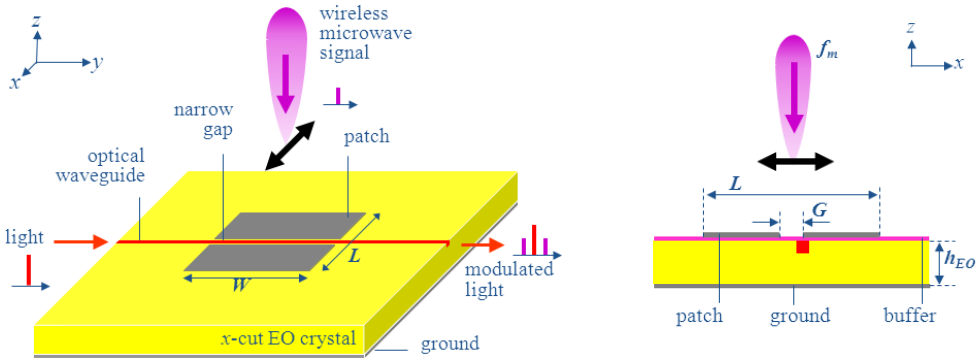

(a) (b)

Figure 3-1 Basic structure of an EO modulator using a patch antenna embedded with a gap, (a) whole and (b) cross-sectional views.

Figure 3-1 shows the basic structure of the proposed EO modulator using a patch antenna embedded with a narrow gap [65]. The proposed device is fabricated on an EO crystal substrate. In this structure a *z*-cut $LiTaO_3$ crystal is used for the substrate. A metal patch is fabricated on the substrate, where the antenna length, *L*, is set a half wavelength, $\Lambda_m/2$, of the designed microwave signal and the antenna width, *W*, is set below one wavelength, Λ_m, of the designed microwave signal to avoid unwanted higher order mode effect. A narrow gap in micrometer order is introduced at the center of the metal patch. A channel optical waveguide is located under the gap for effective optical modulation as shown in Figure 3-1(b). A buffer layer is inserted between the EO crystal and metal patch. The reversed side of the substrate is covered by ground metal.

The characteristics of the standard patch antenna with no gap were discussed in the Chapter 2. When the wireless microwave signal at the designed frequency with linear polarization along the *x*-axis is irradiated to the standard patch antenna with no gap, a resonant standing-wave microwave current is induced on the surface of the metal patch [41]. The direction of the induced standing-wave current on the metal patch surface is parallel to the wireless signal polarization along the *x*-axis and the current magnitude becomes a maximum at the center for the standard patch antenna with no gap [48]. Then, a narrow gap is introduced at the center of the metal patch perpendicular to the standing-wave current direction. In this device structure, a displacement current is induced across the gap due to the requirement of the continuity of the current flow and a strong electric field is also induced across the gap [66]. The induced strong electric field across the gap can be used for optical modulation by use of Pockels effects of an EO crystal. When a lightwave propagates through the optical waveguide located under the gap, the lightwave can be modulated by the induced electric field across gap. Therefore, a wireless microwave signal can be received and converted directly to a lightwave signal through EO modulation by utilizing the displacement current across the narrow gap [64].

3.2.2 Operational principle

3.2.2.1 Standing-wave current

Figure 3-2 shows the cross-sectional view of the standard patch antenna with no gap, where the center of the gap is indicated the origin of the *x*-axis ($x = 0$) and the substrate surface is indicated the origin of the *z*-axis ($z = 0$). When wireless microwave signal is irradiated to the device, a standing-wave microwave surface current in a standard patch antenna can be expressed as [41]

$$K_{pq}(x, y, t) = K_0 \cos(\omega_m t) \cos\left(p\frac{2\pi}{\Lambda_m}x\right) \cos\left(q\frac{2\pi}{\Lambda_m}y\right) \tag{3-1}$$

where p and q are integers indicating modes of the patch antenna, ω_m is the wireless microwave angular frequency and Λ_m is the microwave wavelength. The patch antenna is usually operated in the fundamental mode (p = 1, q = 0). In this case, the standing wave current with a half-wavelength resonances along the x-axis. Therefore, the standing wave surface current can be expressed as

$$K_{10}(x,t) = K_0 \cos(\omega_m t) \cos\left(p\frac{2\pi}{\Lambda_m}x\right) \tag{3-2}$$

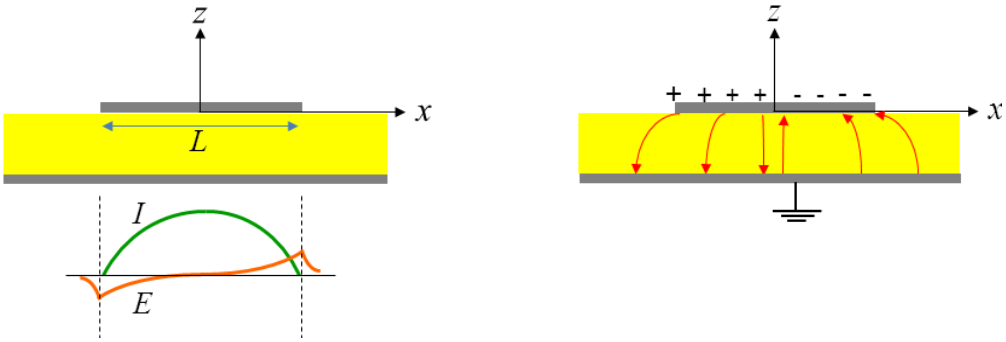

(a) (b)

Figure 3-2 (a) Cross-sectional view and (b) electric field distribution in the standard patch antenna with no gap.

3.2.2.2 Displacement current

Then, a narrow gap is introduced at the center of the patch antenna (x = 0) as shown in Figure 3-3. The narrow gap is perpendicular to the standing-wave current direction. Owing to the requirement of the current flow continuity on the metal patch, a displacement current is induced across the gap [48]. A strong electric field is also induced across the gap [66].

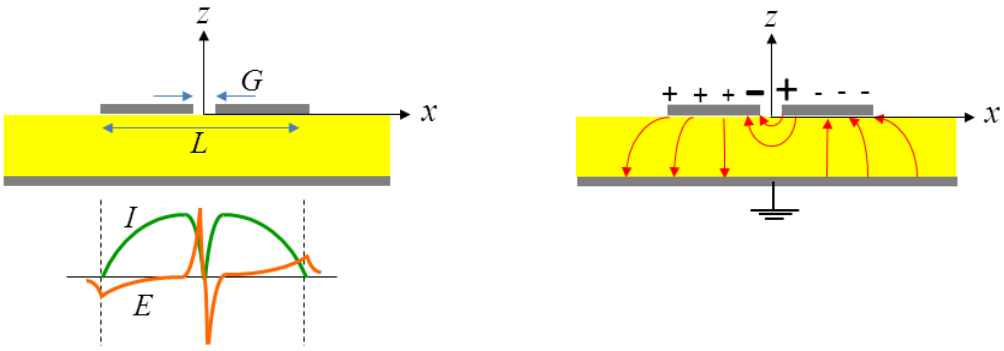

(a) (b)

Figure 3-3 (a) Cross-sectional view and (b) electric field distribution in the patch antenna with a narrow gap.

The displacement current, $\mathbf{J_d}$, in the Maxwell equation (ampere law) can be expressed as

$$\nabla \times \mathbf{H} = \mathbf{J_c} + \mathbf{J_d} \tag{3-3)}$$

$$\mathbf{J_d} = \frac{\partial \mathbf{D}}{\partial t} = \varepsilon \frac{\partial \mathbf{E}}{\partial t} \tag{3-4}$$

where $\mathbf{H}$ is the magnetic field, $\mathbf{J_c}$ is the conduction current density, $\mathbf{D}$ is the electric flux density, ε is the permittivity, and $\mathbf{E}$ is the electric field.

Therefore, the electric field in the scalar value is obtained by time integration of the displacement current. It is expressed as

$$E = \frac{1}{\varepsilon} \int J_d \, dt \tag{3-5}$$

By considering the standing wave surface current in Eq. (3-2), the induced microwave electric field across the gap is obtained by the time integration of the displacement current. Therefore, it can be represented as

$$E_m(t) \propto \int K_{10}(0,t) \, dt = \int K_0 \cos(\omega_m t) \, dt \tag{3-6}$$

$$E_m(t) \propto K_0 \sin(\omega_m t) \tag{3-7}$$

The microwave electric fields across the gap are always induced from one edge to the other edge of the gap. Therefore, the microwave electric fields for the *z*-component under the gap edges have opposite direction between both gap edges.

3.2.2.3 Optical modulation

The induced microwave electric field across the gap can be used for EO modulation. The microwave induced electric field can be observed by a lightwave propagating in an optical waveguide located under the gap. The transit time for the lightwave to pass under the antenna along optical waveguide (y = 0 to y = W) can be considered for accurate calculation [67]. This transit time can be expressed as

$$t = \frac{y - y'}{v_g} \tag{3-8}$$

where y and y' are the position of the lightwave and v_g is the group velocity of the lightwave.

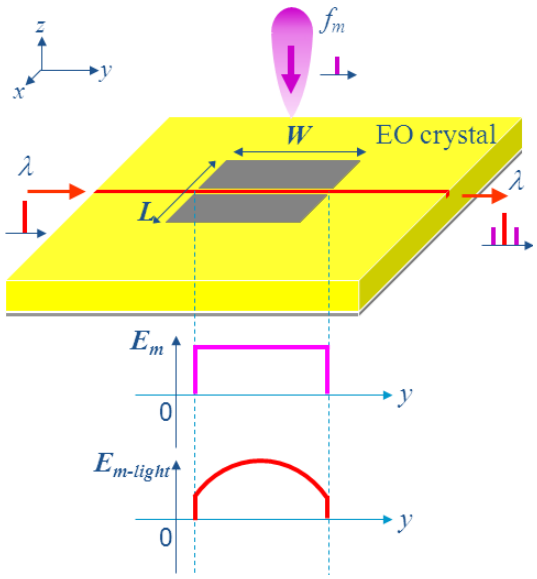

Figure 3-4 Electric field profile along the gap and the microwave electric field observed by lightwave.

Based on the previous discussion, the induced electric field across and along the gap can be shown in the Figure 3-4 and expressed by following equation

$$E_m(t) = E_0 \sin(\omega_m t) \tag{3-9}$$

The induced microwave electric field observed by the lightwave can be calculated by considering the transit time of the lightwave. It can be transformed as

$$\begin{aligned} E_{m-light}(y) &= E_0 \sin\left(\omega_m \frac{y - y'}{v_g}\right) \\ &= E_0 \sin\left(k_m c \frac{y - y'}{v_g}\right) \\ &= E_0 \sin\left[k_m n_g (y - y')\right] \\ &= E_0 \sin\left(k_m n_g y + \zeta\right) \end{aligned} \tag{3-10}$$

$$k_m = \frac{\omega_m}{c} \quad ; \quad c = n_g v_g \quad ; \quad \zeta = -k_m n_g y'$$

where k_m is the wave number of the microwave in the vacuum, n_g is the group index of the lightwave propagating in the waveguide, ζ is an initial phase of the lightwave in the waveguide, and c is the light velocity in the vacuum. The initial phase of the lightwave is important for obtaining the effective modulation.

The output lightwave from the optical waveguide in the proposed device is phase modulated lightwave. The modulation index, $\Delta\phi$, can be determined by taking account of the overlapping field between the induced microwave electric field and the lightwave in the cross section along the gap. It can be calculated by integration of the microwave electric field observed by the lightwave along the antenna width (from $y = 0$ to $y = W$). It can be expressed as [65]

$$\Delta\phi = \frac{\pi r_{33} n_e^3}{\lambda} \Gamma \int_0^W E_0 \sin\left(k_m n_g y + \zeta\right) dy \tag{3-11}$$

where λ is wavelength of the lightwave propagating in the waveguide, r_{33} is the EO coefficient, n_e is the extraordinary refractive index of the EO crystal, and Γ is the overlapping factor between the induced microwave and lightwave electric fields. A wireless microwave signal can be received by the antenna and directly converted to a lightwave signal along the narrow gap through EO modulation [64] [65].

3.2.3 Analysis

3.2.3.1 Equivalent circuit

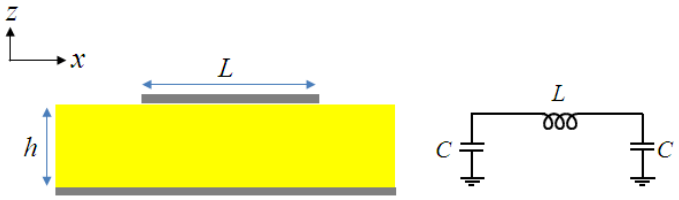

Figure 3-5 Equivalent circuit for the standard patch antenna with no gap.

The characteristics of the standard patch antenna with no gap were reported and discussed in detail [40] [47]. The equivalent circuit of the patch antenna with no gap is shown in Figure 3-5. Its resonant frequency, f_{m0}, can be transformed using simple LC circuit as following equations

$$j2\pi f_{m0}C = -\frac{1}{\frac{1}{j2\pi f_{m0}C} + j2\pi f_{m0}L}$$

$$j2\pi f_{m0}C\left(\frac{1}{j2\pi f_{m0}C} + j2\pi f_{m0}L\right) = -1$$

$$1 - 4\pi^2 f_{m0}^2 LC = -1$$

$$f_{m0} = \frac{1}{2\pi\sqrt{LC/2}} \tag{3-12}$$

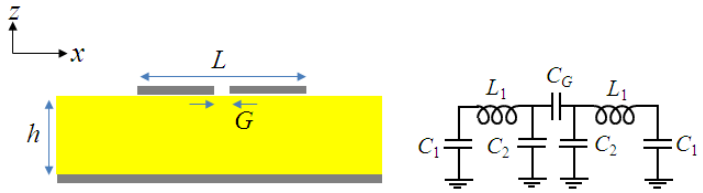

Figure 3-6 Equivalent circuit for the patch antenna embedded with narrow gap.

When a gap is introduced at the center of the metal patch, displacement current and strong electric field are induced due to continuity of the current flow [45]. The equivalent circuits of the gap-embedded patch antenna can be shown as Figure 3-6. The new circuits of C_2 and C_G represent the narrow gap when a gap width, G, is sufficiently small compared to the antenna length, L, and substrate thickness, h. The parasitic capacitances between the edge of the gap and the ground, C_2, can be assumed negligibly small when the gap width, G, is sufficiently small. I assume that the C is equal to C_1 and L is equal to $2L_1$. The resonant frequency of the gap-embedded patch antenna, f_m, can be also transformed using LC circuit as following equations

$$j2\pi f_m C_1 = -\frac{1}{\frac{1}{j2\pi f_m C_1} + \frac{1}{j2\pi f_m C_G} + j2\pi f_m 2L_1}$$

$$j2\pi f_m C_1\left(\frac{1}{j2\pi f_m C_1} + \frac{1}{j2\pi f_m C_G} + j2\pi f_m 2L_1\right) = -1$$

$$1 + \frac{C_1}{C_G} - 8\pi^2 f_m^2 L_1 C_1 = -1$$

$$f_m^2 = \frac{2C_G + C_1}{8\pi^2 L_1 C_1 C_G}$$

$$f_m = \frac{1}{2\pi\sqrt{2L_1\frac{C_1 C_G}{2C_1 + C_G}}}$$

when, we assume that 2 $L_1 = L$ and $C_1 = C$,

$$f_m = \frac{1}{2\pi\sqrt{L\frac{CC_G}{2C + C_G}}} \tag{3-13}$$

Therefore, the resonant frequency of the gap-embedded patch antenna is shifted respected to the resonant frequency of the standard patch antenna with no gap, it can be represented as

$$\Delta f_m = f_m - f_{m0} \tag{3-14}$$

$$\Delta f_m = \frac{1}{2\pi\sqrt{LC/2}}\left(\sqrt{\frac{2C+C_G}{2C_G}} - 1\right) \tag{3-15}$$

where Δf_m is the resonant frequency shift due to the gap. We can see that the resonant frequency shift is inversely proportional to the capacitance of the gap, C_G.

In the patch antenna embedded with a narrow gap, the C_G value contributes mainly to the shifting resonant frequency. The capacitance, C_G, is inversely proportional to the gap width, G. It can be shown as

$$C_G = \varepsilon\frac{A}{G} \tag{3-16}$$

where ε is the permittivity of the substrate, and A is the area of the antenna. I assume that the area of the antenna is not changed and proportional to the antenna length. Therefore, the resonant frequency shift, Δf_m, becomes as

$$\Delta f_m \propto \sqrt{G} \tag{3-17}$$

Based on the equation, the resonant frequency shift becomes higher when the width of the gap becomes wider for the same patch antenna size. Therefore, the gap width contributes slightly to changes the resonant frequency of the patch antenna embedded with a narrow gap. The calculation results of this characteristic are presented in the next sub-section.

3.2.3.2 Resonant frequency

The effective resonant frequency of the patch antenna embedded with a narrow gap was calculated using electromagnetic analysis software, which is High-Frequency Structural Simulator (HFSS) software. The device parameters for microwave analysis are shown in Table 3-1.

Table 3-1 Device parameters for analysis of the patch antenna embedded with a narrow gap.

	Values
Substrate: *z*-cut $LiTaO_3$	
Dielectric constant (ε_x, ε_y, ε_z)	(43,43,41)
Thickness, *h*	0.4 mm
Patch antenna: aluminum	
Antenna size, *L*x*W*	0.8 x 1.3 mm
Gap width, *G*	5 μm

In the calculation results, the resonant frequency of the patch antennas with no gap ($G = 0$) was about 23 GHz under the parameters by observing electric field magnitude under the antenna edge. In order to analyze the proposed device, the observation point for taking the microwave magnitude is located under the edge of the gap as shown in Figure 3-7 (a) since the *z*-cut EO crystal is used.

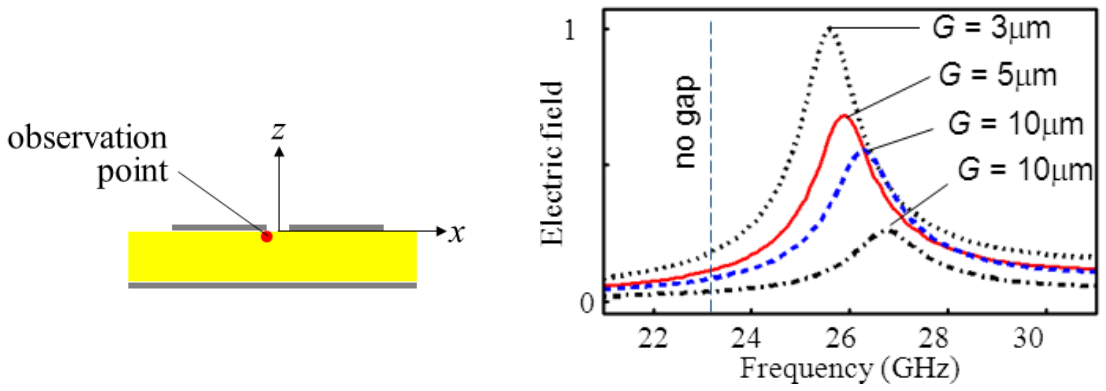

(a) (b)

Figure 3-7 (a) Observation point for calculating the magnitudes of the electric field for the *z*-cut EO crystal (b) Calculated magnitude of electric field across the gap as a function of microwave frequency for several gap width values.

The calculated magnitudes of the electric field of the patch antennas embedded with a narrow gap for several gap width values, *G*, in order micrometer are shown in Figure 3-7 (b). We can see that the gap width contributes to change the effective resonant frequency. The resonant frequencies of the patch antenna embedded with a narrow gap are shifted to be higher than the resonant frequency of the patch antenna with no gap. Based on the calculation results, the equivalent circuits and equations of the patch antenna embedded with a gap as mentioned before were verified because of their same tendency of the resonant frequency shift. Additionally, in the Figure 3-7 (b) shows that the larger electric field can be obtained using narrower gap. This characteristic can be expressed by

$$E = \frac{V}{G} \tag{3-18}$$

where *E* is the electric field in unit of Volt/meter and *V* is the electric voltage in unit of Volt. Therefore, the electric field is inversely proportional to the gap width. It was verified also in the calculation results.

3.2.3.3 Radiation pattern

In here, the radiation pattern of the patch antenna is reported. The calculated radiation pattern for the standard patch antenna with no gap is shown in Figure 3-8(a). The radiation pattern of the patch antenna embedded with a narrow gap was also analyzed, where width of the narrow gap is much smaller than the antenna length in micrometer order. The calculated radiation pattern for the patch antenna embedded with a narrow gap is shown in Figure 3-8(b).

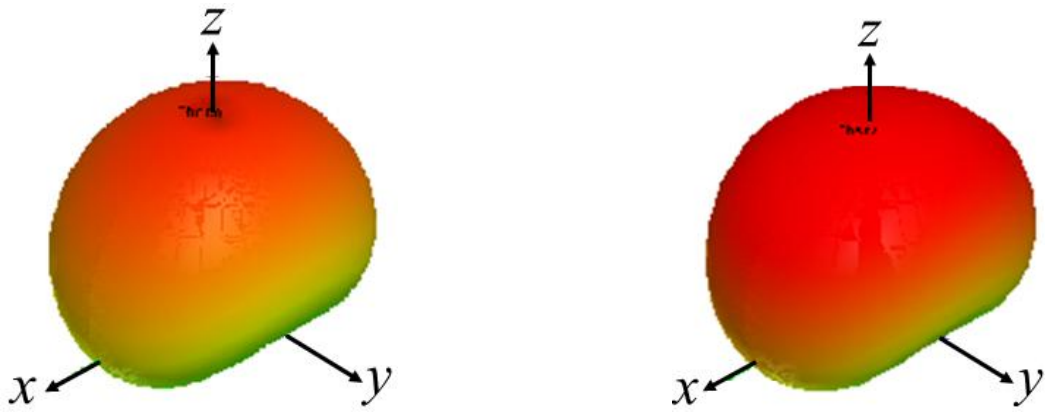

(a) (b)

Figure 3-8 Radiation pattern for (a) the standard patch antenna and (b) the patch antenna embedded with a narrow gap.

We can see that the radiation pattern of the patch antenna embedded with a narrow gap has the same as the radiation pattern of the standard patch antenna with no gap. Based on that, the antenna characteristics of the patch antenna embedded with a narrow gap are similar to the characteristics of the standard patch antenna.

3.2.3.4 Microwave electric field distribution

The microwave characteristics of the patch antennas embedded with a narrow gap were calculated. The calculated electric field distributions on the substrate surface are shown in Figure 3-9 under the irradiation of the wireless microwave signal. In Figure 3-9(a) shows the calculated electric field distribution on the substrate surface by irradiating wireless microwave signal with *x*-polarization (perpendicular to the gap) from the free space above the device. We can see that a strong electric field is induced across the gap. The electric field distribution in the *z*-component for the irradiation of the microwave with the *y*-polarization (parallel to the gap) is also calculated, as shown in Figure 3-9(b). We can see that almost no electric field is induced across the gap.

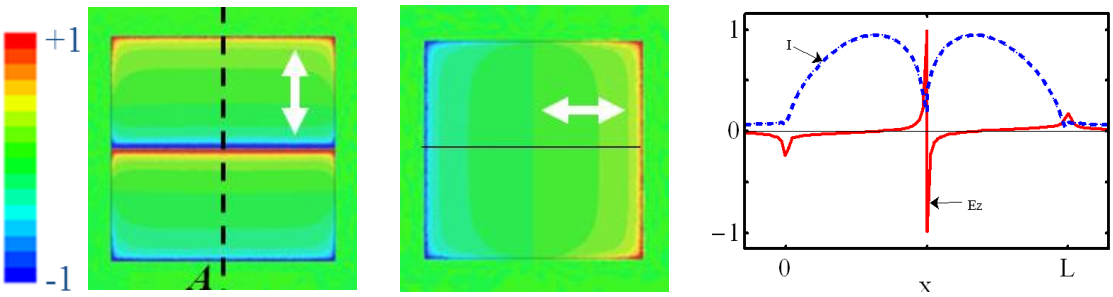

(a) (b) (c)

Figure 3-9 Electric field distribution on the substrate surface for wireless microwave signal with linier polarization in (a) *x*-direction and (b) *y*-direction. (c) Current profile and electric field profile along line *A*.

Additionally, Figure 3-9(c) shows the calculated current profile and electric field profile on the surface along the line-*A*. We can see that, the electric field across the gap is stronger than electric field at the antenna edges since the gap width is much smaller than the substrate thickness. As a result, the electric field across the gap is effective for optical modulation through the Pockels effects.

3.2.4 Fabrication

In order to verify the operations of the new fusion EO modulator, the device fabrication was done using mature fabrication technology. The device fabrication with several processes is explained

clearly such as for fabricating optical waveguide, buffer layer, metal patch, and ground metal. The device parameters for the fabrication are shown in Table 3-2.

Table 3-2 Device parameters for fabrication of the EO modulator using patch antenna embedded with a narrow gap.

	Values
Substrate: *z*-cut $LiTaO_3$	
Dielectric constant (ε_x, ε_y, ε_z)	(43,43,41)
Thickness, h	0.4 mm
Patch antenna: aluminum	
Frequency, f_m	26 GHz
Size, LxW	0.8 x 1.3 mm
Gap width, G	5 μm
Array structure	
Element number, N	4
Distance, D	5.4 mm
Buffer layer: SiO_2	
Thickness	0.2 μm
Optical waveguide	
Single mode	
Wavelength, λ	1.55 μm

3.2.4.1 Optical waveguide

First, a channel optical waveguide was fabricated on a *z*-cut $LiTaO_3$ crystal using an annealed proton exchange method, which is illustrated in Figure 3-10. The top surface of the EO crystal was covered using 3000 Å-thick aluminum by use of a thermal vapor deposition machine. Then, the deposited aluminum was covered with photoresist by use of spin-coating machine. After that, the sample was illuminated by ultraviolet light with a mask pattern for the optical waveguide and continued development process. In order to make the pattern, the aluminum with no photoresist was etched by using acid liquid and then the sample was cleaned by removing the remained photoresist. Next, a proton exchange process using benzoic acid at 240 ^{O}C in 12 hours was done. After finishing the proton exchange process, the aluminum was etched completely. As a result, the optical waveguide was fabricated successfully. The proposed device will be annealed with 350 ^{O}C in 1 hour after all device fabrication process for the final step.

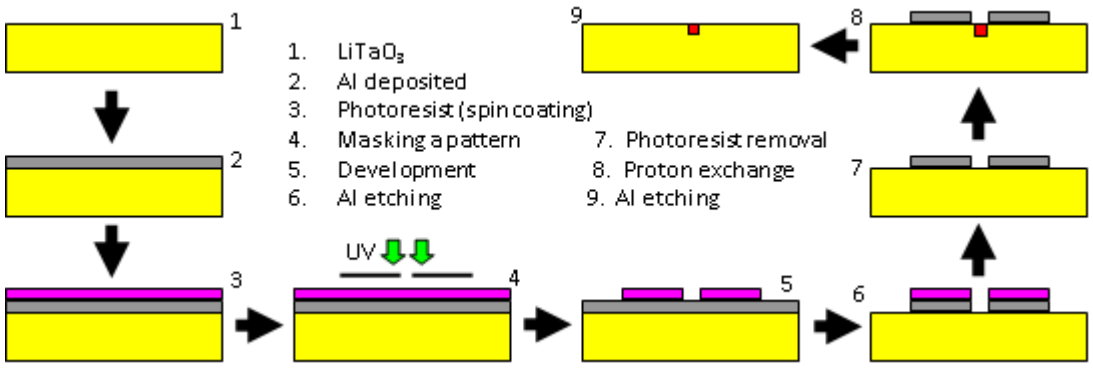

Figure 3-10 Fabrication steps for optical waveguide using annealed proton exchange methods.

3.2.4.2 Buffer layer

After optical waveguide fabrication, a buffer layer is fabricated on the surface of the *z*-cut $LiTaO_3$ crystal. A 200 nm-thick silicon dioxide (SiO_2) was deposited by use of sputtering machine. A buffer layer is necessary for optical integrated circuit where metal electrodes are used and located on waveguides. Therefore, the waveguide performance especially for TM mode operation can be improved significantly due to its propagation loss characteristics.

3.2.4.3 Patch antenna embedded with a narrow gap

A metal patch embedded with a narrow gap on the buffer layer is fabricated. The fabrication processes are illustrated in Figure 3-11. The metal patch embedded with a narrow gap was fabricated with a 1 μm-thick aluminum by use of thermal vapor deposition, a standard photolithography, and a wet etching. Since the *z*-cut $LiTaO_3$ crystal is used, the optical waveguide should be located under one edge of the narrow gap for obtain effective optical modulation.

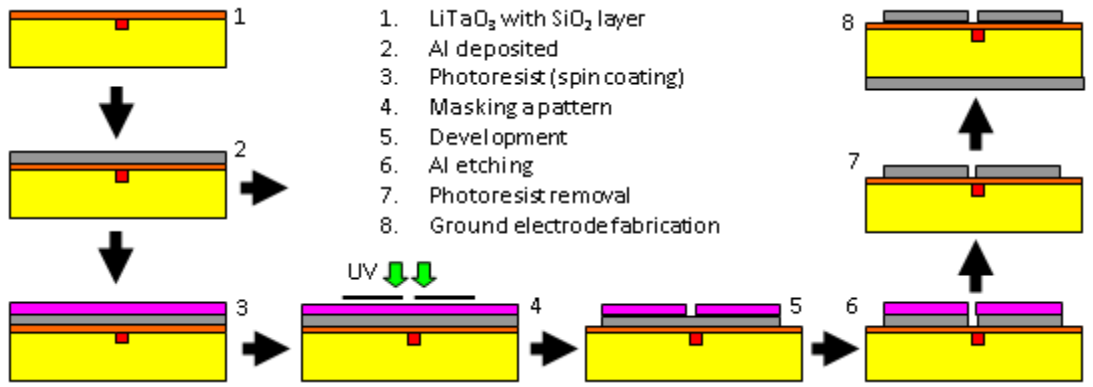

Figure 3-11 Fabrication steps for metal patch using an aluminum.

Then, a ground metal was fabricated on the bottom surface of the substrate. The ground metal was deposited with a 1 μm-thick aluminum by use of thermal vapor deposition. The photograph of the fabricated device before ground metal fabrication is shown in Figure 3-12.

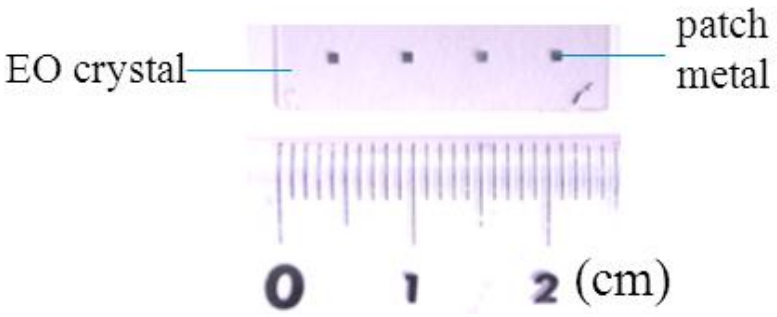

Figure 3-12 Photograph of the fabricated device.

3.2.5 Measurement

In order to verify the operation of the proposed device for wireless microwave-lightwave signal conversion, the fabricated device is measured experimentally. In here, the device measurement is presented for verifying the device operation.

3.2.5.1 Experimental setup

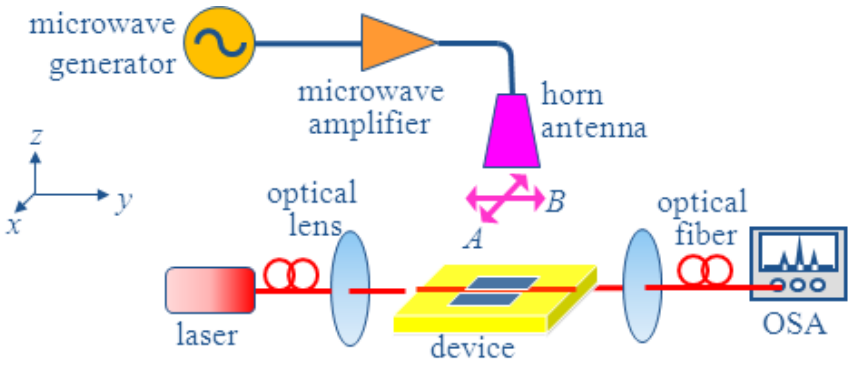

Figure 3-13 Experimental setup for measuring basic operation and performance of the fabricated devices.

The measurement setup for verifying the device operation is shown Figure 3-13. A microwave signal of 26 GHz was generated using a microwave signal generator. Then, the generated microwave signal was amplified using a microwave amplifier. After that, the amplified microwave signal was irradiated to the fabricated device using a horn antenna. The wireless microwave signal with linear polarization was irradiated with +23 dBm radiated power and 100 mm separation between the horn

antenna and fabricated device. A lightwave of 1.55 μm wavelength from a distributed feed-back (DFB) laser was coupled to the fabricated device using an objective lens. The output lightwave signal from the fabricated device was observed using an optical spectrum analyzer (OSA).

3.2.5.2 Measurement results

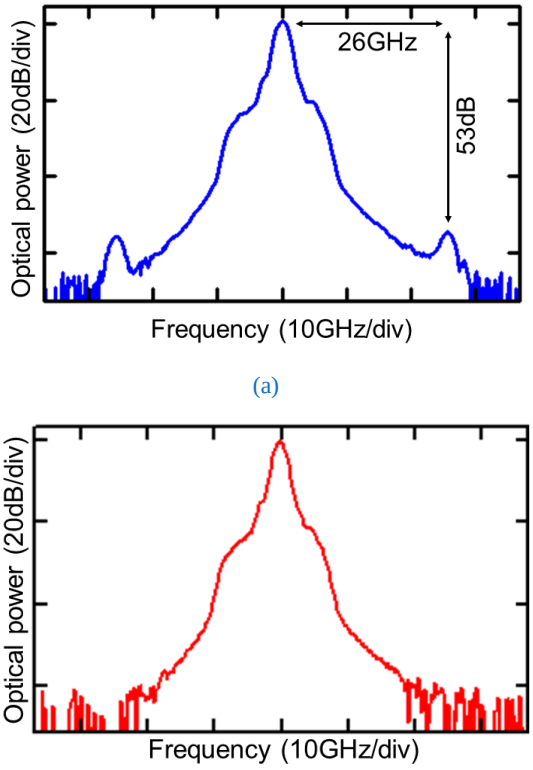

Figure 3-14 Example of the output lighwave with irradiation of wireless microwave signal for (a) *A*-polarization and (b) *B*-polarization.

The measured optical spectra of the lightwave output are shown in Figure 3-14. The Figure 3-14 (a) shows the measured optical spectrum, when the wireless microwave signal with *A*-linear polarization is irradiated to the fabricated device. We can see that, clear optical sidebands were observed since the strong microwave electric field is induced across the gap. The Figure 3-14 (b) shows the measured light spectrum, when the wireless microwave signal with *B*-linear polarization. No optical sideband was observed due to no microwave electric field is induced across the gap. As a result, optical modulation is obtained effectively when the wireless microwave signal with linear polarization perpendicular to the narrow gap.

3.3 *X*-cut $LiNbO_3$ optical modulators using a patch antenna embedded with a narrow gap

In this chapter, two fusion EO modulators are discussed based on *z*-cut $LiTaO_3$ and *x*-cut $LiNbO_3$ crystal substrates. A *z*-cut $LiTaO_3$ optical modulator using a patch antenna embedded with a narrow gap was discussed in the previous section [64] [68]. The basic operations of the new fusion device were verified experimentally. In order to verify in further the proposed device, the new fusion EO modulator fabricated on an *x*-cut $LiNbO_3$ crystal are also presented.

In this section, an *x*-cut Ti:$LiNbO_3$ optical modulator using a patch antenna embedded with a narrow gap is proposed for wireless microwave-lightwave signal conversion in the ROF systems [69] [70]. An *x*-cut $LiNbO_3$ crystal has relatively lower dielectric constant than a *z*-cut $LiTaO_3$ crystal. Since the optical waveguide is located at the center of the gap for *x*-cut $LiNbO_3$ device, a buffer layer is not required because the transverse electric (TE) mode of lightwave has small influence of metal. I expect that large modulation index are obtained since the antenna size becomes larger due to lower dielectric constant of the substrate and no buffer utilization.

3.3.1 Device structure

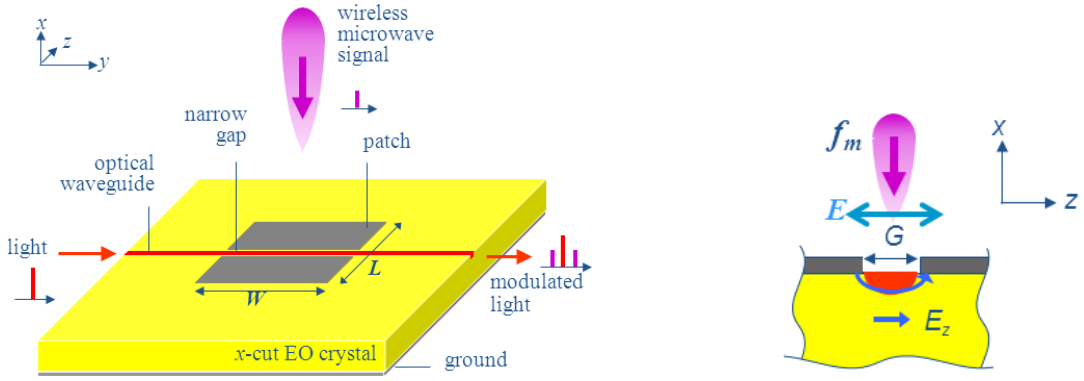

Figure 3-15 Device structure of the *x*-cut $LiNbO_3$, (a) whole and (b) cross-sectional views.

Figure 3-15 shows the structure of the proposed *x*-cut $LiNbO_3$ optical modulator using a patch antenna embedded with a narrow gap. It consists of a channel optical waveguide and a patch antenna embedded with a narrow gap onto an *x*-cut $LiNbO_3$ as a substrate. The length, *L*, of each antenna along the *x*-axis is set as half a wavelength of the wireless microwave signal. The width, *W*, of each antenna along the *y*-axis is set as below a one wavelength of the wireless microwave signal to avoid unwanted higher-order mode effects. The narrow gap in micrometer-order is set at the center of each antenna, along the *y*-axis. The optical waveguide is located at the center of the gap, where the magnified cross-

sectional view is shown in Figure 3-15(b). The reverse side of the substrate is covered with a ground metal.

3.3.2 Operational principle

The operational principle of the EO modulator using patch antennas embedded with a narrow gap has been discussed [64] [65]. The strong electric field induced across the gap can be used for optical modulation through Pockels effect. By considering the dielectric constant values of the EO crystal substrate, where the dielectric constant of the *x*-cut $LiNbO_3$ is $\varepsilon_x = 43$, $\varepsilon_y = 43$, $\varepsilon_z = 28$ and the dielectric constant of the *z*-cut $LiTaO_3$ is $\varepsilon_x = 43$, $\varepsilon_y = 43$, $\varepsilon_z = 41$, the *x*-cut $LiNbO_3$ crystal has relatively low dielectric constant compared with the *z*-cut $LiTaO_3$ crystal [71]. Therefore, I expect that a large antenna size and long interaction length on an *x*-cut $LiNbO_3$ crystal substrate are obtained at the same operational frequency compared to the device using the *z*-cut $LiTaO_3$ crystal substrate

The length of the antenna is inversely proportional to the effective dielectric constant of the substrate, ε_{eff}, which can be expressed as Eq. (2-1). Additionally, a buffer layer is not required for the *x*-cut $LiNbO_3$ devices. Therefore, modulation efficiency improvement can be achieved due to the larger size of the patch metal.

3.3.3 Analysis

3.3.3.1 Peak frequency operation

The microwave characteristics of the patch antenna embedded with a narrow gap on the for several substrate types, which are *x*-cut/ *z*-cut $LiNbO_3$/ $LiTaO_3$ crystals, were analyzed. The device parameters for the analysis are shown in Table 3-3. In this analysis, a rectangular patch type was used for extending the interaction length between microwave and lightwave electric fields, where the patch width is below one wavelength to avoid unwanted higher order mode effects. As a result, larger modulation index can be obtained than the device using square patch type.

The calculated microwave electric field magnitudes across the gap as function of the microwave frequency are shown in Figure 3-16 for several types of EO crystals, which are *x*-cut / *z*-cut $LiNbO_3$/ $LiTaO_3$, for the same size of the patch antenna embedded with a narrow gap. We can see that the patch antenna embedded with a narrow gap fabricated on the *x*-cut $LiNbO_3$ crystal substrate has the highest peak frequency than other devices. The patch antenna embedded with a narrow gap fabricated on the *z*-cut $LiTaO_3$ crystal substrate is lower peak frequency operation than the device fabricated on the *x*-cut $LiNbO_3$ crystal substrate. The shifting microwave frequency operation might be caused by the dielectric constants differences of the EO crystal substrates and utilization buffer layer.

Table 3-3 Device parameters for microwave analysis of *x*-cut Ti:$LiNbO_3$ optical modulators using patch antennas embedded with a narrow gap.

	Values
Substrate: *x*-cut/ *z*-cut $LiNbO_3$/ $LiTaO_3$	
Dielectric constant	
$LiNbO_3$ (ε_x, ε_y, ε_z)	(43, 43, 28)
$LiTaO_3$ (ε_x, ε_y, ε_z)	(43, 43, 41)
Thickness, *h*	0.5 mm
Operational frequency, f_m	26 GHz
Patch antenna: aluminum	
Size, *LxW*	0.7 x 1.3 mm
Gap width, *G*	5 μm
Buffer layer: SiO_2	
for *z*-cut $LiNbO_3$/ $LiTaO_3$	
Thickness	0.2 μm

Based on the calculation results, the *x*-cut $LiNbO_3$ optical modulators have strong microwave electric field across the gap than other devices at the effective microwave operation. The *x*-cut $LiNbO_3$ optical modulators have about two-times stronger microwave electric field across the gap compared to the *z*-cut $LiTaO_3$ optical modulators. The stronger electric field is induced due to the larger antenna aperture on lower dielectric constant of the EO substrate and no buffer layer utilization.

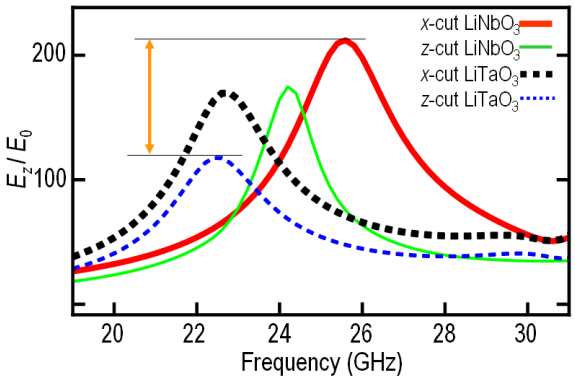

Figure 3-16 Calculated microwave electric field magnitudes across the gap as function of the microwave frequency for several types of the EO crystal (*x*-cut/ *z*-cut $LiNbO_3$/ $LiTaO_3$).

3.3.3.2 *Microwave electric field profile*

By considering orientation of the EO crystal for driving the strong Pockels effects, I analyzed in detail the EO modulators with *x*-cut $LiNbO_3$ and *z*-cut $LiTaO_3$ substrates. The device configurations are shown in Figure 3-17. The optical waveguide is located at the center of the gap for the *x*-cut $LiNbO_3$ optical modulators and located under the edge of the gap for the *z*-cut $LiTaO_3$ optical modulators.

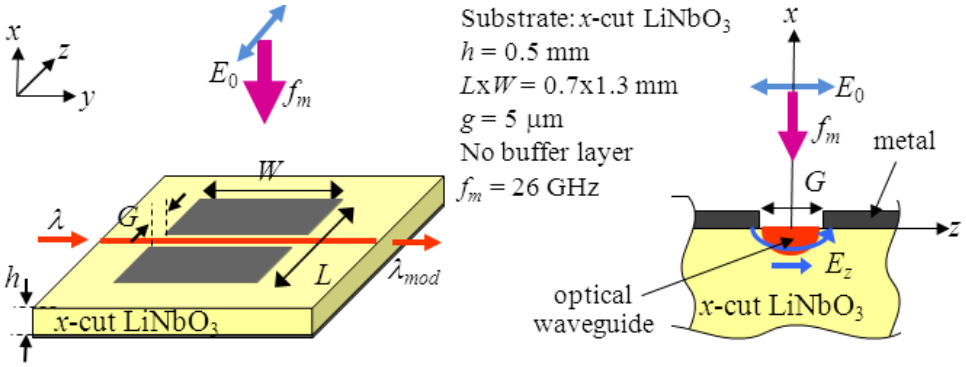

(a)

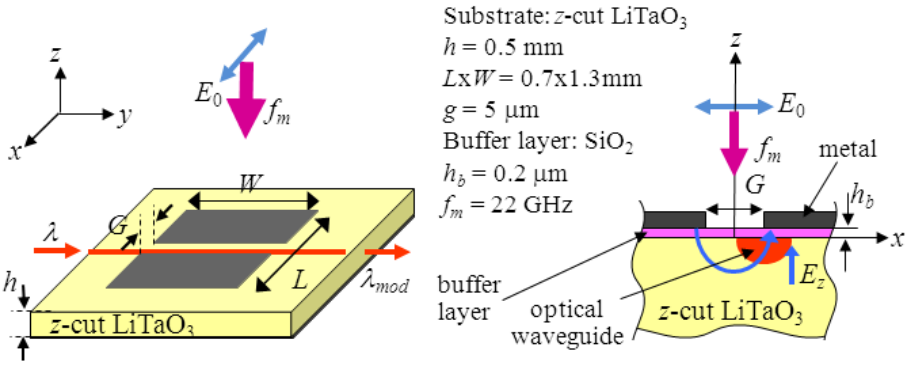

(b)

Figure 3-17 Configuration of EO modulators using (a) *x*-cut $LiNbO_3$ and (b) *z*-cut $LiTaO_3$ substrates.

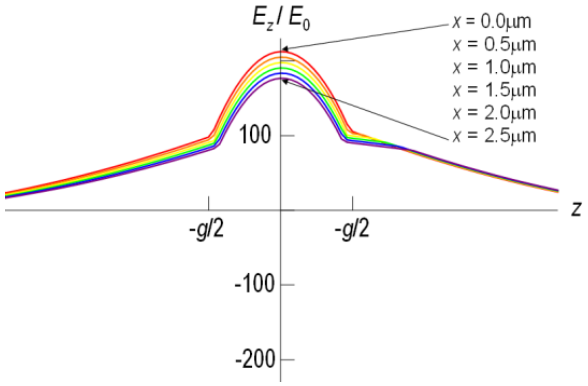

(a)

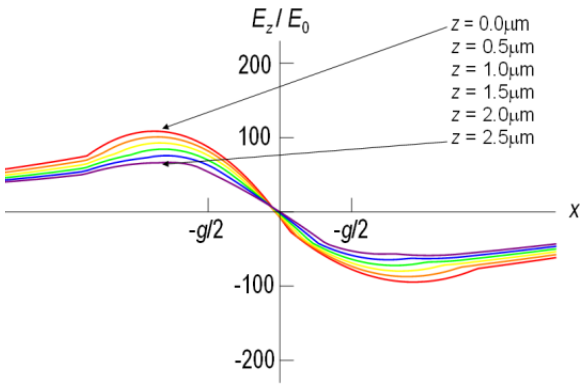

(b)

Figure 3-18 Calculated microwave electric field profiles for (a) *x*-cut $LiNbO_3$ and (b) *z*-cut $LiTaO_3$ optical modulators with several observation point.

3.3.3.3 Modulation index

The modulation index of the EO modulators is proportional to the microwave electric field magnitude across the gap. By considering the calculated microwave electric fields as shown in Figure 3-18, improved modulation index about two-times can be achieved by using the *x*-cut $LiNbO_3$ optical modulators compared with the *z*-cut $LiTaO_3$ optical modulators, when the overlapping factor between the electric fields of the microwave and lightwave is almost same in both devices.

The proposed device is an optical phase modulator. The modulation index, $\Delta\phi$, of the proposed device can be calculated using Eq. (3-11). In the experiment, the modulation index can be calculated by comparing power ratio of carrier, P_c, to sidebands, P_s, since the modulation index is relatively small ($\Delta\phi \ll 1$). The signal level with modulation $J_1(\Delta\phi)$ and no modulation $J_0(\Delta\phi)$ are considered. It can be expressed as following equations

$$E_c = E_0 J_0(\Delta\phi)$$
$$E_s = E_0 J_1(\Delta\phi)$$
$$\frac{P_c}{P_s} = \frac{E_c^2}{E_s^2}$$
$$\frac{P_c}{P_s} = \frac{J_0^2(\Delta\phi)}{J_1^2(\Delta\phi)} \quad (3\text{-}19)$$

It can be simplified for low modulation index as following equation

$$\frac{P_c}{P_s} \sim \frac{\Delta\phi^2}{4} \quad (3\text{-}20)$$

3.3.4 Fabrication

The designed *x*-cut $LiNbO_3$ optical modulators with parameters as shown in Table 3-4 were fabricated. First, a single-mode straight optical channel waveguide for the wavelength of 1.55 μm was fabricated by using the titanium-diffused method. A patch antenna embedded with a narrow gap was fabricated with a 1 μm-thick aluminum film on the substrate by use of thermal vapor deposition, a standard photolithography, and a lift-off technique. Finally, the reverse side of the device was covered with a 1 μm-thick aluminum film as a ground electrode. The photographs of the fabricated prototype device are shown in Figure 3-19.

Table 3-4 Device parameters for fabrication of the *x*-cut Ti:$LiNbO_3$ optical modulators using patch antennas embedded with a narrow gap.

	Values
Substrate: *x*-cut $LiNbO_3$	
Dielectric constant	
x-cut $LiNbO_3$ (ε_x, ε_z, ε_z)	(43, 43, 28)
Thickness, h	0.5 mm
Frequency, f_m	26 GHz
Patch antenna: aluminum	
Size, LxW	0.7 x 1.3 mm
Gap width, G	5 μm
Optical waveguide: titanium diffusion	
Wavelength, λ	1.55 μm

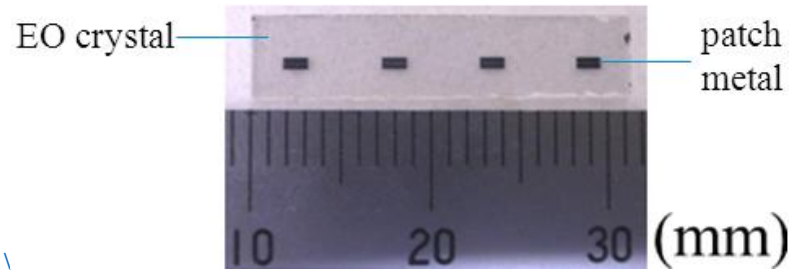

Figure 3-19 Photograph of the fabricated *x*-cut Ti:$LiNbO_3$ optical modulators using patch antennas embedded with a narrow gap.

3.3.5 Measurement

The experimental setup for measuring performances of the fabricated device is shown in Figure 3-20. A 26 GHz microwave signal from a microwave signal generator was amplified using microwave

amplifier and then irradiated to the fabricated device using a horn antenna. A 1.55 μm wavelength lightwave from a laser was passed through a lightwave polarizer for setting light polarization in TM or TE modes. Then, the polarized lightwave is coupled to the optical waveguide in the fabricated device by use of an objective lens. The output light spectrum was measured and monitored using an OSA.

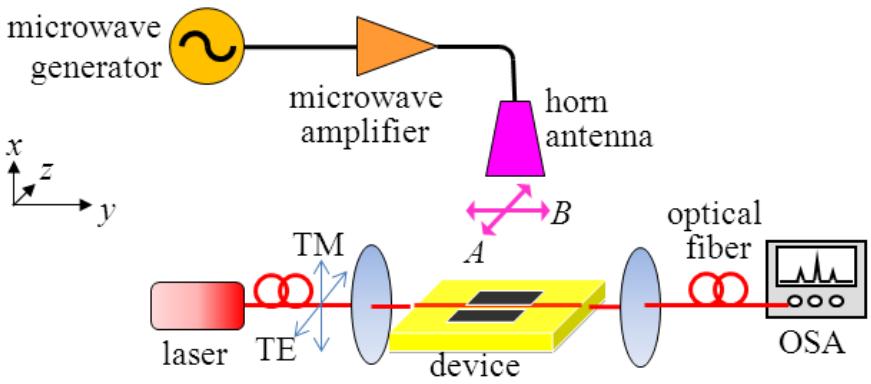

Figure 3-20 Measurement setup for measuring performance of the *x*-cut Ti:$LiNbO_3$ optical modulators using patch antennas embedded with a narrow gap.

The examples of the output light spectra measured by an OSA are shown in Figure 3-21, where the wireless microwave signal with frequency of 26 GHz was irradiated to the fabricated device. Figure 3-21(a) and Figure 3-21(b) show the measured output light spectra for the transverse electric (TE) and transverse magnetic (TM) modes of the lightwave signal, respectively, when a linear-polarized wireless microwave signal with the *A*-polarization was irradiated. We can see that the optical modulation is obtained effectively for TE-mode of the lightwave signal as shown in Figure 3-21(a) due to the larger EO coefficient in the *z*-direction of the *x*-cut $LiNbO_3$ crystal. Optical modulation was obtained with TM-mode of the lightwave as shown in Figure 3-21(b) by using EO effect in the *x*-direction of the *x*-cut $LiNbO_3$ crystal. Figure 3-21(c) shows the output light spectrum when the polarization of the wireless microwave signal polarization was rotated to 90-degrees, which corresponds to the *B*-polarization. In the Figure 3-21(c), small optical sidebands are occurred. It might be caused by reflected microwave signals from the measurement tools.

The measured modulation efficiency as a function of the microwave frequency is shown by the dotted-curve in Figure 3-22, when the microwave polarization was set to the *A*-polarization and lightwave was set to TE-mode. The fabricated device was an optical phase modulator, the modulation index can be calculated from the spectrum intensity ratio between the first sideband and the optical carrier as long as the modulation index value is rather smaller than unity. The peak frequency for effective optical modulation for wireless microwave-lightwave signal conversion was about 25.7 GHz, which almost coincides with the calculation of the microwave frequency dependence as shown by solid-curve in Figure 3-22. The calculated result is obtained by taking the electric field magnitude

across the gap as a function of the microwave frequency from the simulation result using electromagnetic analysis software, HFSS.

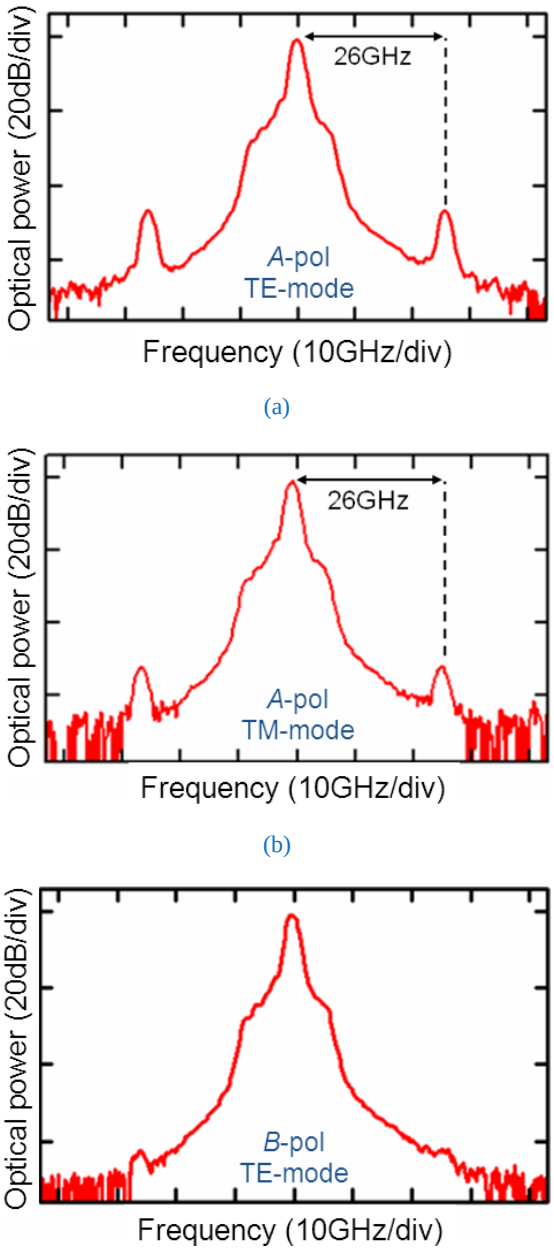

Figure 3-21 Measured light output spectra for: (a) TE mode lightwave and *A*-polarization microwave, (b) TM mode lightwave and *A*-polarization microwave, and (c) TE mode lightwave and *B*-polarization microwave

Figure 3-23 shows the measured modulation efficiency, which is the spectrum intensity ratio between the first sideband and the optical carrier, as a function of the separation between the transmitted antenna (horn antenna) and the fabricated device. The calculation result is obtained by

considering the Friis transmission equation, when the received power of the proposed device is inversely proportional to the separation [72].

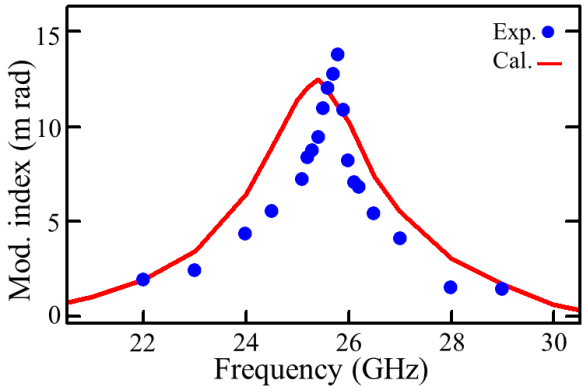

Figure 3-22 Measured modulation index as a function of microwave frequency for the fabricated *x*-cut Ti:$LiNbO_3$ optical modulator using patch antennas embedded with a narrow gap.

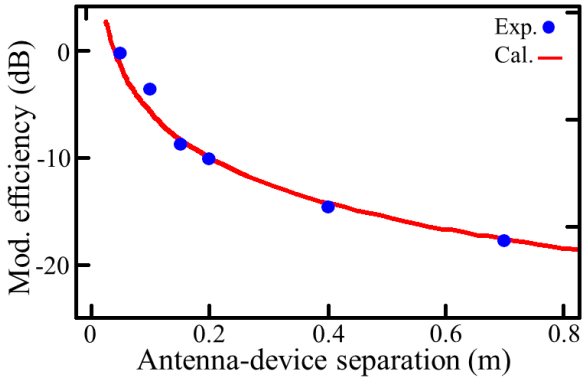

Figure 3-23 Measured modulation efficiency as a function of the separation between the transmitting antenna (horn antenna) and the fabricated *x*-cut Ti:$LiNbO_3$ optical modulator using patch antennas embedded with a narrow gap.

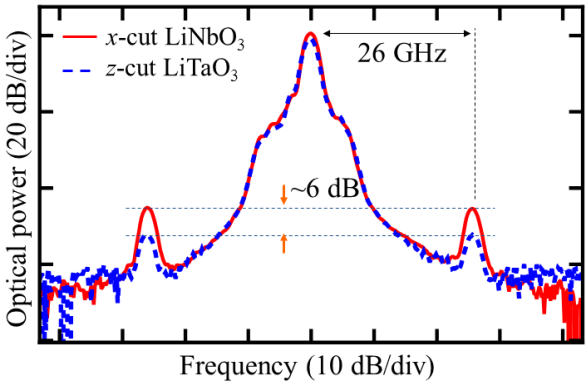

Figure 3-24 Measured optical spectra of the *x*-cut Ti:$LiNbO_3$ optical modulators (solid-line) and the *z*-cut $LiTaO_3$ optical modulators (dashed-line).

The proposed *x*-cut Ti:$LiNbO_3$ optical modulators using a patch antenna embedded with a narrow gap were measured. Operations of the new fusion EO modulator were also verified using *x*-cut $LiNbO_3$ crystal substrate. Furthermore, the measured optical spectra of the modulated lightwave signal using the fabricated *x*-cut $LiNbO_3$ and *z*-cut $LiTaO_3$ optical modulators are shown in Figure 3-24. We can see that, the *x*-cut $LiNbO_3$-based device has modulation efficiency 6 dB larger than the *z*-cut $LiTaO_3$-based device.

Additionally, the insertion loss of the *x*-cut Ti:$LiNbO_3$ optical modulator was measured approximately 11 dB by use of objective lenses as the lightwave coupling. It can be reduced by using optical fibers as the lightwave coupling. The insertion loss is not directly affected to the modulation index of the device since the modulation index expresses by the spectrum intensity ratio between the first sideband and the optical carrier. However, low insertion loss is an important issue to realize low power consumption of the optical modulators in the ROF technology.

3.4 Discussion and summary

In this chapter, new fusion EO modulators using a patch antenna embedded with a narrow gap were proposed for wireless microwave-lightwave signal conversion and optical modulation by radiating wireless microwave signal. The displacement current and electric field across the narrow gap are induced due to the current flow continuity. The electric field across the gap has stronger magnitude than the electric field at the edge of the antenna since the gap width is much smaller than the substrate thickness. It can be used effectively for optical modulation through Pockels effects.

Stronger microwave electric field across the gap can be induced using narrower gap width. However, it has a limitation since optical waveguide is used lightwave trajectory. The optical waveguide is located under the gap depending on the EO crystal orientation by considering the strongest EO coefficient. In order to obtain effective modulation, the gap width of the proposed devices should be over to the width of the optical waveguide core. When the gap width is smaller than the optical waveguide core width, degradation of the optical modulation might be occurred.

The device analysis and fabrication for a 26 GHz microwave signal were done. In order to verify the basic operation of the new fusion EO modulators, two EO modulators using a patch antenna embedded with a narrow gap were fabricated on a *z*-cut $LiTaO_3$ and *x*-cut $LiNbO_3$ crystals. In measurement, the basic operations of the proposed devices were experimentally verified by observing the optical spectra of the light output from the optical waveguide. Clear optical sidebands were observed. Therefore, the proposed device can be used for direct wireless microwave-lightwave signal conversion. Additionally, the *x*-cut $LiNbO_3$-based device has larger modulation efficiency of 6 dB than the *z*-cut $LiTaO_3$-based device since the $LiNbO_3$-based device has lower dielectric constant, larger patch size, and larger EO coefficient.

The new invention of the fusion EO modulators using a patch antennas embedded with a narrow gap was verified. They have simple compact structure and can be operated with low microwave loss and no external power supply. Furthermore, design and fabrication of the proposed devices are easy. The microwave frequency can be designed easily by changing the antenna length.

The proposed device is operated effectively for certain microwave polarization, single modulated lightwave signal, and relatively low modulation index. Techniques to improve performance and enhance functionality of the fusion device are still required for attractive applications. The techniques will be discussed also in this dissertation.

Chapter 4 Electro-Optic Modulators Using a Patch Antenna Embedded with Double Narrow Gaps

4.1 Introduction

In the Chapter 3, I have proposed new fusion EO modulators using a patch antenna embedded with a narrow gap [64] [69]. Their basic operations for direct wireless microwave-lightwave signal conversion were verified experimentally. The new fusion proposed devices are composed of a single optical waveguide under a single narrow gap. Therefore, a modulated lightwave signal can be obtained using the new fusion devices.

In this chapter, in order to enhance functionality of the new fusion EO modulator, I propose EO modulators using a patch antenna embedded with double narrow gaps. The proposed devices are basically for wireless microwave-lightwave signal conversion. By modifying the new device structure, the device functionality can be enhanced. Firstly, an EO modulator using a patch antenna embedded parallel narrow gaps is proposed. This proposed device can be used for realizing optical intensity modulation using the Mach-Zehnder interferometer. Secondly, an EO modulator using a patch antenna embedded with orthogonal narrow gaps is proposed. This proposed device can be used for receiving wireless microwave signal with orthogonal linear polarization and for identifying microwave polarization and for 1D/ 2D wireless irradiation angle (beamforming) control.

In the following sections, I will present the structure of the modified fusion EO modulators using a patch antenna embedded with double narrow gaps. The device analysis, fabrication, and measurement are presented for enhancing device functionality [68] [73]. The proposed device advantages/ disadvantages and applications for functionality enhancement are also discussed.

4.2 EO modulators using a patch antenna embedded with parallel gaps

4.2.1 Device structure

Figure 4-5 shows the structure of an EO modulator using a patch antenna embedded with two parallel gaps. It is composed of two parallel optical waveguides and a square patch embedded with two parallel gaps fabricated on an EO crystal. The two parallel gaps with a few tens micrometer distance are located at the center of the metal patch. The two parallel optical waveguides are located under the parallel gaps. The length of the metal patch is set at half a wavelength for the designed microwave wireless signal. The width of the metal patch is set below a wavelength of the designed

microwave wireless signal. The width of the gaps is set in micrometer order. A buffer layer can be inserted between the substrate and the patch antenna. The reverse side of the substrate is covered with a ground electrode.

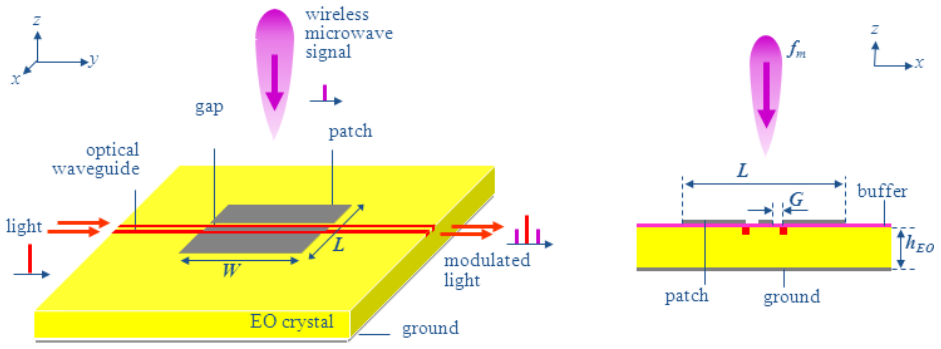

Figure 4-1 Device structure of an EO modulator using a patch antenna embedded with parallel narrow gaps.

In the Chapter 3, the basic operational principle of the fusion EO modulators using a patch antenna embedded with a narrow gap was discussed [64] [69]. Displacement current and electric field across the gap are used for optical modulation through the Pockels effects [22] [54]. When wireless microwave signal is irradiated to the proposed device, the displacement current and electric field are also induced across the parallel gaps. The strong induced electric field across the gaps can be used for optical modulation through the Pockels effects. Therefore, two modulated lightwave signals can be obtained using this proposed device. Furthermore, the Mach-Zehnder optical interferometer can be obtained using the two modulated lightwave signals from the proposed device.

4.2.2 Analysis

Table 4-1 Device parameters for microwave analysis of the EO modulators using a patch antenna embedded with parallel narrow gap.

	Values
Substrate: *z*-cut $LiTaO_3$	
Thickness, *h*	0.5 mm
Operational frequency, f_m	26 GHz
Patch antenna: aluminum	
Size, *LxW*	0.8 x 0.8 mm
Gap width, *G*	5 μm
Buffer layer: SiO_2	
Thickness	0.2 μm

The microwave characteristics of the proposed device were analyzed for two parallel gaps at the center of the patch antenna. The device parameters for the microwave analysis are shown in Table 4-1.

4.2.2.1 Electric field distribution

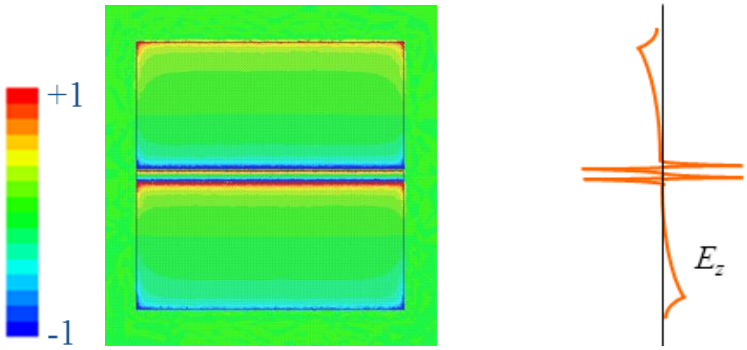

(a) (b)

Figure 4-2 (a) Electric field distribution and (b) electric field profile of the EO modulators using a patch antenna embedded with two parallel narrow gaps.

The microwave characteristics of the patch antennas embedded with parallel narrow gaps was calculated. The calculated electric field distributions on the substrate surface are shown in Figure 4-2 under the irradiation of the wireless microwave signal. We can see that the strong electric field is induced across the two parallel narrow gaps.

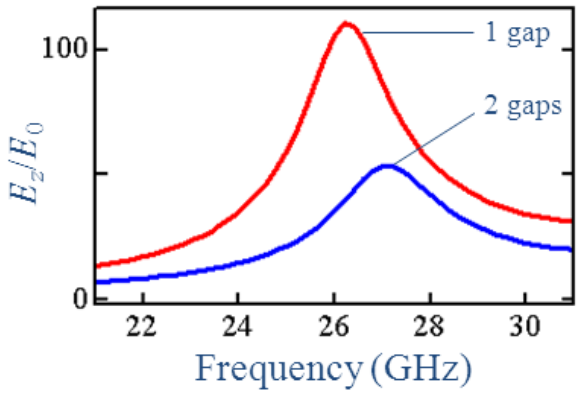

Figure 4-3 Calculated electric field across the gap of the EO modulators using a patch antenna embedded with two parallel narrow gaps and single gap.

The magnitude of the electric field across the gaps was also calculated. The calculated electric field across the gaps as a function of microwave frequency is shown in Figure 4-3. The proposed

device has electric field magnitude across the gaps with a half value compared to the EO modulator using a patch antenna embedded with a single narrow gap. The electric field across the two parallel gaps can be expressed as

$$E_m(t) = \frac{E_0}{2} sin(\omega_m t) \tag{4-1}$$

The peak microwave frequency of the proposed device is also slightly shifted to higher than the EO modulators using a patch antenna embedded with a single narrow gap.

4.2.3 Mach-Zehnder Interferometer

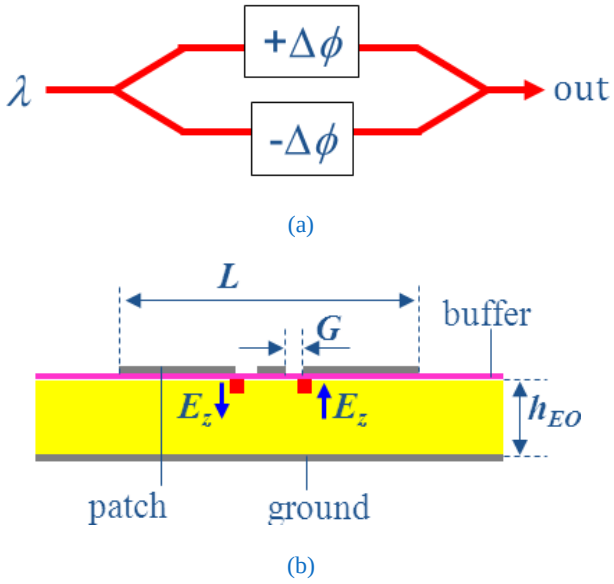

Figure 4-4 Configuration of the Mach-Zehnder interferometer by the EO modulator using a patch antenna embedded with two parallel narrow gap, (a) simple configuration and (b) cross-sectional view of the device.

The proposed device can be used for the Mach-Zehnder interferometer by irradiating wireless microwave signal. The Mach-Zehnder interferometer using the proposed device is shown in Figure 4-4. Intensity optical modulation might be induced by using the proposed device. However, the modulation index might be still low. Improvement of the modulation index is required for increasing the device performance. The technique for enhancing the modulation index will be discussion in the Chapter 6 and Chapter 7.

4.3 EO modulators using a patch antenna embedded with orthogonal gaps

4.3.1 Device Structure

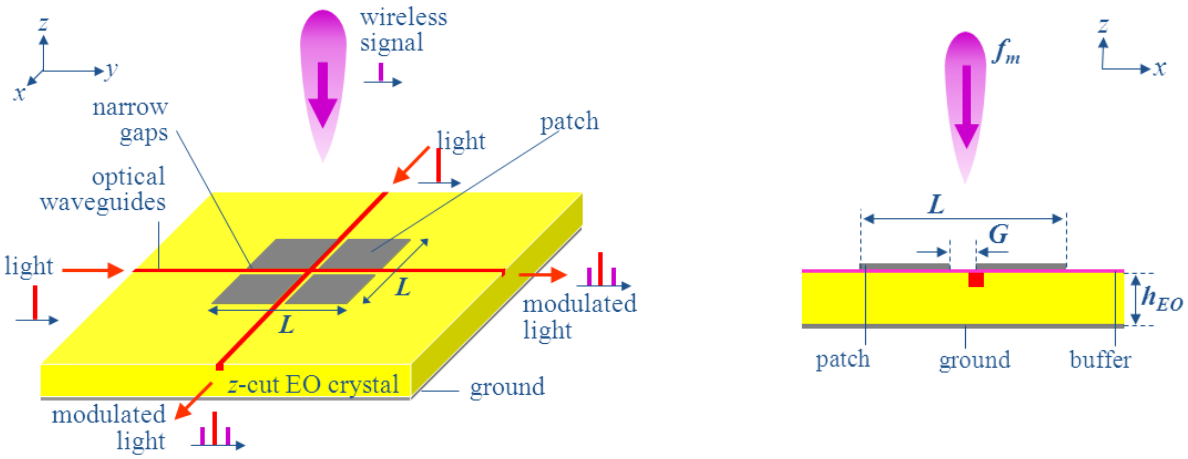

Figure 4-5 Device structure of an EO modulator using a patch antenna embedded with orthogonal narrow gaps.

Figure 4-5 shows the structure of an EO modulator using a patch antenna embedded with two orthogonal gaps. It is composed of two optical waveguides and a square patch embedded with two orthogonal gaps. It is fabricated on a *z*-cut EO crystal by considering the strongest EO coefficient for the two optical waveguides in the *xy*-plane. The length of the square metal patch is set at half a wavelength for the designed microwave wireless signal. The gap widths are set in micrometer order. The two optical waveguides are located under the edges of the two orthogonal gaps. A buffer layer is inserted between the substrate and the patch antenna. The reverse side of the substrate is covered with a ground electrode.

An EO modulator using patch antennas embedded with a narrow gap was reported and discussed [64] [69]. Now, I would explain briefly the basic principle of the EO modulator using patch antennas embedded with orthogonal gaps. When a wireless microwave signal at the design frequency with an arbitrary polarization is irradiated to the proposed device, a resonant standing-wave microwave current is induced on the patch antenna surface. The induced current can be separated into two components along the *x*- and *y*-axes. In the proposed device, displacement currents are induced across the gap normal to the *x*-axis and the gap normal to the *y*-axis, due to the continuity of the current flow. As a result, strong electric fields are also induced across the gaps. The strong electric field across the gaps can be used for optical modulation. Therefore, the wireless microwave signal can be converted to the lightwave signal through optical modulation by the induced electric field across the gaps.

The modulated lightwave signals are obtained from two optical waveguides. Wireless signal with two orthogonal polarizations can be received and converted to two orthogonal lightwave signals independently. The magnitude and phase of the wireless signal can be obtained by detecting the modulated lightwave signals. The polarization of the wireless signal can also be identified by comparing the two orthogonal modulated lightwave signals.

4.3.2 Operational principle

4.3.2.1 Standing-wave current

In the standard patch antenna with no gap, when a wireless microwave signal with an arbitrary polarization condition is irradiated to the device, a standing-wave microwave surface current, K, is induced on the metal patch. It can be expressed as

$$K = \hat{x}K_x + \hat{y}K_y \tag{4-2}$$

where, K_x and K_y are the surface current components along x- and y-axes, respectively, and $\hat{x}$ and $\hat{y}$ are the unit vectors along x- and y-axes, respectively. K_x and K_y can be expressed as

$$K_x(x,t) = K_{xp}\cos(\omega_m t)\cos\left(p\frac{2\pi}{\Lambda_m}x\right) \tag{4-3}$$

$$K_y(y,t) = K_{yq}\cos(\omega_m t + \varphi)\cos\left(q\frac{2\pi}{\Lambda_m}y\right) \tag{4-4}$$

where, K_{xp} and K_{yq} are the amplitude of the surface current, ω_m is the wireless microwave signal angular frequency, Λ_m is the microwave wavelength and φ is the mutual phase shift between the x- and y-current components. For simplicity, I focus on the fundamental mode case, that is p = 1 and q = 1. In this mode, the surface current becomes maximum at x = 0 along the x-axis and at y = 0 along the y-axis.

4.3.2.2 Displacement current

Then, two narrow orthogonal gaps G_y and G_x are introduced at x = 0 and y = 0, respectively. The displacement currents must be induced across both the gaps for the current continuity requirement as shown in Figure 4-6 [66]. They can be formulated as

$$G_y: \frac{\partial D_x}{\partial t} \propto K_x(0,t) = K_{x0}\cos(\omega_m t) \tag{4-5}$$

$$G_x: \frac{\partial D_y}{\partial t} \propto K_y(0,t) = K_{y0}\cos(\omega_m t + \varphi) \tag{4-6}$$

where D is the electric flux density ($D = \varepsilon E$), and ε is the permittivity. Therefore, the induced electric fields across the gaps are obtained by the time integration of the displacement currents as shown in Figure 4-6 [74]. It can be shown as follows

$$E_x(t) \propto K_{x0}\sin(\omega_m t) \tag{4-7}$$

$$E_y(t) \propto K_{y0}\sin(\omega_m t + \varphi) \tag{4-8}$$

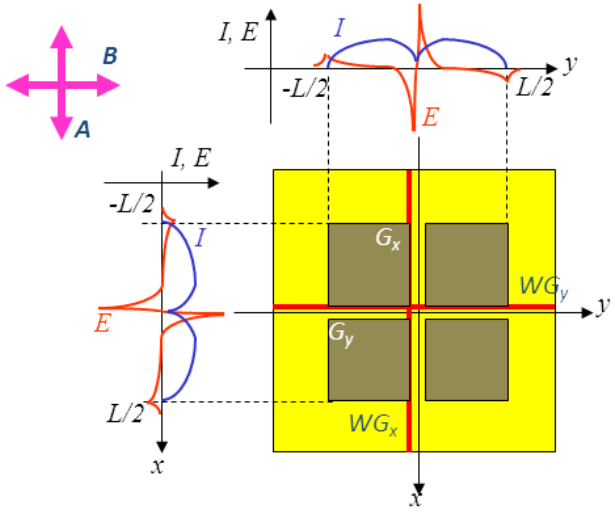

Figure 4-6 Current profile and electric field profile of the EO modulator using patch antennas embedded orthogonal gaps.

4.3.2.3 Optical modulation

The optical modulation characteristics driven by the electric fields across the gaps were also analyzed. In order to calculate modulation indices through the EO effect, the microwave electric field observed by the lightwave propagating in the optical waveguides should be considered by taking into account of the transit-time effect [67]

First, the transformation for considering the transit-time effect for the lightwave propagating in the optical waveguide WG_y along the y-axis, can be expressed by $y' = y - v_{gy}t$, where y'denotes the point of the lightwave in the coordinate system moving with the lightwave, and v_{gy} is the group

velocity of the lightwave in the optical waveguide WG_y. Therefore, the microwave electric fields observed by the lightwave along the optical waveguide WG_y become as

$$\begin{aligned} E_{x-light}(y) &= E_x\left(\frac{y-y'}{v_{gy}}\right) \\ &\propto K_{x0}\sin\left(\omega_m\frac{y-y'}{v_{gy}}\right) \\ &= E_{x0}\sin\left(k_m n_{gy} y + \zeta_y\right) \end{aligned} \tag{4-9}$$

where k_m is the wave number of the microwave in vacuum ($k_m = \omega_m/c$), n_{gy} is the group index of the lightwave propagating in the optical waveguide WG_y ($n_{gy} = c/v_{gy}$), ζ_y is an initial phase of the lightwave in the optical waveguide WG_y ($\zeta_y = -k_m n_{gy} y'$), and c is the light velocity in vacuum.

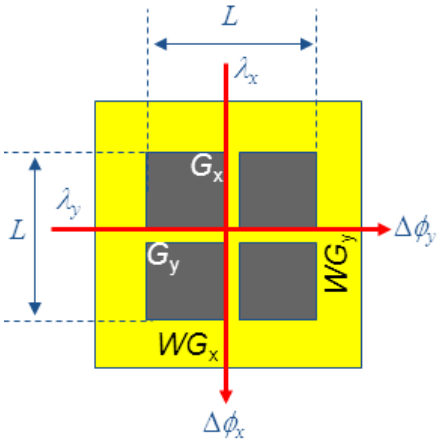

Figure 4-7 Top-view of the EO modulator EO modulator using patch antennas embedded orthogonal gaps.

The lightwave propagating in the optical waveguide WG_y is modulated by the induced electric field across the gap G_y through the EO effect. The obtained lightwave from the WG_y is phase-modulated light by the wireless microwave signal with the *A*-polarization. Its modulation index, $\Delta\phi_y$, can be determined taking account of the overlapping between of the induced microwave electric field and the lightwave electric fields in the cross section. It is expressed as follows,

$$\Delta\phi_y = \frac{\pi r_{33} n_e^3}{\lambda_y}\Gamma\int_0^L E_{x-light}(y)dy \tag{4-10}$$

where λ_y is the lightwave wavelength propagating in the optical waveguide WG_y, r_{33} is the EO coefficient, n_e is the extraordinary refractive index of the substrate, Γ is a factor expressing the overlapping between the induced microwave electric field and the lightwave, and L is the length of the patch antenna as the interaction length of the EO modulation.

For the lightwave propagating in the optical waveguide WG_x, the transit time of the lightwave is expressed as by $x' = x - v_{gx}t$, where x' denotes the point of the lightwave in the coordinate system moving with the lightwave, and v_{gx} is the group velocity of the lightwave in the optical waveguide WG_x. Therefore, the microwave electric fields observed by the lightwave along the WG_x become as

$$E_{y-light}(x) = E_{y0}\sin\left(k_m n_{gx} x + \zeta_x + \varphi\right) \tag{4-11}$$

where n_{gx} is the group index of the lightwave propagating in the optical waveguide WG_x ($n_{gx} = c/v_{gx}$), and ζ_x is an initial phase of the lightwave in the optical waveguide WG_x ($\zeta_x = k_m\, n_{gx}\, y'$).

Then, the lightwave propagating in the optical waveguide WG_x is modulated by the induced electric field across the gap G_x through the EO effect. The obtained lightwave from the WG_x is phase-modulated light by the wireless microwave signal with the *A*-polarization. Its modulation index, $\Delta\phi_x$ can be determined taking account of the overlapping between of the induced electric field and the lightwave in the cross section. It is expressed as follows,

$$\Delta\phi_y = \frac{\pi r_{33} n_e^3}{\lambda_x}\Gamma\int_0^L E_{y-light}(x)dx \tag{4-12}$$

where λ_x is the lightwave wavelength propagating in the optical waveguide WG_x.

By using two orthogonal gaps and optical waveguides, wireless microwave signals with two orthogonal linear polarizations can be received, separated, and converted to lightwave signals directly, independently, and simultaneously. Therefore, the polarization condition of a wireless signal can be identified using the proposed device. The magnitude and phase of the wireless signal can be also observed. Additionally, a circular polarization of the wireless microwave signal can be received and converted to lightwave signals using the device. The two modulated lightwave signals with 90 degree phase difference of the microwave signal can be detected using the proposed device.

4.3.3 Analysis

4.3.3.1 Microwave polarization

The microwave characteristics of the proposed device were analyzed in detail using electromagnetic software, HFSS. The device parameters for microwave analysis are shown in Table 4-2.

Table 4-2 Device parameters for microwave analysis of EO modulators using patch antennas embedded with orthogonal gaps.

	Values
Substrate: *z*-cut $LiTaO_3$	
Dielectric constant (ε_x, ε_y, ε_z)	(43,43,41)
Thickness, *h*	0.4 mm
Patch antenna: aluminum	
Antenna size, *L*x*W*	0.8 x 0.8 mm
Gap width, *G*	5 μm

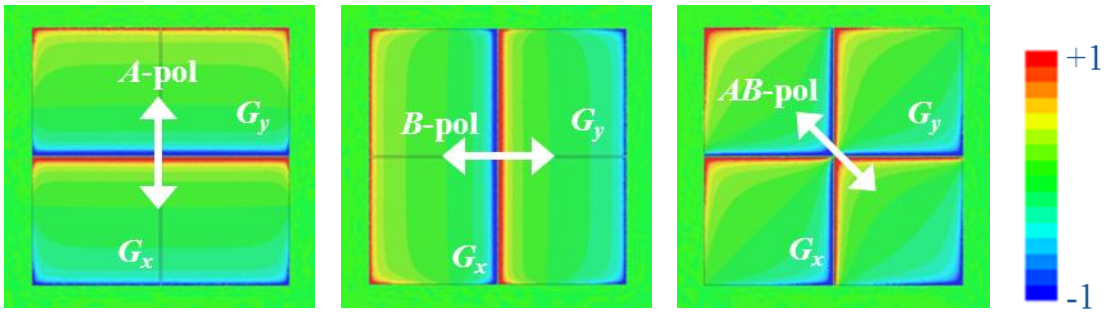

(a) (b) (c)

Figure 4-8 Electric field distributions (top-view) for several wireless microwave polarizations.

Figure 4-8 shows the calculated microwave electric field distributions under the patch metal when the designed microwave signals with several wireless microwave polarizations are irradiated to the device. When the wireless microwave signal with a linear polarization along *x*-axis (*A*-polarization) is irradiated to the device, the strong microwave electric field is induced across the gap G_y and no microwave electric field across the gap G_x as shown in Figure 4-8(a). On the contrary, when the polarization of the radiated wireless microwave signal is rotated 90-degrees (along *y*-axis/ *B*-polarization), the strong microwave electric field is induced across the gap G_x and extremely weak microwave electric field under the gap G_y as shown in Figure 4-8(b). When the polarization of the radiated wireless microwave signal is rotated 45-degrees (between *x*- and *y*-axes/ *AB*-polarization),

strong microwave electric fields are induced across both two orthogonal gaps as shown in Figure 4-8(c).

In this case, the induced electric fields across the gap G_y and G_x are completely in-phase. When wireless microwave signals with circular polarization state are irradiated to the device, the induced electric fields across the gap G_y and G_x have the same magnitude with a 90-degrees phase differences. The induced electric field can be used for optical modulation through Pockels effects. By using these characteristics, the polarization condition of the wireless microwave signal can be identified using the device by adopting the ROF technology.

4.3.4 Fabrication

I have fabricated the proposed device for microwave operational frequency of 26 GHz using *z*-cut $LiTaO_3$ crystal with thickness of 0.4 mm. The detail device parameters for fabrication are shown in Table 4-3. The fabrication processes of the EO modulators using patch antennas embedded with orthogonal gaps will be briefly reported, where the processes have almost same sequence with the previous devices explained in the Chapter 3.

Table 4-3 Device parameters for fabrication of EO modulators using a patch antenna embedded with orthogonal gaps.

	Values
Substrate: *z*-cut $LiTaO_3$	
Dielectric constant (ε_x, ε_y, ε_z)	(43,43,41)
Thickness, h	0.4 mm
Frequency, f_m	26 GHz
Patch antenna: aluminum	
Size, LxW	0.8 x 0.8 mm
Gap width, G	5 μm
Buffer layer: SiO_2	
Thickness	
Optical waveguide	0.2 μm
Single mode	
Wavelength, λ	1.55 μm

In the device fabrication, two orthogonal channel optical waveguides for single-mode operation at the wavelength of 1.55 μm was fabricated by using the annealed proton-exchange method with benzoic acid at 240 ^{O}C [56] [57]. The exchange time of 12 hours was used for fabricating waveguide

with 2 μm thickness. Then, a thin SiO_2 buffer layer was deposited on the surface of the substrate after the optical waveguide fabrication using a sputtering machine. Next, a square patch antenna embedded with orthogonal gaps was fabricated with a 1 μm-thick aluminum film on the buffer layer surface by use of thermal vapor deposition, a standard photolithography technique, and a lift-off process. The edges of the gaps were set onto the optical waveguides for effective optical modulation. Thermal annealing process at 350 ^{O}C in 1 hour was also done to increase the optical waveguide performance. Finally, an aluminum film with thickness of 1μm was deposited on the reverse side of the substrate as a ground electrode.

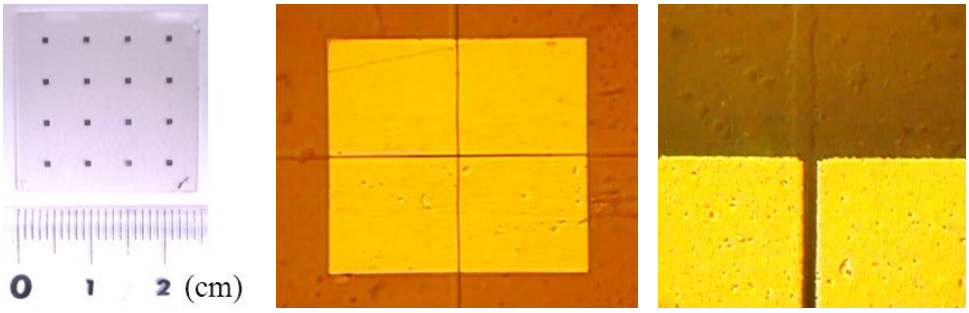

(a) (b) (c)

Figure 4-9 Photographs of the fabricated device. (a) EO modulators using a patch antenna embedded with orthogonal gaps. (b) Microscopy picture of a patch antenna embedded with orthogonal gaps and (c) intersection area of the optical waveguide and the gap.

The photographs of the fabricated prototype device are shown in Figure 4-9. Figure 4-9(a) shows the picture of the whole fabricated device. Figure 4-9(b) and Figure 4-9(c) show the magnified pictures of the patch antenna embedded with orthogonal gaps and intersection area of the optical waveguide and the narrow gap, respectively. The optical waveguides was located under the edge of the narrow gaps.

4.3.5 Measurement

4.3.5.1 Experimental setup

The measurement setup is shown in Figure 4-10. Two lightwaves of 1.55 μm wavelength from a laser were coupled to the optical waveguides WG_x and WG_y in the fabricated device. A wireless microwave signal from a microwave signal generator with an operational frequency of 26 GHz was amplified by use of an amplifier and irradiated to the fabricated device by use of a horn antenna with irradiated power of +24 dBm. The light output spectra as the modulated lightwave signals were observed and monitored by use of an optical spectrum analyzer (OSA).

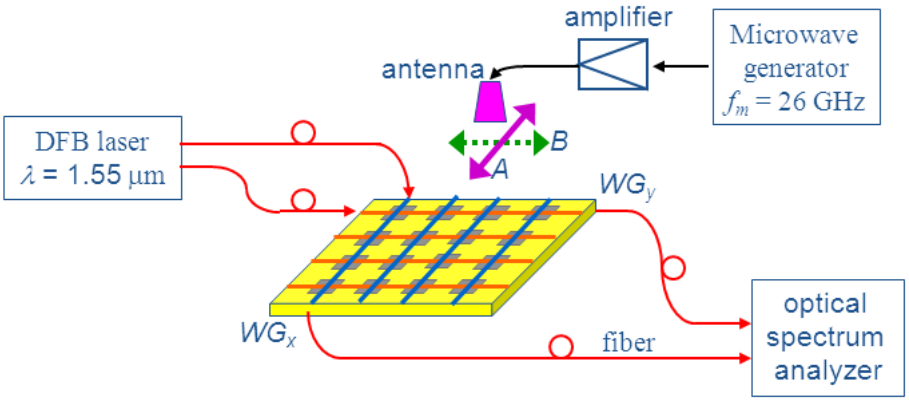

Figure 4-10 Measurement setup for the EO modulators using a patch antenna embedded with orthogonal gaps.

4.3.5.2 Measurement results

First, the polarization of the wireless microwave signal was set with the *A*-polarization (0 degree). In this case, optical sidebands were observed clearly in the output lightwave from the WG_y and no optical sideband was observed from the WG_x. Figure 4-11 shows the measured optical spectra of the modulated lightwave signals from WG_y (solid-line) and WG_x (dashed-line) by irradiating wireless microwave signal with the *A*-polarization.

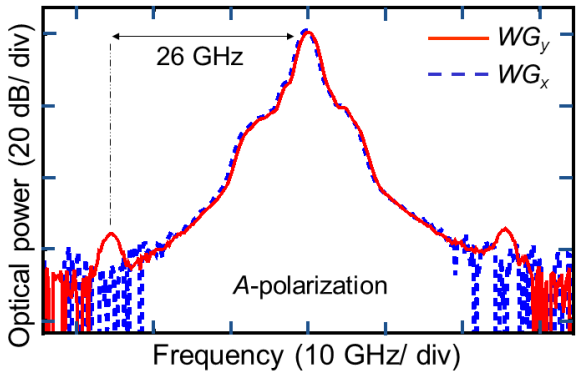

Figure 4-11 Measured optical spectra of the lightwave signals from the optical waveguides WG_y and WG_x for *A*-polarization (0 degree)

In contrary, Figure 4-12 shows the measured optical spectra of the modulated lightwave signals from WG_y (solid-line) and WG_x (dashed-line) by irradiating wireless microwave signal with the *B*-polarization (rotate to 90 degree). We can see that optical sidebands were observed clearly in the

output from the WG_x (dashed-line) and no optical sideband was observed from the WG_y (solid-line) as shown in Figure 4-12.

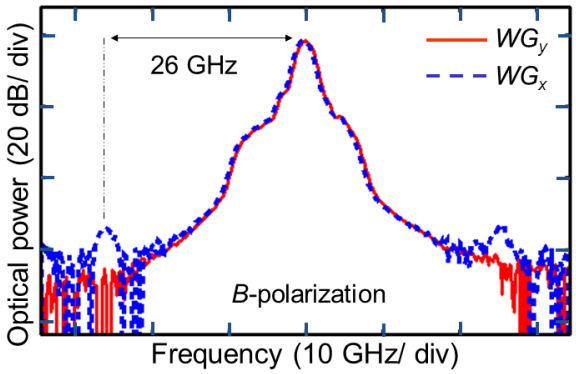

Figure 4-12 Measured optical spectra of the lightwave signals from the optical waveguides WG_y and WG_x for *B*-polarization (90 degree).

Additionally, I have measured also the modulated lightwave signals by irradiating wireless microwave signal with *AB*-polarization (45 degree) as shown in Figure 4-13. We can see that the optical sidebands of the two orthogonal modulated lightwave signals from the optical waveguides WG_y and WG_x are almost the same values.

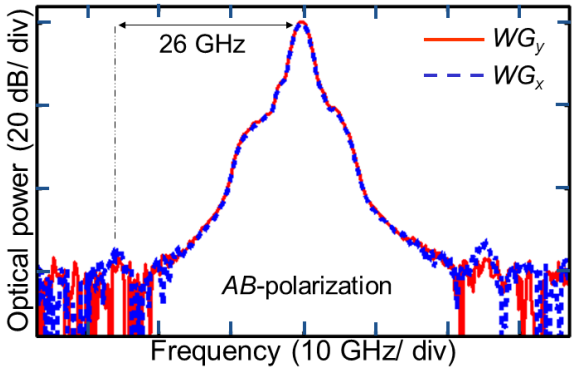

Figure 4-13 Measured optical spectra of the lightwave signals from the optical waveguides WG_y and WG_x for *AB*-polarization (45 degree).

Based on the results of the device measurement, optical sidebands were clearly observed from the optical waveguides when the microwave polarization is perpendicular to the gaps as shown in Figure 4-11 and Figure 4-12. When microwave polarization is parallel to the gaps and optical waveguide, no optical sideband was induced. When the microwave polarization is not completely perpendicular and parallel to the gaps, optical modulation are induced from the two optical waveguides as shown in Figure 4-13.

The modulation index of from the optical waveguides can be obtained using Eq. (3-20). The measured modulation indices of the proposed device from the two optical waveguides as a function of the microwave polarization direction in degree (where the *A*-polarization is 0 degree) are shown in Figure 4-14. We can see that measured modulation indices from the two optical waveguides depend on the microwave polarization direction. The measurement results have a good agreement to the calculation results.

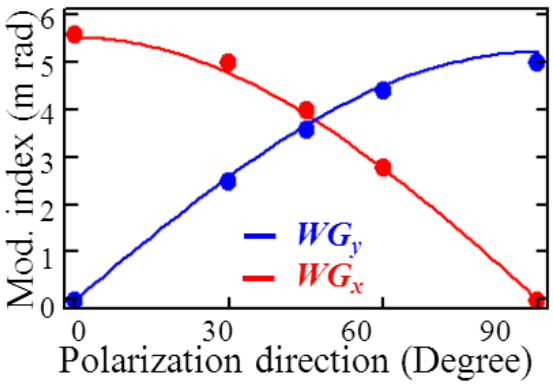

Figure 4-14 Measured modulation index from WG_x and WG_y as a function of microwave polarization direction in degree, where *A*-polarization is 0 degree.

By using the proposed device, a wireless microwave signals with two orthogonal polarizations can be received and converted to lightwave signal directly, simultaneously, and independently. Furthermore, the proposed device can be used for identifying the microwave linear polarizations direction by considering two orthogonal modulated lightwave signals. Additionally, wireless microwave signals with circular polarization can be received and converted to lightwave using the proposed device, where the microwave phase difference between two orthogonal gaps is 90 degrees.

4.4 Discussion and Summary

In this chapter, new fusion EO modulators using a patch antenna embedded with double narrow gaps were proposed for wireless microwave-lightwave signal conversion with functionality improvement. The EO modulators using a patch antenna embedded with two parallel gaps and orthogonal gaps were proposed. The displacement current and electric field across the narrow gaps are induced for EO modulation.

The EO modulators using a patch antenna embedded with two parallel gaps can be used for an optical intensity modulator through the Mach-Zehnder interferometry. Analysis of the proposed device was done. Two modulated lightwave signals can be obtained using the proposed device. However,

modulation index improvement is required for better performance. The technique for enhancing the modulation index will be discussion in the Chapter 6 and Chapter 7 [75] [76].

The EO modulators using a patch antenna embedded with two orthogonal gaps can be used for receiving two orthogonal microwave polarizations and identifying microwave polarization. The operations of the proposed devices for microwave polarization identification were verified experimentally. The measurement results have a good agreement to the calculation results. Furthermore, these proposed devices can be used for receiving wireless microwave signal with circular polarization. Based on this proposed devices with array structures, new device functionality for 2-D beamforming receiving can be realized. The detail discussion of the new device functionality will be presented in the Chapter 6 [75].

Chapter 5 Electro-Optic Modulators Using a Planar Yagi Antenna Coupled to a Resonant Electrode

5.1 Introduction

Conversion from microwave to lightwave signals can be composed of microwave antennas and optical modulators. Several configurations based on the antennas and optical modulators were discussed in the Chapter 2 [60]. In this thesis, electro-optic (EO) modulators using planar antennas with integrated and fusion structures are discussed in detail.

I have proposed EO modulators using a patch antenna embedded with narrow gaps [64] [70]. These devices are basically used for wireless microwave-lightwave signal conversion. They have simple and compact structure and can be operated with low microwave distortion and with no external power supply. An additional connection line is not required in the devices. However, the modulation efficiency from microwave to lightwave signals (modulation index) reminds low. It might be caused by several reasons, such as the small gain of the patch antennas (~8 dBi) and short interaction length between the microwave and lightwave electric fields.

In this chapter, I propose a new EO modulator using a planar Yagi antenna coupled to a resonant electrode [77]. The proposed device is composed of optical waveguides and a planar Yagi antenna coupled a coplanar waveguide resonant modulation electrode fabricated on an EO crystal such as $LiNbO_3$ or $LiTaO_3$. The optical waveguides are designed for single mode operation for the designed lightwave wavelength. The Yagi antenna is composed of a main planar dipole, planar directors, and a planar reflector. High antenna gain can be obtained using the Yagi antennas (~14 dBi). The resonant electrodes are structure by a standing-wave coplanar waveguide. A planar connection lines is required for connecting the Yagi antenna and resonant electrode. Optical modulation can be obtained by use of the induced electric field along the resonant electrode through Pockels effects of the EO crystal substrate. Therefore, the modulation efficiency improvement can be obtained using the proposed device.

In the following sections, I will present the device structure and operational principles of the proposed EO modulators using a planar Yagi antenna coupled a resonant electrode. Analysis of the proposed device for millimeter-wave signal at operational frequency of 40 GHz is presented [77].

5.2 Device structure

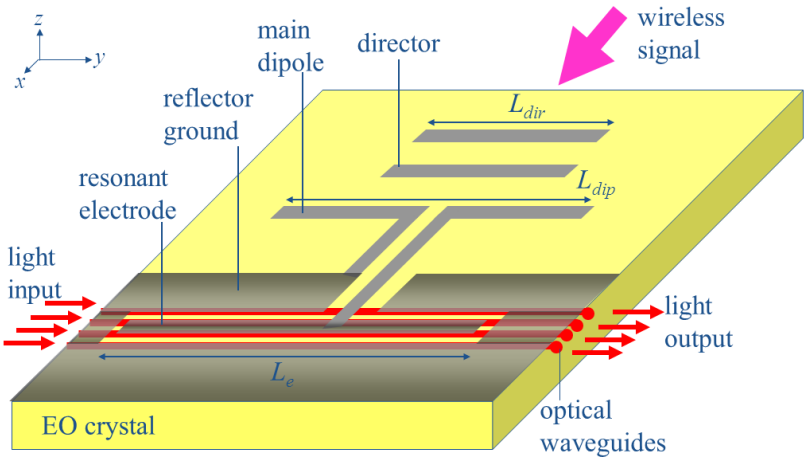

Figure 5-1 Device structure of the EO modulator using a Yagi antenna coupled to a resonant electrode.

Figure 5-1 shows the basic structure of the proposed EO modulator using a planar Yagi antenna coupled to a resonant electrode. It is composed of several optical waveguides and a planar antenna coupled to a resonant electrode, which are fabricated onto an EO crystal. The antenna is composed of a planar Yagi antenna for receiving wireless signals. It consists of a main dipole, directors, and a reflector with planar structure. The resonant electrode for EO modulation is composed of a coplanar waveguide with open-ends. Its length is set to one-wavelength for the designed millimeter-wave signal. The antenna is coupled to the resonant electrode using a planar connection line for connecting between the balanced and unbalanced millimeter-wave circuits (baluns). The optical waveguides are located under the standing-wave resonant electrode. A buffer layer is inserted between the substrate and the planar resonant electrode.

5.3 Operational principle

The Yagi antenna has a high-gain and a narrow radiation pattern. The length of the main dipole, directors, and reflector in the planar Yagi antenna are generally determined close to $0.5\Lambda_{eff}$, $0.45\Lambda_{eff}$, and $0.55\Lambda_{eff}$, respectively, where Λ_{eff} is the effective wavelength of the wireless signals [78]. When the wireless signal at the designed frequency is irradiated to the antenna, resonant currents are induced in the all elements of the planar Yagi antenna. The most sensitive direction to receive the signal is that along the array (x-axis) owing to the mutual coupling among the directors, main dipole, and reflector. Then the induced currents are transferred along the array directors and reflected by the reflector. As a result, the strong electromagnetic fields are coupled to the main dipole antenna and it is also improved

by dipole resonance. The received and improved millimeter-wave electromagnetic fields are transferred to the coplanar waveguide resonant electrode for optical modulation. When the lightwaves propagate along the optical waveguides, they are modulated by the standing-wave resonant electric field along the resonant electrode. The antenna gain can be improved by increasing the number of the directors in the planar Yagi antennas. As a result, the induced electric field along the resonant electrode becomes large. Therefore, the large modulation efficiency can be obtained using the planar Yagi antenna coupled to the resonant electrode due to higher antenna gain and longer interaction length compared to the EO modulators using patch antennas embedded with narrow gaps.

5.3.1 Standing-wave electric field

The operational principle of the proposed device is discussed briefly. A standing-wave millimeter-wave resonant electrode is used. In this study, I concern the standing-wave resonant electrode with a one wavelength as the length. The standing-wave millimeter-wave electric field along the resonant electrode can be used for optical modulation.

The standing-waves electric field in the resonant electrode along the *y*-axis can be generated by calculating the forward and backward travelling electric field. The forward and backward travelling electric field can be expressed as

$$E_m^+(y,t) = E_0 \sin\left[2\,\pi\, f_m\left(t - \frac{y}{v_m}\right)\right] \tag{5-1}$$

$$E_m^-(y,t) = E_0 \sin\left[2\,\pi\, f_m\left(t + \frac{y}{v_m}\right)\right] \tag{5-2}$$

Then, the standing-wave electric field can be transformed as following equation

$$\begin{aligned} E_m^{st}(y,t) &= E_m^+(t,y) + E_m^-(t,y) \\ &= E_0 \sin\left[2\,\pi\, f_m\left(t - \frac{y}{v_m}\right)\right] + E_0 \sin\left[2\,\pi\, f_m\left(t + \frac{y}{v_m}\right)\right] \\ &= 2E_0 \sin(2\,\pi\, f_m\, t)\cos\left(2\,\pi\, f_m \frac{y}{v_m}\right) \end{aligned} \tag{5-3}$$

where f_m is the operational frequency of the millimeter-wave signal, v_m is the phase velocity of the millimeter-wave signal.

5.3.2 Optical modulation

The induced standing-wave millimeter-wave electric field along the resonant electrode can be used for EO modulation. The induced millimeter-wave electric field can be observed by lightwave propagating in optical waveguides located along the resonant electrode. The transit time for the lightwave to pass under the antenna along optical waveguide (y = 0 to $y = L_{ele}$) is also considered [67]. This transit time can be expressed as $y' = y - v_g t$, where y and y' are the position of the lightwave and v_g is the group velocity of the lightwave.

By considering the transit time of the lightwave, the induced millimeter-wave electric field observed by the lightwave can be calculated. It can be transformed as

$$\begin{aligned} E_{m-light}^{st}(y) &= E_m^{st}\left(y, \frac{y-y'}{v_g}\right) \\ &= 2E_0 \sin\left[2\,\pi\, f_m \left(\frac{y-y'}{v_g}\right)\right] \cos\left[2\,\pi\, f_m \frac{y}{v_m}\right] \\ &= 2E_0 \sin\left[k_m\, n_g\, y + \zeta\right] \cos[k_m\, n_m y] \end{aligned} \tag{5-4}$$

$$k_m = \frac{2\,\pi\, f_m}{c} \quad ; \quad c = n_g v_g = n_m v_m \quad ; \quad \zeta = -k_m n_g y'$$

where k_m is the wave number of the microwave in the vacuum, n_m is the effective refractive index of the millimeter-wave along resonant electrode, n_g is the group index of the lightwave propagating in the waveguide, ζ is an initial phase of the lightwave in the waveguide, and c is the light velocity in the vacuum.

The modulation index, $\Delta\phi$, can be determined by taking account of the overlapping field between the induced millimeter-wave electric field and the lightwave along the resonant electrode. It can be calculated by integration of the millimeter-wave electric field observed by the lightwave along the resonant electrode length (from y = 0 to $y = L_{ele}$). It can be expressed as

$$\Delta\phi = \frac{\pi r_{33} n_e^3}{\lambda} \Gamma \int_0^{L_{ele}} E_{m-light}^{st}(y)\, dy \tag{5-5}$$

where λ is wavelength of the lightwave propagating in the waveguide, r_{33} is the EO coefficient, n_e is the extraordinary refractive index of the EO crystal, and Γ is the overlapping factor between the induced microwave and lightwave electric fields.

A wireless microwave signal can be received by the Yagi antenna and directly converted to a lightwave signal along the resonant electrode through EO modulation. Large modulation index are obtained using the proposed device with high gain of the Yagi antenna and long interaction length of the resonant electrode. The proposed device can be operated passively with low microwave distortion. Simple and compact device structure is also advantages of the proposed device [77].

5.4 Analysis

5.4.1 Millimeter-wave analysis

The proposed EO modulator was designed by using a 0.25 mm-thick *z*-cut $LiTaO_3$ crystal as a substrate. The operational frequency was set at 40 GHz millimeter-wave signal. The length of the standing-wave coplanar waveguide resonant electrode was set one-wavelength of the designed millimeter-wave signal. The planar Yagi antenna coupled to the resonant electrode was analyzed in detail by using electromagnetic analysis software, HFSS. The Yagi antenna and the modulation electrode were analyzed separately as illustrated in Figure 5-2. Then they will be combined each other for realizing the integrated structure.

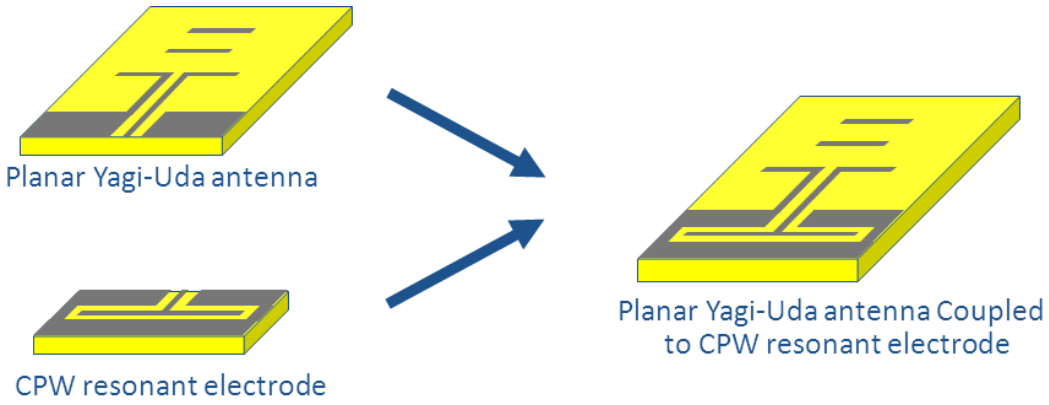

Figure 5-2 Millimeter-wave analysis method for EO modulator using a Yagi antenna couplesd to a resonant electrode.

5.4.1.1 Yagi antenna

Figure 5-3 shows the structure of the planar Yagi antenna on an EO crystal substrate, where two directors were set. I calculated the proposed device by changing the parameter values such as the main dipole length, director length, director separation, and others. The selected parameters of the Yagi antenna for millimeter-wave analysis with 40 GHz operational frequency are shown in Table 5-1.

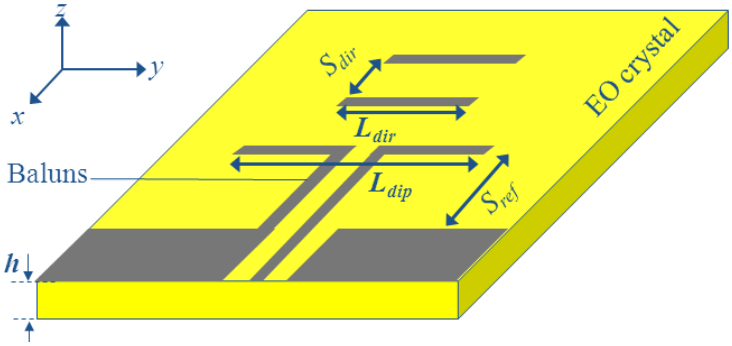

Figure 5-3 Structure of the planar Yagi antenna.

Table 5-1 Parameters for millimeter-wave analysis of the Yagi antenna.

	Values
Substrate: *z*-cut $LiTaO_3$	
Dielectric constant (ε_x, ε_y, ε_z)	(43,43,41)
Thickness, h	0.25 mm
Yagi antenna	
Main dipole length, L_{dip}	1.2 mm
Director length, L_{dir}	0.7 mm
Director separation, S_{dir}	0.4 mm
Reflector separation, S_{ref}	0.9 mm

The simulation setup for analyzing the Yagi antenna is shown in Figure 5-4(a) using a dummy excitation port. The calculated return loss of the designed Yagi antenna is shown in Figure 5-4(b). The calculated return loss has depth around 40 GHz bands, however other depth is also occurred it may be caused by unwanted resonant effects. Figure 5-4(c) shows the calculated electric field distribution on the substrate surface for 40 GHz millimeter-wave frequency. We can see that the electric field is passed through along the planar connection lines (parallel stripline) then resonance is induced along the main dipole and the directors. Furthermore, I also analyzed the radiation pattern of the Yagi antenna at 40 GHz millimeter-wave frequency as shown in Figure 5-4(d). The wireless millimeter-wave signal is mainly radiated along the guided elements (directors) direction, which is in the *x*-axis. However, the back radiation is not much small, it might be caused by the reflector have large distance from the main dipole.

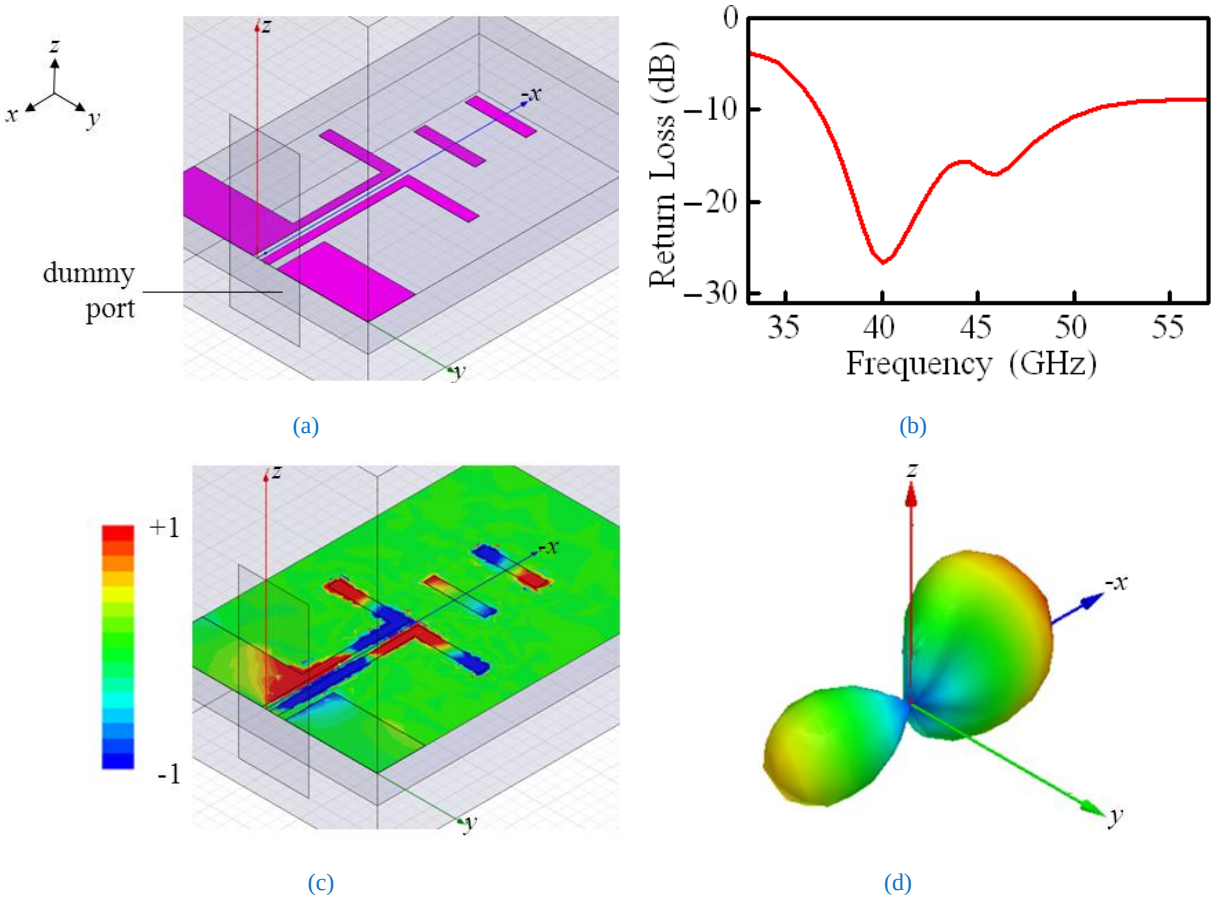

Figure 5-4 Calculation of the Yagi antenna characteristics, (a) simulation setup, (b) calculated return loss, (c) calculated electric field distribution at 40 GHz, and (d) calculated radiation pattern of the Yagi antenna at 40 GHz operational frequency.

5.4.1.2 Resonant electrode

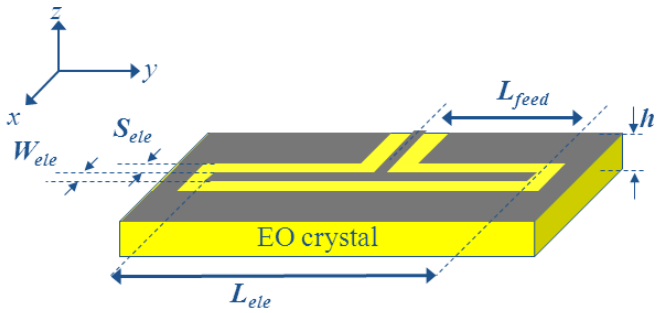

Figure 5-5 Structure of the planar resonant electrode.

Figure 5-5 shows the structure of the planar standing-wave coplanar waveguide resonant electrode on an EO crystal substrate. The detail parameters of the resonant electrode for millimeter-wave analysis with 40 GHz operational frequency are shown in Table 5-2.

Table 5-2 Parameters for millimeter-wave analysis of the resonant electrode.

	Values
Substrate: *z*-cut $LiTaO_3$	
Dielectric constant (ε_x, ε_y, ε_z)	(43,43,41)
Thickness, h	0.25 mm
Resonant electrode	
Coplanar waveguide	
Electrode length, L_{ele}	1.5 mm
Electrode width, W_{ele}	30 μm
Electrode separation, S_{ele}	30 μm
Feeding length, L_{feed}	0.4 mm

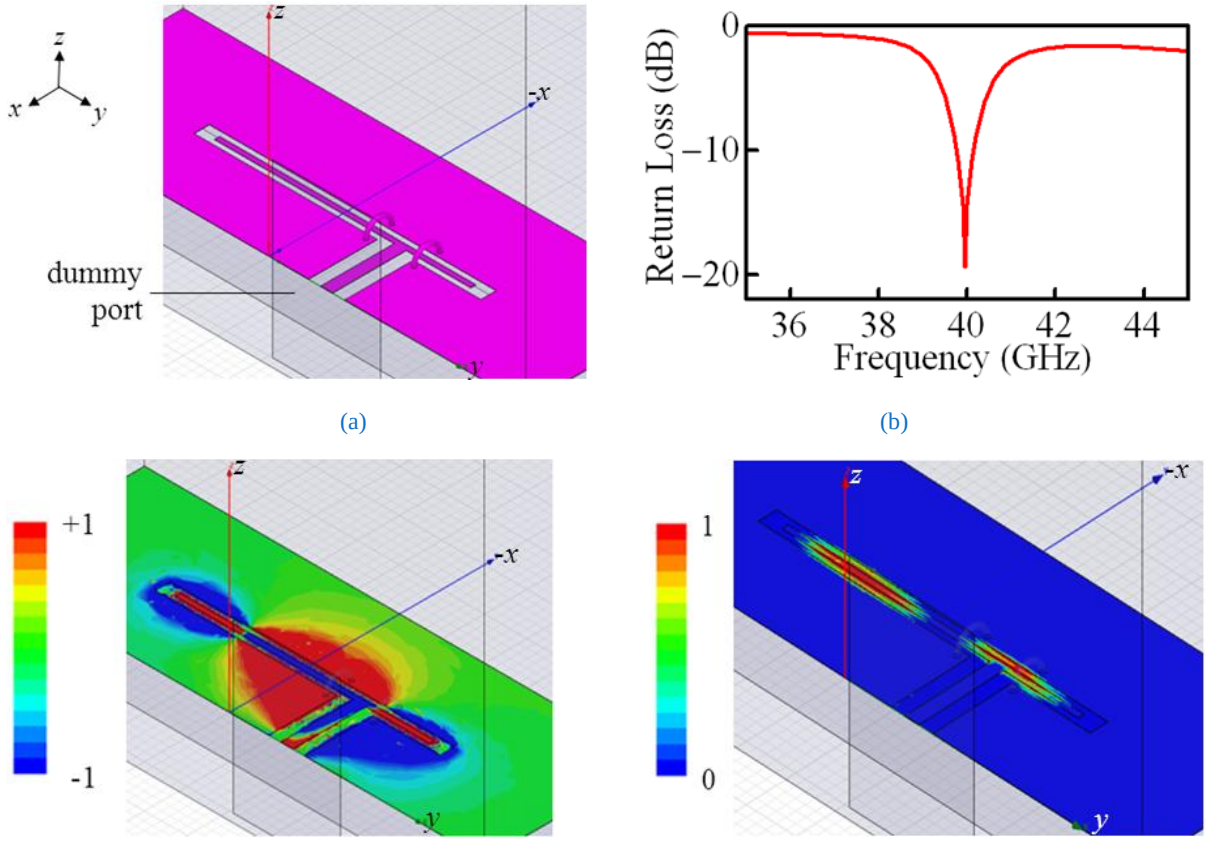

(a) (b)

(c) (d)

Figure 5-6 Calculation of the resonant electrode characteristics, (a) simulation setup, (b) calculated return loss, (c) calculated electric field distribution, and (d) calculated current distribution of the Yagi antenna at 40 GHz operational frequency.

In the analysis, the simulation setup for analyzing resonant electrode is shown in Figure 5-6(a) using a dummy excitation port. The calculated return loss of the designed Yagi antenna is shown in Figure 5-6(b). The calculated return loss has depth close to 40 GHz bands. Figure 5-6(c) shows the calculated electric field distribution on the substrate surface for 40 GHz millimeter-wave frequency. We can see that the standing-wave electric field is induced along the coplanar waveguide resonant electrode. The calculated current distribution on the substrate surface for 40 GHz millimeter-wave frequency is shown in Figure 5-6(d).

5.4.1.3 Yagi antenna couple to resonant electrode

Based on the calculation results of the Yagi antenna and resonant electrode in the millimeter-wave signal, the Yagi antenna coupled to resonant electrode was also analyzed simultaneously. I used electromagnetic analysis software for calculating the device characteristics using dummy excitation incident wave port, which is assumed for wireless millimeter-wave signal from the space.

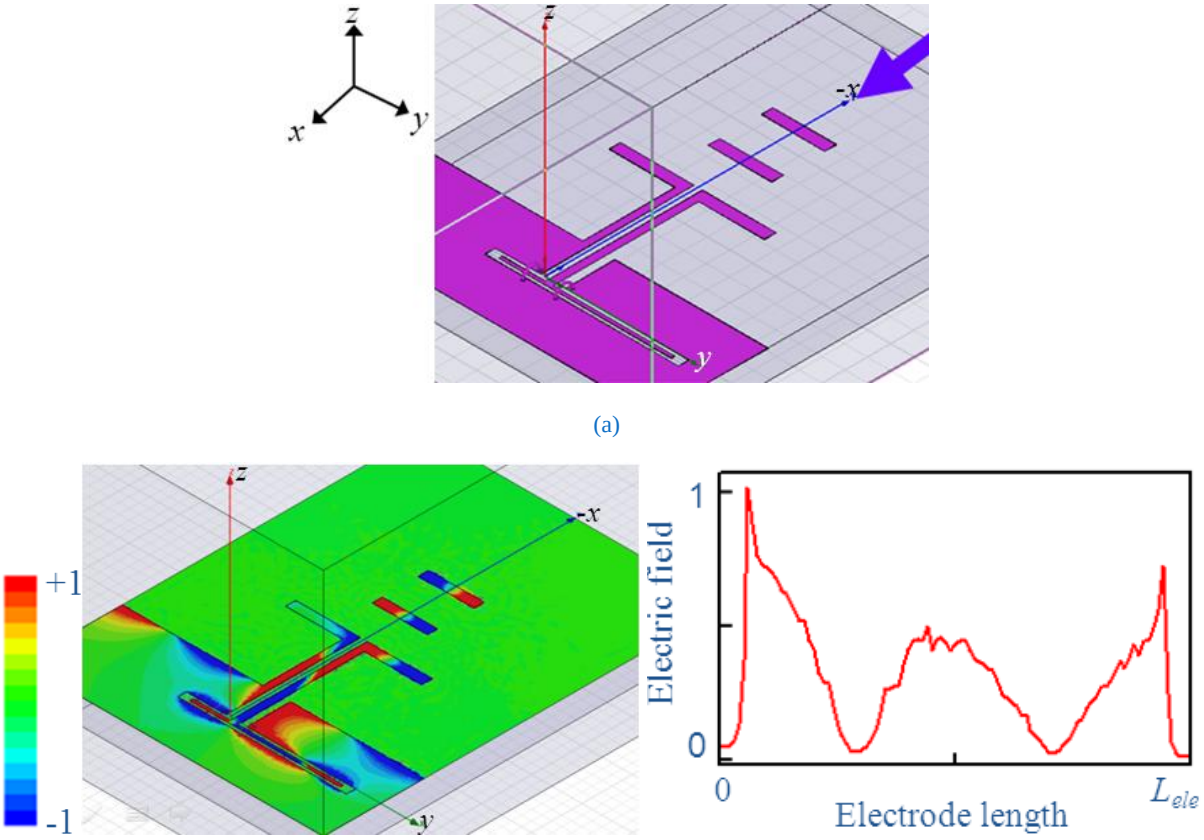

Figure 5-7 Calculation of the resonant electrode characteristics, (a) simulation setup, (b) calculated electric field distribution of the Yagi antenna coupled to resonant electrode at 40 GHz, and (c) calculated electric field profile along the resonant electrode in *y*-axis at 40 GHz.

In the analysis, the simulation setup for analyzing the Yagi antenna coupled to resonant electrode is shown in Figure 5-7(a) by irradiation wireless millimeter-wave signal using a dummy excitation incident wave port. Figure 5-7(b) shows the calculated electric field distribution on the substrate surface for 40 GHz millimeter-wave signal. We can see that the standing-wave electric field is induced along the coplanar waveguide resonant electrode. The induced millimeter-wave electric field along the resonant electrode can be used for optical modulation through Pockels effects.

5.4.2 Modulation index

Modulation index of the proposed device can be calculated using Eq. (5-5). We can see that the modulation index is proportional to the electric field magnitude and interaction length. The proposed device has electric field magnitude about three-times larger and interaction length over two-times longer compared the EO modulators using a patch antenna embedded with narrow gaps for the same frequency operation.

Based on that, modulation index improvement can be obtained using the proposed device compared to the EO modulators using patch antennas embedded with narrow gaps. The modulation efficiency improvement is about 10 dB. Therefore, higher modulation index can be obtained using the proposed device.

5.5 Discussion and summary

A new EO modulator using a planar Yagi antenna coupled with a resonant modulation electrodes are proposed for improving modulation efficiency. The Yagi antenna has high gain about 14 dBi and the standing-wave resonant electrode has long interaction length for optical modulation. High directivity of the wireless microwave signal can be also obtained using the proposed device. Additionally, the gain of the antenna can be improved in further by increasing the number of the directors. By considering them, large modulation efficiency can be obtained for wireless microwave-lightwave signal conversion.

In order to verify the expectation, I have analyzed the characteristics of the proposed EO modulators for millimeter-wave band of 40 GHz. In the analysis, calculated electric field magnitude and interaction length of the proposed device is larger than the EO modulator using a patch antenna embedded with a narrow gap. Therefore, modulation efficiency improvement of about 10 dB can be obtained using the proposed device compared to the EO modulators using a patch antenna embedded a narrow gaps. The modulation efficiency improvement is obtained due to the larger antenna gain and longer interaction length.

In order to obtain effective optical modulation, precise tuning between the planar structures, which are the planar Yagi antenna, resonant electrode, and connection line, are required. The proposed device is rather difficult in the design to achieve matching condition between the planar structures but easy in fabrication since planar structure is used. The microwave loss might be induced, since the proposed device is composed of a planar Yagi antenna, a resonant electrode, and a connection line. Furthermore, the precise tuning is difficult to achieve for effective optical modulation.

The proposed device can be used for broadcasting systems, electromagnetic compatibility measurement, or so on. Additionally, the modulation efficiency can be improved in further using an array structure. The EO modulators using an array of the planar antennas will be discussed in the next chapter.

Chapter 6 Electro-Optic Modulators Using Arrays of Planar Antennas

6.1 Introduction

In the Chapter 3, Chapter 4, and Chapter 5, I have proposed electro-optic (EO) modulators using a planar antenna for wireless microwave-lightwave signal conversion [64] [69] [68]. These devices can be used for realizing microwave-photonic systems [79]. The basic operations of the proposed devices were successfully verified in the experiment. They were fabricated on an electro-optic (EO) crystal substrate. The proposed devices have simple structure and can be operated with low microwave loss and no external power supply. However, the modulation efficiency still remains low.

In this chapter, I propose EO modulators using an array of planar antennas for enhancing modulation efficiency and wireless irradiation angle (beamforming) control. The modulation efficiency is basically proportional to the number of antennas in the array structure. In order to achieve effective optical modulation, transit time of lightwave passing through at each planar antenna should be considered. In here, I propose a new technique to improve modulation efficiency by using a quasi-phase-matching (QPM) array structure. The antenna number of the new proposed device becomes twice as the conventional (standard/ no QPM) array structures. As a result, the modulation efficiency becomes double also with more compact device structure where the QPM array device and the conventional array device have the same device length. The array structures have advantages relating their sensitivity to the wireless irradiation angle (beamforming). Based on that, the beamforming receiving of the wireless signal can be controlled through optical technology by using the EO modulator with an array of planar antennas. In here, EO modulators using 2-D array of planar antennas are also presented for wireless beamforming control. In order to control the beamforming, I propose a new technique to compensate for the optical modulation degradation using orthogonal meandering gaps. Since the antenna distance in the 2-D array structure is the same, the wireless signal beamforming can be controlled using the meandering gaps. 1-D beamforming receiving is obtained by analyzing modulated lightwave signal from the each optical waveguide independently. Furthermore, when two orthogonal modulated lightwave signals are considered simultaneously, 2-D beamforming receiving can be obtained. Based on this, EO modulators using a 2-D array of planar antennas can be used for enhancing modulation efficiency and 1-D and 2-D beamforming receiving of wireless microwave signals.

The proposed EO modulators have more compact structures. They can be operated with low microwave loss and no external power supply. The proposed devices are easy in the design and fabrication.

In the following sections, I will present the device structure, operational principle, analysis, fabrication, and measurement of EO modulators using an array of planar antennas. First, an EO modulator using an array of patch antennas embedded with a narrow gap are discussed. Second, an EO modulator using a QPM array of patch antennas embedded with a narrow gap are proposed. Its performance for a radio-over-fiber (ROF) link is also reported. Then, an EO modulator using 2-D array of patch antennas embedded with orthogonal meandering gaps are discussed.

6.2 EO modulators using an array of patch antennas embedded with a narrow gap

6.2.1 Device structure

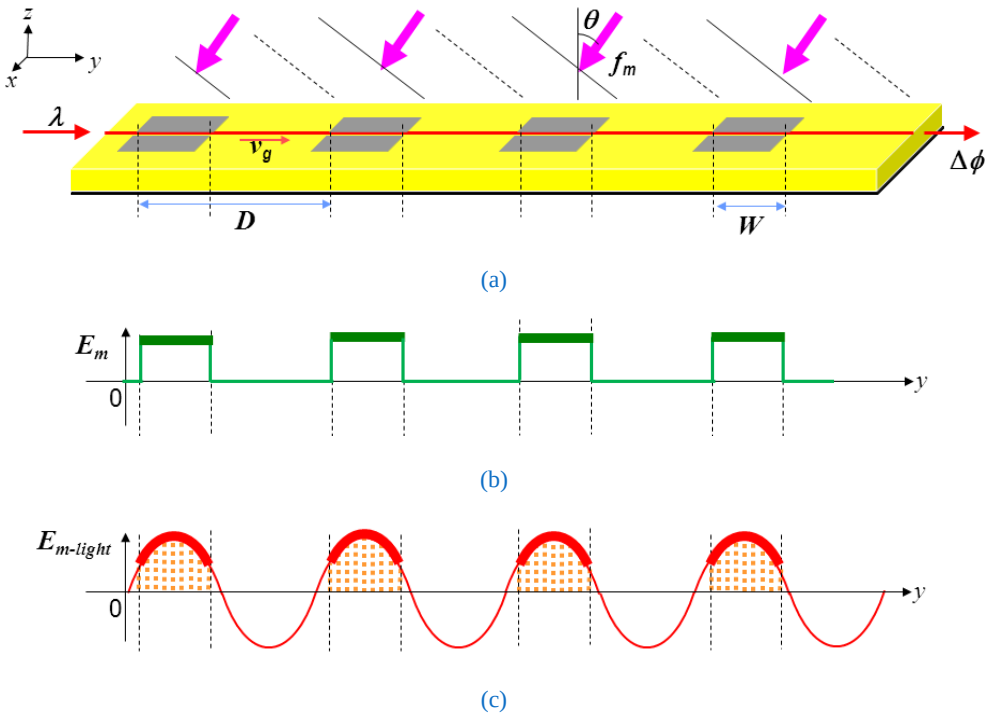

Figure 6-1 Array structure of EO modulators using patch antennas embedded with a narrow gap, (a) whole view, (b) standing-wave microwave electric field profile along the device, and (c) microwave electric field observed by lightwave by considering transit-time of the lightwave.

An array structure of EO modulators using patch antennas embedded with a narrow gap is considered for enhancing the modulation efficiency. The array structure is shown in Figure 6-1(a), where it is composed of several numbers of patch antennas embedded with a narrow gap fabricated on an EO crystal. The distance of the patch antennas embedded with a narrow gap is set by *D*.

When a wireless microwave signal at the angular frequency ω_m with a linear polarization in the *x*-direction is irradiated to the proposed device with an array structure, the displacement current and strong electric field are induced across the gap. The microwave electric field profiles across the gap at each patch antenna are shown in Figure 6-1(b). The magnitude of the microwave electric fields across the gap are temporal changed between minimum and maximum values. The lightwave is propagated to the optical waveguide. In order to pass through each patch antenna, the lightwave propagation is required time. It is called the transit time effect. The typical of the microwave electric field observed by the lightwave is shown by sinusoidal curve in Figure 6-1(c). The antenna distance is necessary to obtain effective modulation, where the microwave electric field observed by lightwave is required in phase condition for each patch antenna. As a result, effective optical modulation can be obtained by considering the lightwave transit time effect.

6.2.2 Operational principle

6.2.2.1 Microwave electric field

In the array structure, the temporal phases of the microwave signal supplied to the patch antennas embedded with a narrow gap are changed according their distance, *D*, and the wireless irradiation angle, θ. When the proposed optical modulator is irradiated with a wireless millimeter-wave signal at an angular frequency of ω_m, the microwave electric field at *h*-th patch antenna embedded with a gap can be transformed as following equations,

$$E_m(t) = E_0 \cos(\omega_m t + \boldsymbol{k} \cdot \boldsymbol{r}) \tag{6-1}$$

where, $\boldsymbol{k} \cdot \boldsymbol{r} = (-\hat{\boldsymbol{y}}\, k_m n_0 \sin\theta - \hat{\boldsymbol{z}}\, k_m n_0 \cos\theta) \cdot (\hat{\boldsymbol{x}}\, x + \hat{\boldsymbol{y}}\, y + \hat{\boldsymbol{z}}\, z)$

$= -y\, k_m n_0 \sin\theta - z\, k_m n_0 \cos\theta$

$$E_m(y, z, t) = E_0 \cos(\omega_m t - y\, k_m n_0 \sin\theta - z\, k_m n_0 \cos\theta)$$

when, $z = 0$ therefore,

$$E_m(y, t) = E_0 \cos(\omega_m t - y\, k_m n_0 \sin\theta)$$

when, $y = (h - 1)D$ in the array structure,

$$E_m^h(t) = E_0 \cos(\omega_m t - (h-1)D\, k_m n_0 \sin\theta) \tag{6-2}$$

where $\boldsymbol{k}$ is a wave vector of the microwave signal, k is the wave number of the microwave signal, n_0 is the refractive index of the microwave in air (=1), h denotes the number of the patch antennas, and D is a distance of the patch antennas in the array structure.

6.2.2.2 Transit time of lightwave

When a lightwave propagates in the optical waveguide, the lightwave passing through the antennas in the array structure is taking time to propagation between them (called transit time of the lightwave) [67]. The transit time of the lightwave can be calculated by considering group velocity of the lightwave and the distance of the antennas in the array structure. This transit time, t, can be expressed as

$$t = \frac{y - y'}{v_g} \tag{6-3}$$

where v_g is the group velocity of the lightwave propagating in the waveguide and y and y' is the position of the antenna along the y-axis.

6.2.2.3 Microwave electric field observed by lightwave

When a lightwave propagates in the optical waveguide, the microwave electric field as would be observed by the lightwave can be expressed by following equation with taking into account the transit-time of the lightwave

$$\begin{aligned} E_{m-light}^h(y,\theta) &= E_m^h\left(\frac{y-y'}{v_g}\right) \\ &= E_0 \cos\left[\omega_m\left(\frac{y-y'}{v_g}\right) - (h-1)D\, k_m n_0 \sin\theta\right] \\ &= E_0 \cos\left[k_m c\left(\frac{y-y'}{v_g}\right) - (h-1)D\, k_m n_0 \sin\theta\right] \\ &= E_0 \cos\left[k_m n_g (y-y') - (h-1)D\, k_m n_0 \sin\theta\right] \\ &= E_0 \cos\left[k_m n_g y - (h-1)D\, k_m n_0 \sin\theta + \zeta\right] \end{aligned} \tag{6-4}$$

where n_g is the group index of the lightwave propagating in the waveguide, ζ is an initial phase of the lightwave in the waveguide corresponds to the phase of the microwave signal when the lightwave propagates in the optical waveguide, and c is the light velocity in the vacuum. The microwave electric fields as would be observed by the lightwave are shown by the sinusoidal-curve in Figure 6-1(c), where the antenna distance in the array structure is set by considering the transit time effect.

6.2.2.4 Optical modulation

The modulation index, $\Delta\phi$, can be determined by taking account of the overlapping between the induced microwave and the lightwave electric fields at each patch antenna embedded with a gap. It can be calculated by summing the integration of the microwave electric field observed by the lightwave along each antenna width, which is from $y = (h-1)D$ to $y = (h-1)D + W$. It can be expressed as [65]

$$\Delta\phi(\theta) = \frac{\pi r_{33} n_e^3}{\lambda} \Gamma \sum_{h=1}^{N} \int_{(h-1)D}^{(h-1)D+W} E_{m-light}^{h}(y,\theta)\, dy \tag{6-5}$$

where λ is wavelength of the lightwave propagating in the waveguide, r_{33} is the EO coefficient, n_e is the extraordinary refractive index of the EO crystal, Γ is the overlapping factor between the induced microwave and lightwave electric fields, and N is the number of antennas.

By using an array structure, the modulation index of the proposed device can be improved. Effective optical modulation can be obtained by tuning the distance of the patch antennas in the array structure, where the microwave electric field observed by lightwave is the same phase in each patch antenna. The modulation index as a function of wireless irradiation angle is able to calculate. The wireless irradiation angle of the microwave signal can set by tuning the distance of the patch antennas embedded with a gap in the array structure.

6.2.3 Analysis

6.2.3.1 Modulation index

Modulation index of the proposed device in the array structure can be calculated using Eq. (6-5). The parameters for modulation index calculation of the proposed device are set as shown in Table 6-1.

The calculated modulation index as a function of the wireless irradiation angle of the microwave signal is shown in Figure 6-2. The proposed device is effective for receiving wireless microwave signal with normal irradiation angle ($\theta = 0$ degree).

Table 6-1 Device parameters for optical modulation analysis of EO modulators using an array of patch antennas embedded with a narrow gap.

	Values
Microwave signal	
Operational frequency, f_m	26 GHz
EO crystal ($LiTaO_3$)	
Thickness	0.4 mm
EO effect, r_{33}	30.3 pm/V
Refractive index, n_e	2.125
Group index, n_g	2.168
Lightwave	
Wavelength, λ	1.55 μm
Patch antenna	
Antenna size, LxW	0.8 x 1.3 mm
Gap width, G	5 μm
Array structure	
Number, N	4 elements
Distance, D	5.4 mm

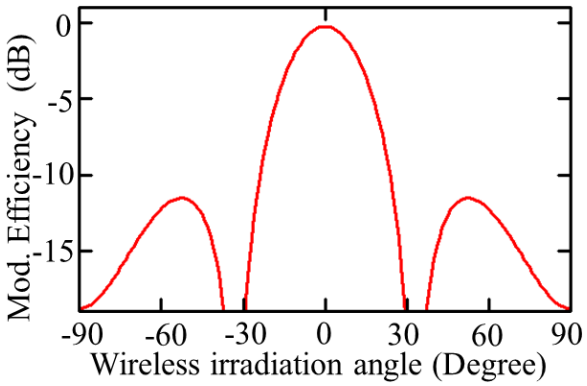

Figure 6-2 Calculated modulation index as a function of wireless irradiation angle of microwave signal.

The wireless irradiation angle of the microwave signal can be tuned by changing the distance, D, of the patch antenna in an array structure. Therefore, effective optical modulation can be obtained, when the wireless irradiation angle is changed. It can be expressed as

$$D = \frac{2\,n\,\pi}{k_m(n_0 \sin\theta + n_g)} \qquad n = 1,2,3,\ldots \qquad (6\text{-}6)$$

I also calculated the modulation index of the array structure for several antenna distance values (D = 4.5 mm, D = 6 mm, and D = 6.5 mm). The calculation results are shown in Figure 6-3. We can see that, the wireless irradiation angle for the most effective optical modulation is shifted by changing the distance of the patch antenna in the array structure.

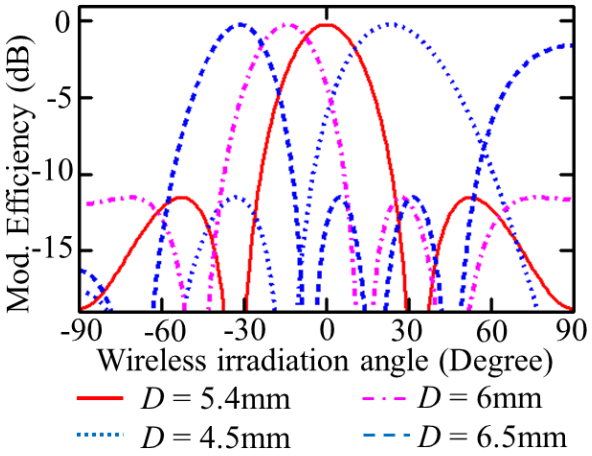

Figure 6-3 Calculated modulation index as a function of wireless irradiation angle of microwave signal for several antenna distance values in an array structure.

6.2.4 Fabrication

The EO modulator using an array of patch antennas embedded with a narrow gap was fabricated for 26 GHz bands. The detailed parameters for the device fabrication are shown in Table 6-1.

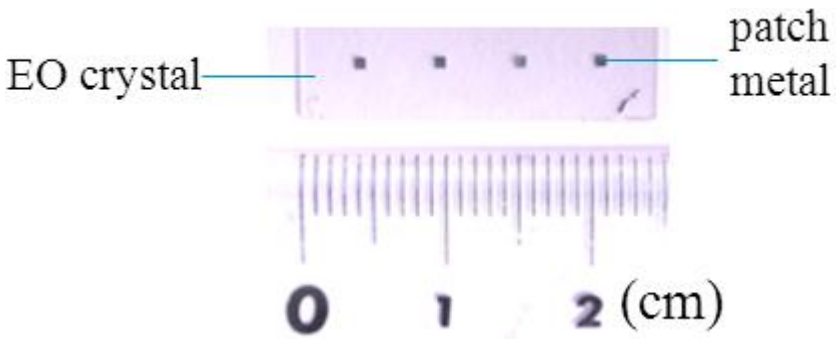

Figure 6-4 Photograph of the fabricated EO modulator using an array of patch antennas embedded with a narrow gap.

The processes of the fabrication were the same with the previous device fabrication as reported in the Chapter 3. The proposed device is fabricated on 0.4 mm-thick *z*-cut $LiTaO_3$ crystal. A straight optical waveguide was fabricated using annealed proton exchange method. Then, buffer layer was covered on the substrate surface. After that, an array of patch antennas embedded with a narrow gap was fabricated with 1 μm-thick aluminum using thermal deposition, standard lithography, and lift-off method. Finally, a 1 mm-thick aluminum was deposited on the reverse side of the substrate as the ground. The photograph of the fabricated device is shown in Figure 6-4.

6.2.5 Measurement

In this device measurement, the measurement setup is basically the same with as the previous measurement setup in the Chapter 3. The measurement setup of the proposed device is shown in Figure 6-5. A 26 GHz microwave signal from a microwave signal generator was amplified using microwave amplifier and then irradiated to the fabricated device using a horn antenna. A 1.55 μm wavelength lightwave from a laser was coupled to the optical waveguide in the fabricated device by use of an objective lens. The output light spectrum was measured and monitored using an optical spectrum analyzer (OSA).

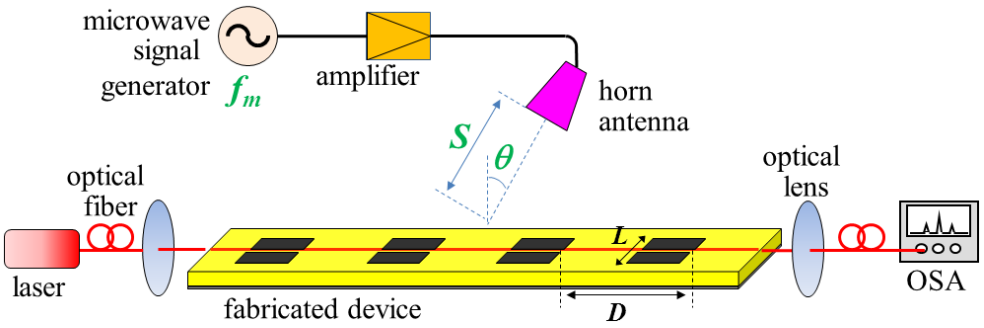

Figure 6-5 Measurement setup of the EO modulator using an array of patch antennas embedded with a narrow gap.

By irradiation wireless microwave signal to the fabricated device and coupling lightwave to the optical waveguide, the modulated lightwave signal can be obtained at the output. Modulation index can be improved and proportional to the number of the patch antennas since effective optical modulation is induced at each patch antenna in the array structure.

Since the modulation index is still remind low, the ratio between carrier and sideband powers can be represented for the modulation index. The modulation index can be transformed using Eq. (3-20). The measured modulation index of the fabricated device as a function of microwave frequency is shown by dotted in Figure 6-6. The solid line in Figure 6-6 shows the calculated modulation index

by considering the induced microwave electric field across the gap. We can see that the measurement results are coincided well to the calculation results.

Measured modulation efficiency as a function of wireless signal irradiation angles (directivity) was also done for the fabricated device. The measurement results are shown by the dotted in Figure 6-7. The solid line in Figure 6-7 is the calculated directivity of the array metal patch with element number of 4 by considering the transit time effect of the lightwave passing through at each metal patch. We can see that the measurement results have good agreement to the calculation results. In this array structure, the wireless directivity can be controlled by changing the distance of antennas in the array structures.

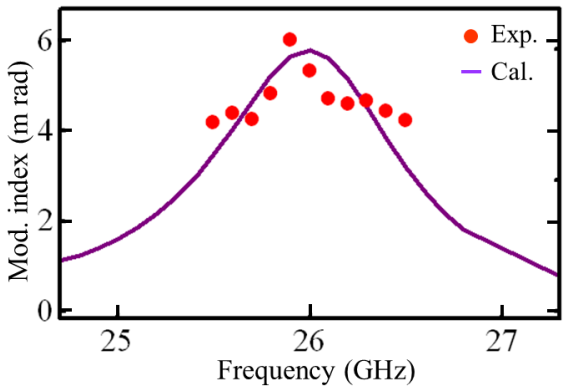

Figure 6-6 Measured modulation index as a function of microwave frequency.

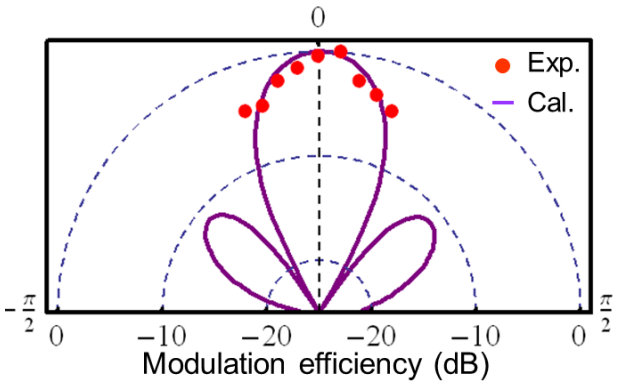

Figure 6-7 Measured modulation index as a function of wireless irradiation angle (directivity/ beamforming).

6.3 EO modulator using a new QPM array of patch antennas embedded with a narrow gap

We have discussed the EO modulator using an array of patch antennas embedded with narrow gaps [64] [69] [68]. This array structure has long antenna distance between each other. The long

distance can be utilized for increasing modulation efficiency by adding new antennas between the previous antennas.

In this section, I propose an EO modulator using a new QPM array of patch antennas embedded with a narrow gap for enhancing modulation efficiency. Twice patch antennas with the same device length can be obtained using the proposed device compared with the EO modulator using a conventional array of patch antennas embedded a narrow gap. By considering the transit time of the lightwave passing through each patch antenna, effective optical modulation can be achieved [67]. Modulation efficiency can be improved using this proposed device. The analysis and experiment of the proposed device are discussed and presented in here.

6.3.1 Device structure

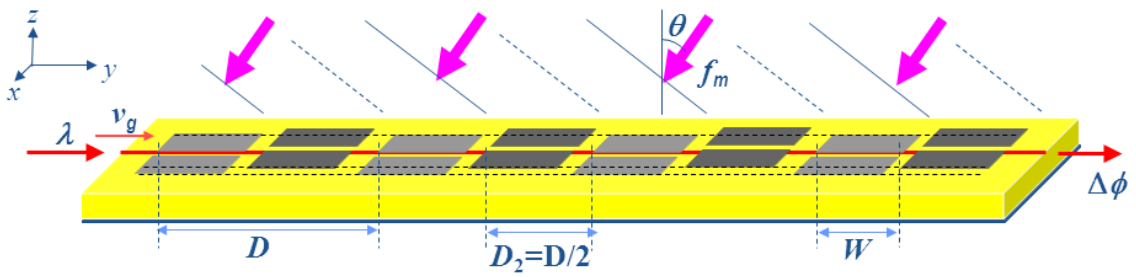

(a)

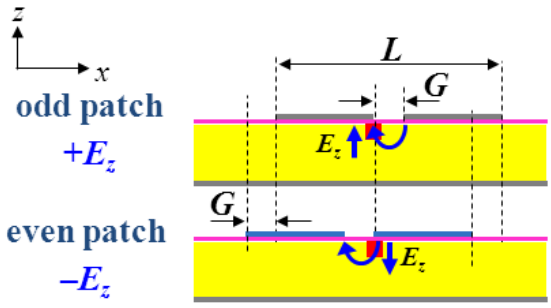

(b)

Figure 6-8 Device structures of the EO modulator using a new QPM array of patch antenna embedded with a narrow gap. (a) Whole device structure (3-D view). (b) Cross-sectional view configuration of the device structure along odd-antennas, and even-antennas.

Figure 6-8 shows the structure of the EO modulator using a new QPM array of patch antennas embedded a narrow gap. It consists of a channel optical waveguide and patch antennas embedded with a narrow gap onto a *z*-cut EO crystal like $LiNbO_3$, $LiTaO_3$, or KTP. EO polymers with single polarized molecules in the *z*-direction are also applicable for the substrate. An array of the patch antennas embedded with a narrow gap is set onto the substrate with a distance, D_2, which corresponds to half of

the period in conventional array structures in Figure 6-1. The number of antennas in the proposed device is double compared to the conventional array structure. The patch antenna size is set to *L*x*W*. The narrow gap in micrometer-order is set at the center of each antenna, along the *y*-axis. The optical waveguide is located under the one-side edge of the gap, where the cross-sectional views are shown in Figure 6-8 (b) for odd- and even-antennas. The buffer layer is inserted between the substrate and the antennas. The reverse side of the substrate is covered with a ground electrode.

The basic operations of the new fusion EO modulators using a patch antenna embedded with narrow gaps were discussed in the Chapter 3 and Chapter 4 [64] [69] [68]. The displacement current and electric field across the gap is used for optical modulation through EO effects [22] [54].

The modulation efficiency can be improved using a QPM array structure. In conventional array structures, the distance of the patch-antennas, *D*, is determined by the phase-matching condition, which is expressed as

$$n_g \, k_m \, D = 2 \, n \, \pi \qquad n = 1,2,3, \ldots \qquad (6\text{-}7)$$

where v_g is the group velocity of the lightwave, ω_m is the angular frequency of microwave signal, n_g is the group index of the lightwave propagating in the optical waveguide (n_g = c/v_g), k_m is the wave number of the microwave in vacuum ($k_m = \omega_m/c$) , and c is the light velocity in vacuum. Therefore, the spacing between antennas for the conventional array structure is relatively large than the patch antenna size. In the large free spaces on the conventional array structures, we introduce new patch-antennas with the QPM technique. Therefore, the distance of the antennas in the new array structure, D_2, becomes half compared to the distance of the antennas in the conventional array structure ($D_2 = D/2$). The degradation by phase-mismatching in densely allocated array structures can be compensated for using the QPM technique by switching alternately of the spatial relationship between the gap edges and the optical waveguide for odd- and even-antennas. Therefore, modulation efficiency improvement can be obtained using the proposed QPM EO modulator.

6.3.2 Operational principle

When a wireless microwave signal at the angular frequency ω_m is irradiated to the proposed QPM device, the displacement current and strong electric field are induced across the gap. The induced electric field can be expressed by Eq. (3-9).

For an array of patch antennas embedded with narrow gap as shown in Figure 6-9, the temporal phases of the microwave signal supplied to the patch antennas embedded a narrow gap are changed

according their distance, D_2, and the wireless irradiation angle, θ. The microwave electric field at h-th patch antennas, $E^h_{m-light}$, can be expressed by

$$E^h_{m-light}(t) = E_o \cos[\omega_m\, t + 2D_2(h-1)k_m n_0 \sin\theta] \tag{6-8}$$

where h denotes the number of the gap-embedded patch-antennas, D_2 is a distance of the patch-antennas as shown in Figure 6-9, and n_0 is the refractive index of the microwave in air (=1).

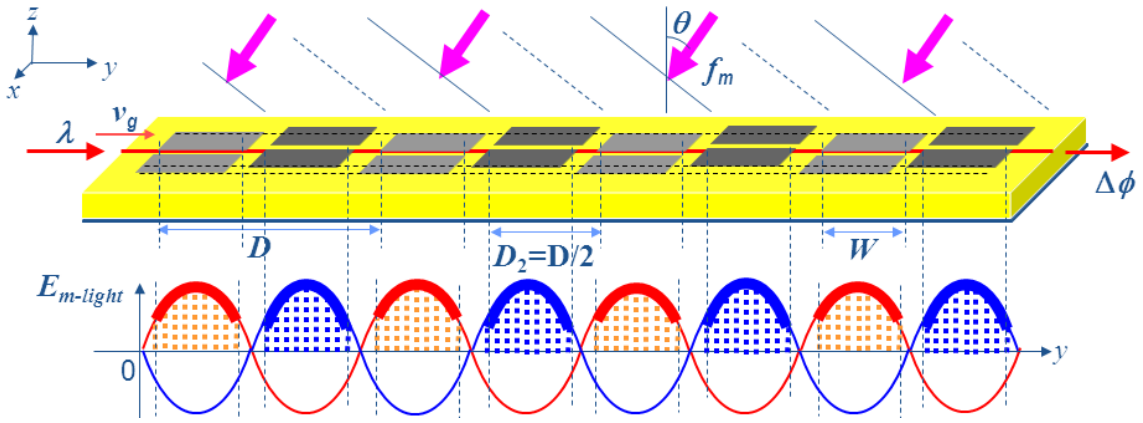

Figure 6-9 Operational principle of the QPM EO modulator. Microwave electric field observed by propagating lightwave along odd- and even-antennas. Modulation efficiency corresponds to taking into account the shaded-areas.

When a lightwave propagates in the optical waveguide, the microwave electric field as would be observed by the lightwave can be expressed by following equation with taking into account the transit-time of the lightwave

$$E^h_{m-light}(t) = E^h_{m-light}\left(\frac{y-y'}{v_g}\right)$$

$$E^h_{m-light}(y) = E_o \cos\left[k_m\, n_g\, y + 2D_2(h-1)k_m n_0 \sin\theta + \zeta\right] \tag{6-9}$$

where ζ is an initial phase of the lightwave in the optical waveguide ($\zeta = -k_m\ n_g\ y'$) corresponds to the phase of the microwave signal when the lightwave propagates in the optical waveguide. The microwave electric fields as would be observed by the lightwave are shown by the sinusoidal-curve in Figure 6-9.

The modulation efficiency from the wireless microwave to lightwave signals in this proposed devices is proportional to the modulation index, $\Delta\phi$, when $\Delta\phi << 1$. The modulation index is calculated by the integration of microwave electric field as would be observed by the lightwave along the gap-embedded patch-antennas, it can be expressed as

$$\Delta\phi(\theta) = \frac{\pi r_{33} n_e^3}{\lambda} \Gamma \sum_{h=1}^{N} \int_{(h-1)D_2}^{(h-1)D_2+W} P_{QPM}(y) E_{m-light}^{h}(y) dy \tag{6-10}$$

where λ is the wavelength of lightwave propagating in the optical waveguides, r_{33} is the EO coefficient, n_e is the extraordinary refractive index of the substrate, Γ is a factor expressing the overlapping between the induced microwave electric field and the lightwave, W are the width of the patch-antenna as the interaction length of the microwave and lightwave, and N is the number of gap-embedded patch-antennas in the array structure. $P_{QPM}(y)$ expresses the polarity sign of the microwave electric field in z-component under the gap edge along the optical waveguide. $P_{QPM}(y)$ is set +1 for the odd-elements and -1 for the even-elements. The modulation index of the QPM device corresponds to the sum of the shaded areas in Figure 6-9(b). Since the modulation index is also a function of wireless irradiation angle, θ, the directivity in the modulation efficiency can be also calculated using Eq.(6-10).

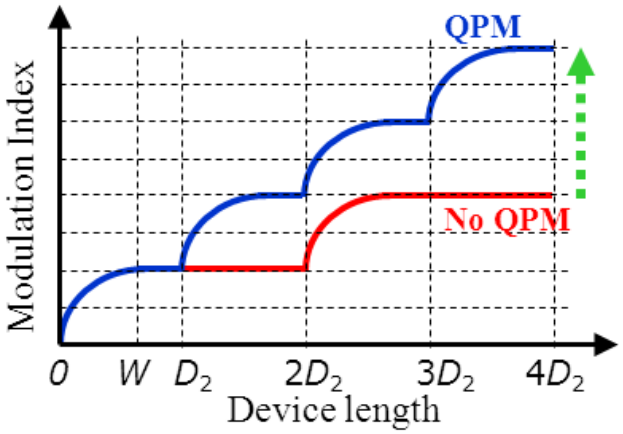

Figure 6-10 Improved modulation index of the EO modulators with a QPM structure compared to the EO modulators without a QPM structure.

The modulation index of the proposed device is represented by an integration of microwave electric field observed by lightwave (shaded-areas). The comparison of modulation indices between the EO modulators with a QPM structure and the EO modulators without a QPM structure are shown Figure 6-10. We can see that improved modulation index can be obtained due to the additional elements between the previous elements, where the microwave electric field observed by the

lightwave along each antenna should be considered for effective optical modulation. Therefore, the modulation index of the EO modulators with a QPM structure is improved double compared to the EO modulators without a QPM structure.

6.3.3 QPM Structures

The microwave electric fields in the *z*-component between two-edges of the gap have different polarities [80]. The different polarities enable us to obtain the QPM condition. The QPM structures on the *z*-cut EO crystals are obtainable by switching the spatial relationship between the gap edge and optical waveguide along the odd- and even-antennas as shown in Figure 6-11(a) and (b). In here, I propose several possible configurations for QPM condition.

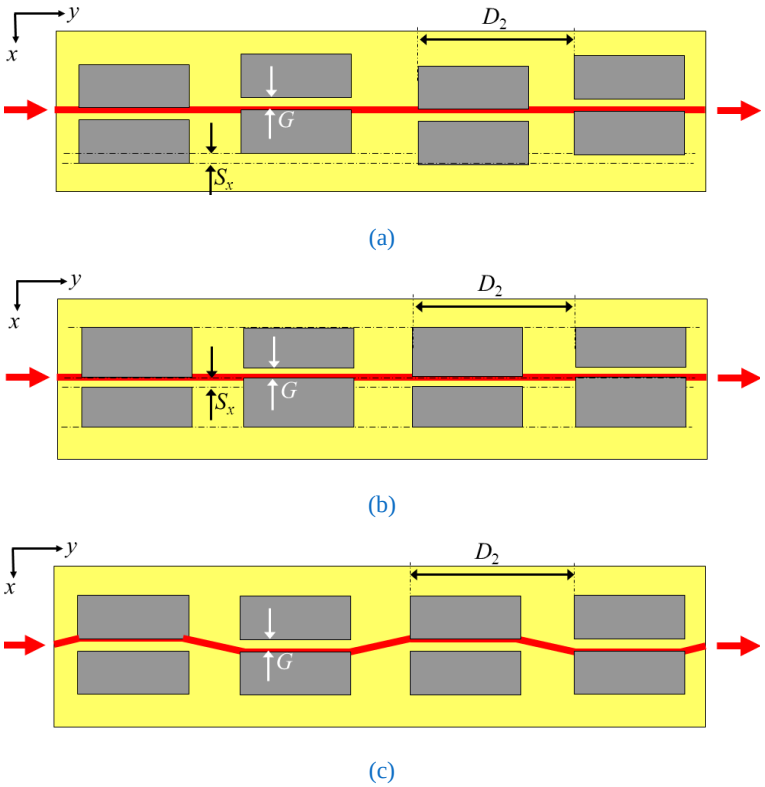

Figure 6-11 Several QPM techniques for the EO modulator on the *z*-cut EO crystal. (a) Shifting position of antennas along the *x*-axis. (b) Shifting position of gap along the *x*-axis. (c) Meandering optical waveguide.

The QPM condition can be obtained using phase-inversed structures by considering the polarity of the microwave electric field under the gap edges. Figure 6-11 shows top-views of QPM devices with three configurations of the phase-inversed structures on a *z*-cut EO crystal. They are promising techniques for increasing modulation efficiency in the EO modulators using gap-embedded patch-antennas.

The QPM structure using shifted position of the patch antennas by S_x along the x-axis is shown in Figure 6-11(a). The narrow-gap is located at the center of the patch-antennas with the gap width of G. The spatial relative relationship between the straight optical waveguide and the gap edges is switched alternately by shifting the position of the antennas in the array structure for the QPM condition.

The phase-inversed structure using shifted position of the narrow gap is shown in Figure 6-11 (b). The patch antennas are aligned in completely parallel to the straight optical waveguide. However, the narrow gap positions in the odd- and even-antennas are slightly shifted by S_x along the x-axis. By shifting the gap in the antennas, the induced electric fields across the gap are almost the same as long as the gap shift is within micrometer-order. Therefore, the relatively spatial relationship between the optical waveguide and the gap edges is also switched alternately.

Figure 6-11(c) shows the QPM structure using meandering optical waveguide. The patch antennas are aligned in parallel. All narrow-gaps are located at the center of each patch antenna with the gap width of G. However, the optical waveguide is meandered between the odd- and even-antennas. Therefore, the QPM condition can be also obtained.

6.3.4 Analysis

Table 6-2 Device parameters for analysis of the EO modulator using a QPM array of gap-embedded patch antennas.

	Values
Operational frequency	26 GHz
Substrate: z-cut $LiTaO_3$	
Dielectric constant (ε_x, ε_y, ε_z)	(43,43,41)
Thickness, h	0.4 mm
Patch antenna: aluminum	
Antenna size, LxW	0.8 x 1.3 mm
Gap width, G	5 μm
Array structure	
Antenna number, N	8 elements
Distance, D_2	2.7 mm

The proposed QPM device with configuration of shifting position of the antennas as shown in Figure 6-11(a) was designed at a 26 GHz microwave operational frequency. The detail parameters for analyzing the proposed device are shown in Table 6-2.

The microwave characteristics of the device were numerically analyzed using electromagnetic analysis software, HFSS. The calculated frequency dependence of the magnitude of the electric field across the gap in the *z*-component is shown in Figure 6-12(a), when a linearly polarized wireless microwave signal with polarization in along the *x*-axis was irradiated to the device and the observation point (the optical waveguide location) was set under the edge of the gap. The peak resonant frequency of the gap-embedded patch-antenna was matched with the designed microwave frequency. Figure 6-12(b) shows the electric field distribution in the *z*-component on the surface of the substrate. The electric field at two-edges of the gap have different polarity in the *z*-component. The difference polarity of the induced electric field between two edges of the gap enables us to realize QPM condition for improving modulation efficiency in the simple compact QPM devices.

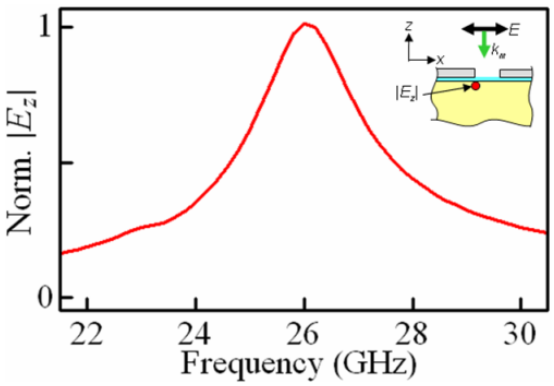

(a)

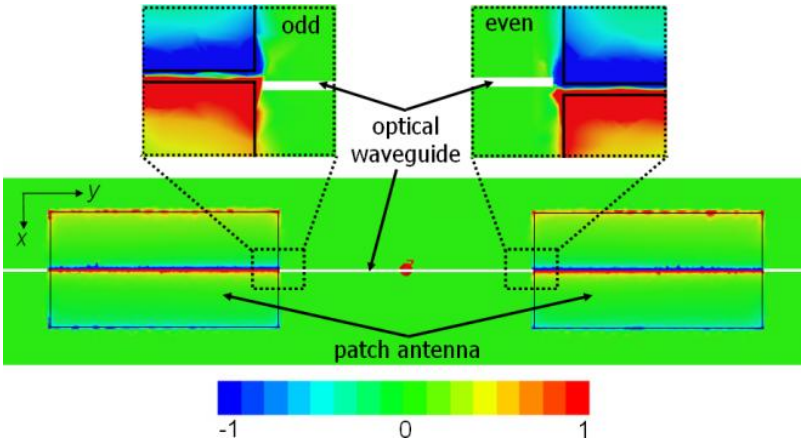

(b)

Figure 6-12 Calculated electric field in the *z*-component under wireless microwave signal irradiation. (a) Magnitude of the electric field across a gap as a function of microwave frequency. (b) Distribution of the electric field on substrate surface.

The directivity in the wireless microwave-lightwave signal conversion using the proposed QPM device can be calculated using Eq. (6-10). The calculated directivity in the designed QPM device is shown in Figure 6-13, when the microwave wireless frequency is set at 26 GHz with 8 antennas and antenna distance of 2.7 mm. The QPM devices with 8 antennas have similar directivity pattern with the conventional array structure with 4 antennas. The same directivity pattern is caused by the same wave number of the microwave electric field observed by the lightwave and their spatial relationship between the gap edge and optical waveguide along each patch for effective optical modulation. This is an advantage of the QPM devices with twice patch numbers as the conventional array structure.

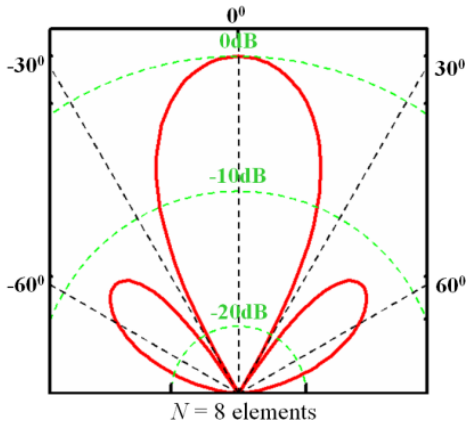

Figure 6-13 Calculated modulation efficiency as a function of wireless irradiation angle of the designed EO modulator using a QPM array of gap-embedded patch-antennas.

In the proposed device, the temporal phase of the microwave signal on the patch and the transit time effect of the lightwave passing through each patch are considered for optical modulation. The directivity pattern of the proposed device can be tuned with the number of the patches in array structure. In addition, the QPM device structure with twice patch numbers has the same directivity pattern compare with the conventional device structure. In this proposed device beside the number of the patch number, the other important factor to control the directivity pattern is the wave number of the microwave electric field observed by the lightwave along the device and their spatial relationship between the gap edge and optical waveguide along each patch.

6.3.5 Experiment

The designed QPM EO modulator with configuration of shifting position of the antennas as shown in Figure 6-11(a) was fabricated. First, a single-mode straight optical channel waveguide for the wavelength of 1.55 μm was fabricated [56] [57]. Then, a thin SiO_2 buffer layer was deposited on the surface of the substrate. Gap-embedded patch-antennas were fabricated with a 1 μm-thick

aluminum film on the buffer layer. Finally, the reverse side of the device was covered using a 1 μm-thick aluminum film as a ground electrode. The photographs of the fabricated prototype device are shown in Figure 6-14.

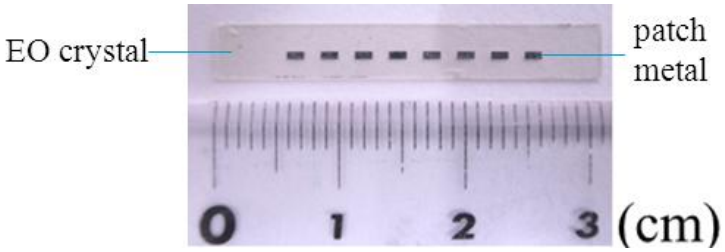

Figure 6-14 A photograph of a fabricated EO modulator using a QPM array of gap-embedded patch antennas.

The experimental setup for measuring the fabricated device is the same as the previous experimental setup as shown in Figure 6-5. A 1.55 μm wavelength lightwave from a laser was coupled to the fabricated device. A 26 GHz microwave signal from a microwave signal generator was irradiated to the fabricated device using a horn antenna. The light output spectrum was measured and monitored using an optical spectrum analyser (OSA).

The modulation efficiency can be calculated from the spectrum intensity ratio between the first sideband and the optical carrier as long as the modulation index value is rather smaller than unity. The examples of the output light spectra measured by an optical spectrum analyzer is shown in Figure 6-15, where the wireless microwave signal was irradiated to the device normally (θ = 0 degree). The modulation sidebands were observed clearly as shown by the solid-curve in Figure 6-15(a), when a linearly-polarized wireless microwave signal perpendicular to the gap was irradiated. The intensity ratio between the sidebands and optical carrier was -42 dB, which corresponds to the modulation index of about 16 mrad.

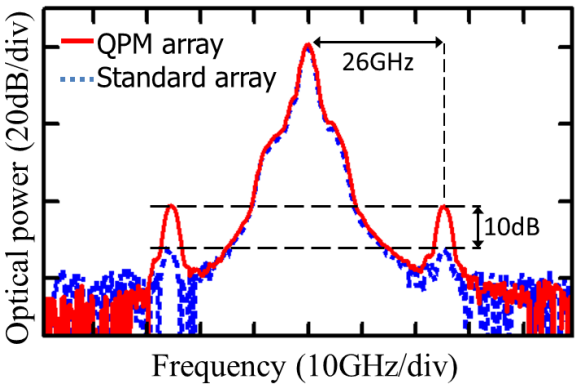

Figure 6-15 Measured output light spectra under microwave wireless signal irradiation of 26 GHz for the QPM array device (solid-curve) and the no QPM array device (dashed-curve).

For comparison, the output light spectrum from the EO wireless microwave-lightwave signal converter using the conventional array structure (no QPM structure) is also shown by the dashed-curve in Figure 6-15(a). In the QPM array structure, the wireless microwave-lightwave signal conversion was improved by about 10 dB compared to the conventional array structure.

Figure 6-16 shows the modulation efficiency as a function of microwave frequency for the QPM devices, when the irradiation angle of wireless microwave signal was set normal to the device (0 degree). The dotted in Figure 6-16 shows the measured modulation efficiency. The peak frequency of the wireless microwave-lightwave signal conversion was about 25 GHz, which almost coincided with the designed operational frequency. The square in Figure 6-16 shows the measured modulation efficiency as a function of microwave frequency for no QPM device (conventional array structure).

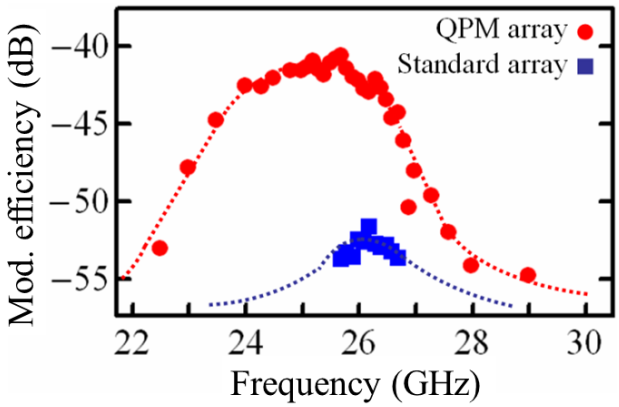

Figure 6-16 Measured frequency dependences of the modulation efficiency with wireless signal irradiation angle of 0 degree (normal direction). The red- and blue-curves show the frequency dependences for QPM array and conventional array structures, respectively.

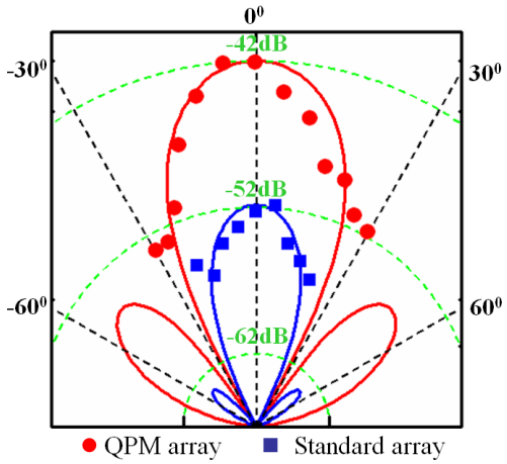

Figure 6-17 Measured modulation efficiency as a function of wireless irradiation angle (directivity). The dotted- and square-shapes show the modulation efficiencies for QPM array and conventional array structures, respectively.

Figure 6-17 shows the modulation efficiency as a function of wireless irradiation angle (directivity), when the operational frequency of the wireless microwave signal was set at 26 GHz. The dotted in Figure 6-17 shows the measured modulation efficiency for the QPM device. The measured directivity is in good agreement with the calculation of the designed device. The square-shape in Figure 6-17 shows the measured directivity of the modulation efficiency in the conventional array structure. We can see that the QPM devices has the same directivity with the conventional array structures, where the QPM device has double antenna number as the conventional array structure.

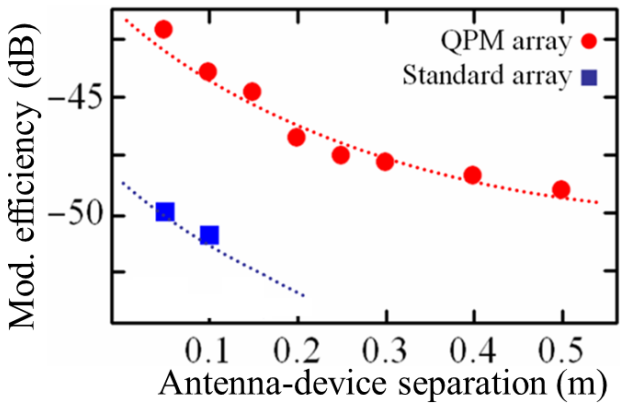

Figure 6-18 Measured modulation efficiency as a function of separation between the antenna and device. The dotted- and square-shapes show the separation dependences for QPM array and conventional array structures, respectively.

Figure 6-18 shows the modulation efficiency as a function of the separation, *R*, between the horn antenna and the fabricated device. The dotted in Figure 6-18 shows the measured modulation efficiency for the QPM device. The optical sidebands were observed with a separation up-to 1 m between the horn antenna and the device. The square-shape in Figure 6-18 shows the measured antenna and device separation dependence of the modulation efficiency in the array structures.

The basic operations of the proposed QPM device were demonstrated successfully. Improved modulation efficiency of about 10 dB was obtained using the proposed QPM device. The QPM technique is effective to improve the modulation efficiency to be double. The proposed device has the same device length and twice antenna compared with the no QPM device.

6.3.6 Modulation efficiency improvement

By adding new planar antennas between the previous antennas in the array structure, the modulation efficiency can be improved. The modulation efficiency is proportional to the number of the antenna in the array structure. In order to achieve the modulation efficiency, the transit time of the lightwave passing through each planar antenna must be considered.

The EO modulators using new QPM array of planar antennas have more compact structure since the antennas become dense in the array structure compared to the conventional array structure. The QPM array device has twice antenna number with the same length compared to the no QPM array device. By considering the transit time of the lightwave using a QPM method, double modulation efficiency can be obtained.

In the experiment, modulation efficiency improvement of 10 dB was obtained experimentally compared to the conventional array structure. The device is easy in the design and fabrication with more compact device and simple QPM method.

6.3.7 Demonstration of ROF links

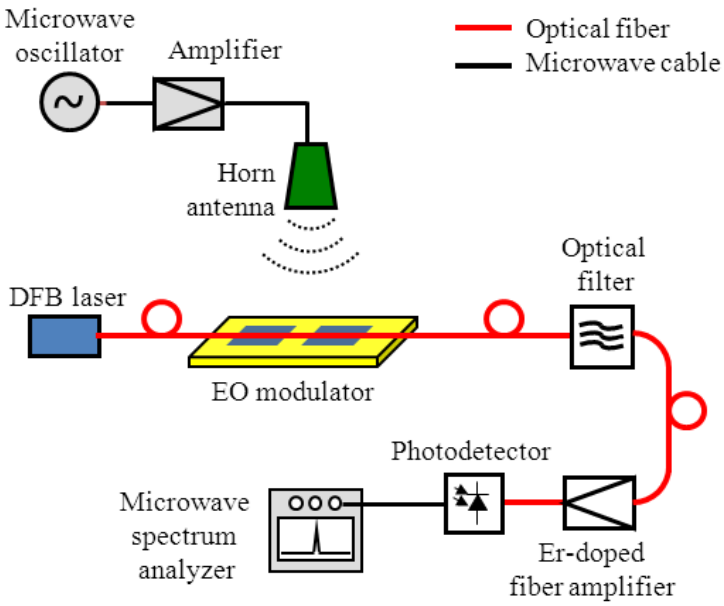

Figure 6-19 Experimental setup for a ROF link demonstration using the proposed device.

In this section, a ROF link using the proposed device is discussed for demonstrating the data transfer. Figure 6-19 shows the experimental setup for demonstration of the ROF links. The lightwave with a wavelength of 1.55 μm from a laser was modulated using the QPM EO modulator with gap-embedded patch antennas under the irradiation of a wireless microwave signal of 26GHz. The phase modulated lightwave signal was propagated through an optical fiber. The propagated lightwave signal was filtered by an optical tunable filter that allows wavelength tuning manually around 1.55 μm wavelength with fixed pass-band width and sharp-cut filtering. The optical filter is operated to cut the lower sideband component and to suppress the optical carrier. As a result, the power ratio between optical sideband and carrier can be enhanced to increase an effective modulation index. After that, it

was amplified by an erbium-doped optical fiber amplifier. Then, the filtered and amplified lightwave signal was detected by use of a high-speed photo-detector. The detected signal (re-converted signal from the lightwave to microwave) was observed using microwave spectrum analyzer.

By using the optical filter, the lower sideband component was cut and the optical carrier was also reduced. As a result, power ratio between the optical carrier and sideband can be improved. The measured optical spectrum after the optical filter is shown in Figure 6-20. Single sideband with -6 dB intensity ratio between the sideband and optical carrier was obtained. Therefore, the effective modulation efficiency (the +1st sideband to optical carrier ratio) was improved about 35dB compared with Figure 6-15 due to optical filtering. The filtered lightwave signal was amplified with optical power of about -25 dBm.

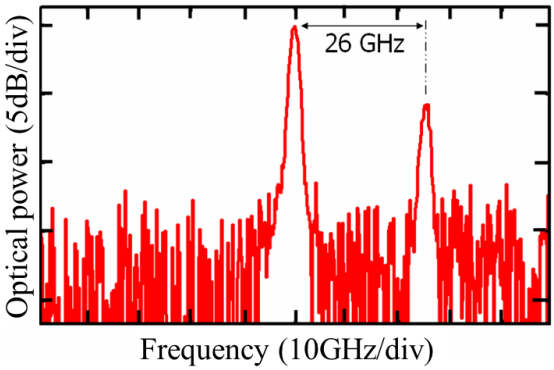

Figure 6-20 Measured light spectrum after pass through an optical filter.

By using the photonic technology, the modulation efficiency of the proposed device can be improved. The single sideband can be also obtained by cutting one sideband with an optical filter. The lightwave with single sideband is easy to detect by a photo-detector for converting the lightwave to microwave signals.

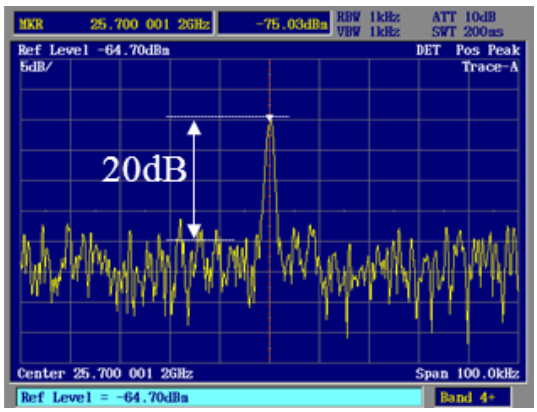

Figure 6-21 Detected microwave signal through radio-over-fiber links.

Figure 6-21 shows the microwave spectrum of the reconverted 26 GHz signal from the photodiode. The spectrum of the reconverted microwave signal is observed clearly. The carrier to noise ratio (CNR) was measured of about 20 dB. The CNR is a one parameter for interpreting the received signal, which has relationship to the data rate and bandwidth. An increased data rate increases bit-error-rate (BER), an increased CNR decreases BER, and an increased bandwidth can be used for increasing data rate [17]. Based on the result when the bandwidth is about 2 KHz, data rate of about 10 Kbps can be achieved.

Regarding the result, higher CNR and large bandwidth are required for transferring data with high data rate through the ROF link. The CNR values can be increased by improving modulation efficiency of the proposed device. The bandwidth can be enlarged by use of high operational frequency. The bandwidth of over 100 MHz can be obtained by using 60 GHz millimeter-wave bands. The modulation efficiency can be improved 12 dB furthermore with four-times numbers of antennas in array structures i.e. 32 antenna numbers. As a result, the CNR of over 30 dB can be achieved. Therefore, the data rate of about 1 Gbps can be realized through ROF link using the proposed device. New 60 GHz millimeter-wave EO modulators using an array of planar antennas on suspended structures are discussed in the Chapter 7.

6.4 EO modulators using a 2-D array of patch antennas embedded with narrow gaps

EO modulators using a 1-D array of patch antennas embedded with a narrow gap were discussed in the sub-chapters 6.2 and 6.3. Modulation efficiency improvement and 1-D wireless irradiation angle control can be obtained using these devices. In this sub-chapter, EO modulators using a 2-D array of patch antennas embedded with orthogonal gaps are proposed and discussed their applications for wireless irradiation angle (beamforming) through optical modulation.

6.4.1 Device structure

Figure 6-22 shows the structure of the EO modulator using 2-D array of patch antennas embedded with orthogonal gaps. The proposed device is fabricated on a *z*-cut EO crystal substrate. The proposed device is composed of optical waveguides and *N*x*N* array of patch antennas embedded with two orthogonal gaps. The antenna size is set to *L*x*L* with a micrometer-order gap width at the center. Meandering gaps are introduced also in the proposed device. The optical waveguides are located under the edge of the gaps. A buffer layer is inserted between the substrate and the antennas. The reverse side of the substrate is covered with a ground electrode.

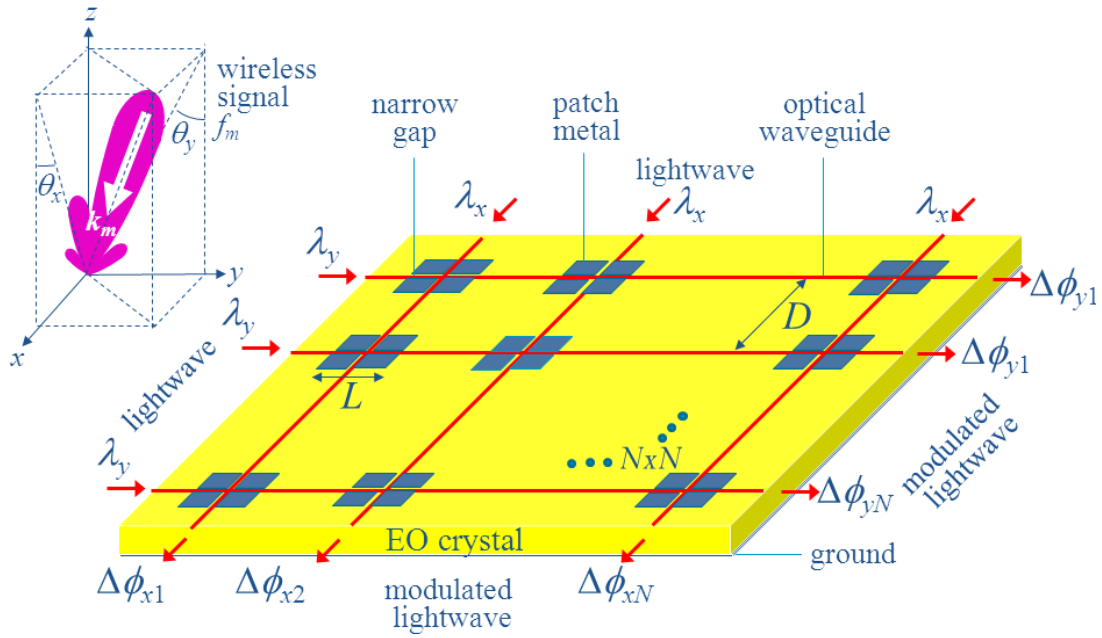

Figure 6-22 Structure of the EO modulator using a 2-D array of patch antennas embedded orthogonal gaps, (a) whole view, (b) cross section view for the *yz*-plane, (c) and cross section view for the *xz*-plane.

The proposed device is basically composed of the patch antennas embedded with orthogonal gaps. The operations of the EO modulator using a patch antenna embedded with orthogonal gaps were discussed in the Chapter 4 [68] [81]. Displacement currents and electric field are induced across the orthogonal gaps for the continuity of the current flow. The strong electric field across the gaps can be used for optical modulation. The modulated lightwave signals are obtained from two optical waveguides. By using array structure, the modulation efficiency can be improved and wireless irradiation angle can be effectively received by controlling the antenna distance. Furthermore, the beamforming of wireless microwave signal can be received using the array structure with meandering gaps and synthesized through optical modulation, when the antenna distance is kept the same for several wireless irradiation angles.

6.4.2 Operational principle

6.4.2.1 Microwave electric field observed by lightwave

The transit time of the lightwave in the array structure was discussed before in the sub-chapters 6.2 and 6.3. In order to improve the modulation index and control wireless beamforming, an array structure of the EO modulators using patch antennas embedded with orthogonal gaps can be adopted as shown in Figure 6-22. When the distance of the patch antennas in the array structure are set D and wireless microwave signal with irradiation angle of θ_y for the *yz*-plane and θ_x for the *xz*-plane is

irradiated to the proposed device, the microwave electric field observed by the lightwave at the h_x- and h_y-th patch antenna can be expressed as following equations for two optical lightwave signal,

$$E^{h}_{x-light}(y) = E_{x0}\cos\left[k_m n_{gy} y - (h_x - 1)D\ k_m n_0 \sin\theta_y + \zeta_y\right] \quad (6\text{-}11)$$

$$E^{h}_{y-light}(x) = E_{y0}\cos\left[k_m n_{gy} x - (h_y - 1)D\ k_m n_0 \sin\theta_y + \zeta_y + \varphi\right] \quad (6\text{-}12)$$

where θ_y and θ_x are the wireless irradiation angles for *yz*- and *xz*-planes, respectively.

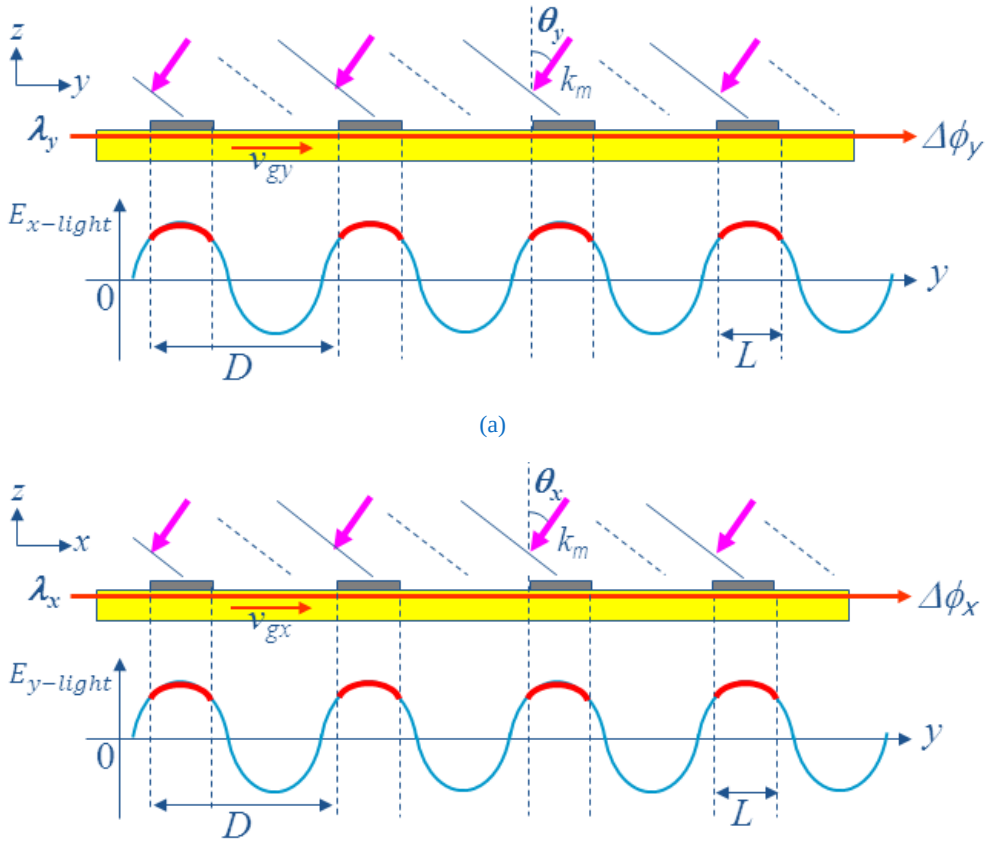

Figure 6-23 Microwave electric field observed by lightwave in the waveguide along (a) *y*-axis and (b) *x*-axis

The microwave electric field observed by lightwave is shown in sinusoidal in the Figure 6-23. Figure 6-23(a) and Figure 6-23(b) show the microwave electric observed by lightwave in the waveguide along the *y*-axis and *x*-axis, respectively.

6.4.2.2 *Optical modulation in orthogonal gaps*

The modulation index, $\Delta\phi$, can be determined by summing the integration of the microwave electric field observed by the lightwave along each antenna width (from $y = (h-1)D$ to $y = (h-1)D + L$). The modulation indices for two orthogonal lightwave signals can be expressed as following equations [65]

$$\Delta\phi_x(\theta_y) = \frac{\pi r_{33} n_e^3}{\lambda_y} \Gamma \sum_{h=1}^{N} \int_{(h-1)D}^{(h-1)D+L} E_{x-light}^{h}(y)dy \tag{6-13}$$

$$\Delta\phi_y(\theta_x) = \frac{\pi r_{33} n_e^3}{\lambda_x} \Gamma \sum_{h=1}^{N} \int_{(h-1)D}^{(h-1)D+L} E_{y-light}^{h}(x)dx \tag{6-14}$$

The modulation indices of the proposed device can be improved by using an array structure. The modulation indices as a function of the wireless irradiation angle can be calculated using Eq. (6-13) for the *yz*-plane and Eq. (6-14) for *xz*-plane.

6.4.2.3 *Meandering gaps*

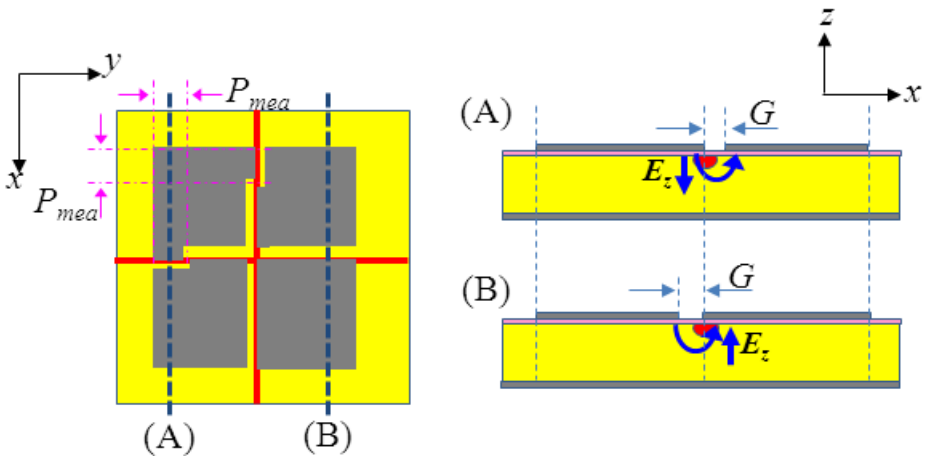

Figure 6-24 Typical of meandering gaps in the EO modulator using a 2-D array of patch antennas embedded orthogonal gaps.

The spatial relationship between the gap edge and optical waveguide was discussed before as shown in Figure 6-11. Since the microwave electric field in the *z*-component is considered, the degradation of optical modulation can be compensated. The modulation index of the proposed device has a function of the wireless irradiation angles. When the distance of the antennas in the proposed device is designed effectively for normal wireless irradiation angle, the optical modulation degradation

might be induced for other wireless irradiation angles. In order to compensate for the degradation, several techniques for change the polarity of interaction between the microwave and lightwave electric fields can be adopted such as polarization reversal of the EO crystal or others [76] [75].

In here, I proposed new technique to solve the problem by using meandering gaps. The typical meandering gaps are shown in Figure 6-24. We can see that the relationship between the gap edge and optical waveguide is spatially changed by introducing the meandering gap. This new technique has a simple structure. By changing interaction between the gap edges and optical waveguide, the optical modulation degradation can be compensated for.

Modulation indices from the two optical waveguides of the proposed device using the meandering gaps are

$$\Delta\phi_y(\theta_y) = \frac{\pi r_{33} n_e^3}{\lambda_y}\Gamma \sum_{h=1}^{N}\left[P_{mea}(y)\int_{(h-1)D-\frac{L}{2}}^{(h-1)D-\frac{L}{2}+P_{mea}} E_{m-light}^{h}(y)\,dy + P_{mea}(y)\int_{(h-1)D-\frac{L}{2}+P_{mea}}^{(h-1)D+\frac{L}{2}} E_{m-light}^{h}(y)dy\right] \quad (6\text{-}15)$$

$$\Delta\phi_x(\theta_x) = \frac{\pi r_{33} n_e^3}{\lambda_x}\Gamma \sum_{h=1}^{N}\left[P_{mea}(x)\int_{(h-1)D-\frac{L}{2}}^{(h-1)D-\frac{L}{2}+P_{mea}} E_{y-light}^{h}(x)\,dx + P_{mea}(x)\int_{(h-1)D-\frac{L}{2}+P_{mea}}^{(h-1)D+\frac{L}{2}} E_{y-light}^{h}(x)dx\right] \quad (6\text{-}16)$$

where $P_{mea}(y)$ is the interaction between the gap edges and optical waveguides as shown in Figure 6-24 with the polarity sign of +1 or –1.

6.4.3 Analysis

6.4.3.1 1-D beamforming receiving

I analyzed the proposed device for microwave signal with operational frequency of 26 GHz. The detailed parameters of the proposed device are shown in Table 6-3. Figure 6-25 shows the patterns of the meandering gaps along *y*-axis in the 2-D array of patch antennas embedded with narrow gaps. The pattern was designed for 1-D beamforming receiving in the *yz*-plane for several wireless irradiation angles. The modulation indices can be calculated using Eq. (6-15). By considering the patterns of the meandering gaps in Figure 6-25, the calculated modulation indices are shown in Figure 6-26 for several wireless irradiation angles. We can see that the modulated lightwave $\Delta\phi_{y1}$ using the

pattern are effectively operated for wireless irradiation angle of -30 degrees. The normal wireless irradiation angle can be obtained from the modulated lightwave $\Delta\phi_{y3}$. The other patterns are used effectively other wireless irradiation angles.

Table 6-3 Device parameters for optical modulation analysis of EO modulators using 2-D array of patch antennas embedded with orthogonal gaps.

	Values
Microwave signal	
Operational frequency, f_m	26 GHz
EO crystal ($LiTaO_3$)	
Thickness, h	0.4 mm
EO effect, r_{33}	30.3 pm/V
Refractive index, n_e	2.125
Group index, n_g	2.168
Lightwave	
Wavelength, λ	1.55 μm
Patch antenna	
Antenna size, LxL	0.8 x 0.8 mm
Gap width, G	5 μm
Array structure	
Number, NxN	5x5 elements
Distance, D	5.4 mm

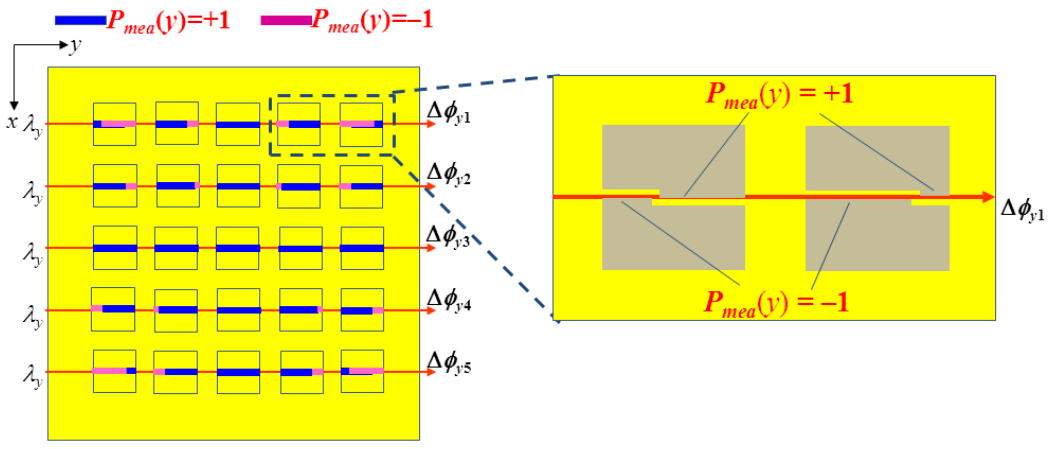

Figure 6-25 Meandering gap pattern for 1-D beam forming receiving of the wireless irradiation angles.

The wireless irradiation angle can be tuned by using meandering gap structures. By adopting the technique, modulation indices along *x*-axis for the *xz*-plane using the EO modulator using a 2-D array patch antennas embedded with orthogonal gaps can be calculated also. Based on that, the modulation indices for wireless irradiation angle in 1-D for *yz*-plane or *xz*-plane can be obtained independently [73].

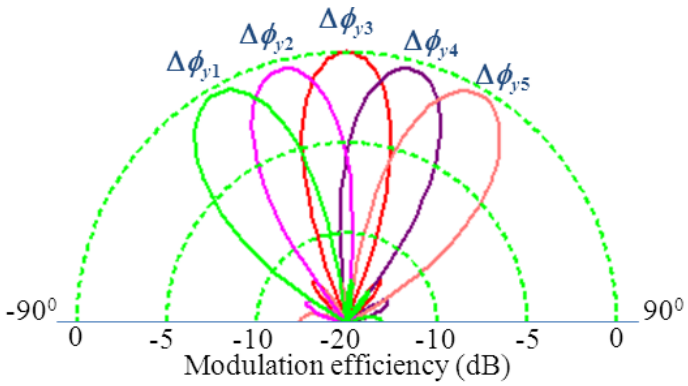

Figure 6-26 Calculated modulation indices as a function of wireless irradiation angle for several patterns of the meandering gaps.

6.4.3.2 2-D beamforming receiving

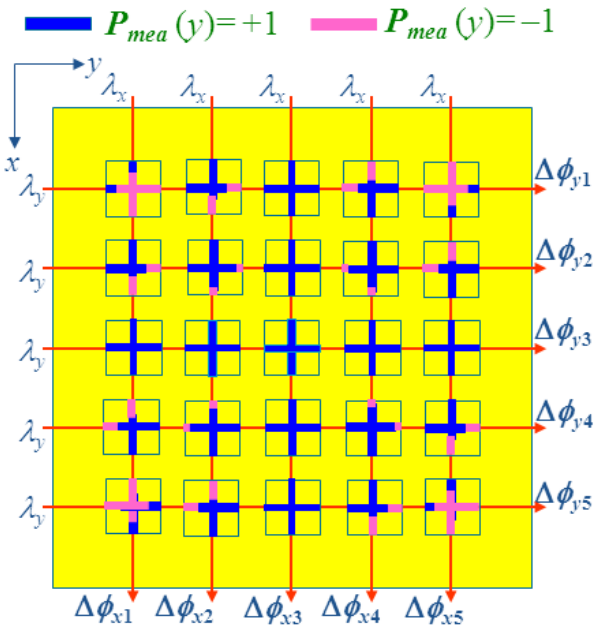

Figure 6-27 Meandering gap pattern for 2-D beamforming receiving of wireless irradiation angles.

In the previous sub-chapter, 1-D beamforming receiving of wireless microwave by use of using 2-D array structure was discussed. In here, an EO modulator using a 2-D array of patch antennas embedded with orthogonal meandering gaps are proposed for 1-D and 2-D beamforming receivers. The pattern of the meandering gaps in EO modulator using a 2-D array of patch antennas embedded with orthogonal gaps is shown in Figure 6-27. 1-D beamforming receiving in *xz*- and *yz*-planes can be obtained independently by calculating the modulation indices using Eq. (6-15) and Eq. (6-16).

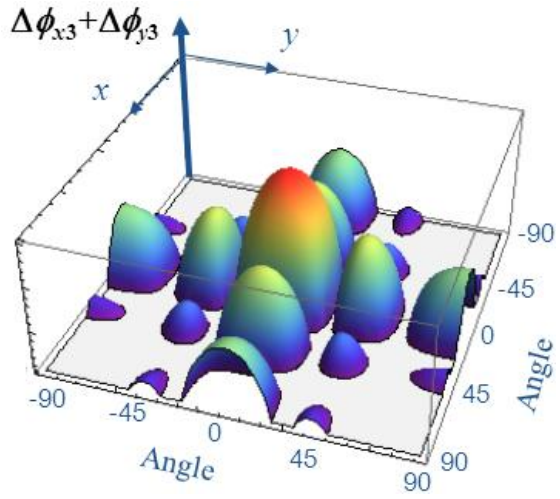

(a)

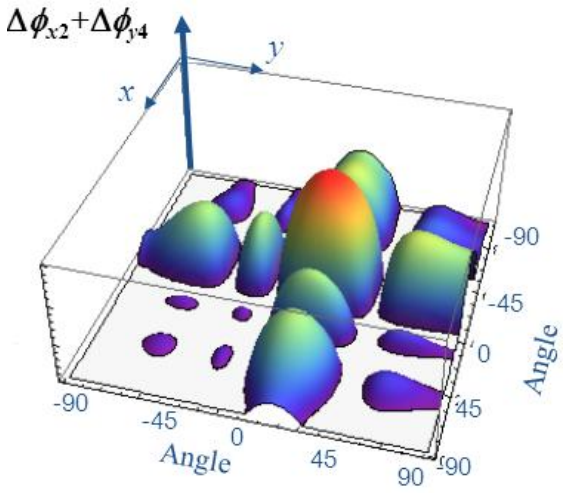

(b)

Figure 6-28 Calculated modulation index as a function of 2-D wireless irradiation angle.

2-D beamforming receiving of wireless microwave signal can be achieved using the proposed device by considering two orthogonal modulated signals simultaneously [68]. The modulation indices as a function of 2-D wireless irradiation angle in *xyz*-space, can be calculated using following equation,

$$\Delta\phi(\theta_x, \theta_y) = \Delta\phi_x(\theta_x) + \Delta\phi_y(\theta_y) \quad (6\text{-}17)$$

By taking into account of the modulation indices of two orthogonal modulated signals, 2-D wireless irradiation angles can be identified using the proposed device. The typical of the calculated modulation index for the proposed device using the parameters in Table 6-3 is shown in Figure 6-28. In Figure 6-28(a) shows the modulation efficiency as a function of 2-D beamforming for effective operation by normal wireless irradiation angle (θ_x = θ_y = 0 degree). In Figure 6-28(b) shows the modulation efficiency as a function of 2-D beamforming for effective operation by normal wireless irradiation angle θ_x = +15 degree, θ_y = – 15 degree). Based on the analysis, the proposed device can be used for receiving wireless microwave signal with 2-D beamforming and converting the signal to the lightwave signal directly. Therefore, EO beamforming receiver using a 2-D array of patch antennas embedded with orthogonal meandering gaps can be realized [73].

6.4.4 Beamforming control

In order to improve the device functionality, an EO modulator using a 2-D array of patch antennas embedded with orthogonal narrow gaps was also proposed. The wireless irradiation angle (beamforming) can be effectively received and controlled by considering the microwave electric field observed by lightwave at each patch antenna.

The certain beamforming of the wireless signal can be controlled by changing the distance of the array structure. When the distance is fixed and beamforming is changed, the degradation of optical modulation might be occurred. In order to compensate for the degradation, a new technique was proposed using meandering gaps. 1-D beamforming receiving can be obtained by EO modulator using a 2-D array of patch antennas embedded with meandering gaps by calculating the modulation lightwave signal separately and independently. Furthermore, an EO modulator using a 2-D array of patch antennas embedded with orthogonal meandering gaps can be used for 2-D beamforming receiving by calculating two orthogonal modulated lightwave signals simultaneously.

6.5 Discussion and summary

EO modulators using an array of planar antennas were proposed for enhancing modulation efficiency and beamforming control [75] [82]. Increasing planar antenna number in array structure is effective for increasing modulation efficiency. Consideration of the transit time of lightwave passing through at each planar antenna is required for achieving effective optical modulation.

A new technique to improve modulation efficiency by using a QPM array structure was proposed. Double modulation efficiency is obtained by twice number of the planar antennas with the

same device length compared to the conventional array devices. In the experiment, modulation efficiency improvement of about 10 dB was obtained experimentally. The EO modulators using QPM array structures have the same radiation pattern as the conventional EO modulator using array structures. A ROF link using this proposed device was also demonstrated. The measured carrier to noise ratio of about 20 dB was obtained. Higher CNR and large bandwidth are required for transferring data with high data rate through the ROF link by improving modulation efficiency of the proposed device with array structures and by use of high operational frequency.

Furthermore, an EO modulator using a 2-D array of patch antennas embedded with orthogonal gaps was proposed. New technique of meandering gaps to compensate for optical modulation degradation was used. It has simple structure and additional fabrication process. By using the proposed device, 1-D beamforming receiving can be obtained by analyzing each modulated lightwave signals independently. By analyzing two orthogonal modulated lightwave signals, 2-D beamforming receiving of wireless microwave signal can be obtained.

The proposed devices have simple and compact structure and can be operated with low microwave loss and no external power supply. Furthermore, they are easy in design and fabrication. This device can be used for communication systems in multiple-input-multiple-output (MIMO), space-division-multiplexing-access (SDMA) schemes, and surveillance radar.

Chapter 7 Optical Modulators Using Electro-Optic Waveguides Suspended to Planar Antennas on Low-*k* Dielectric Substrate

7.1 Introduction

In the Chapter 3, Chapter 4, and Chapter 5, optical modulators using planar antennas for wireless microwave-lightwave signal conversion were proposed and discussed [64] [69] [68]. The basic operations of the proposed device were successfully verified in the experiment. They were fabricated on an electro-optic (EO) crystal substrate. The proposed devices have simple and compact structure and can be operated with low microwave loss and no external power supply. The efforts to improve the modulation efficiency using an array structure were also discussed in the Chapter 6 [75] [80].

In order to improve furthermore the modulation efficiency, the antenna is considered to be a large size to improve the antenna apertures and receiving power. A high-*k* EO crystal such as $LiNbO_3$ or $LiTaO_3$ was used for realizing optical modulators using planar antennas in the previous chapter. The antenna aperture can be enlarged using low effective dielectric constant. As a result, interaction length between microwave and lightwave electric field becomes also longer than the device fabricated on an EO crystal substrate.

In this chapter, I propose new optical modulators using EO waveguides suspended to planar antennas on a low-*k* dielectric substrate for wireless millimeter-wave-lightwave signal conversion. By using a thin EO crystal (<100μm) suspended on the low-*k* dielectric substrate, the effective dielectric constant value becomes low to realize a large size of the planar antennas for obtaining high gain. As a result, high received power can be obtained, since the patch antenna size becomes large. The interaction length of the millimeter-wave and lightwave electric fields can be longer. Therefore, the modulation index can be improved using the proposed devices compared to the devices fabricated on a high-*k* EO crystal substrate. The substrate resonant modes for high frequency operation are also eliminated since the thin EO crystal is used.

The proposed EO modulators have simple and compact structures. They can be operated with low millimeter-wave loss and no external power supply. The proposed devices are easy in the design and fabrication. Basically, the proposed devices are used for converting from wireless millimeter-wave to lightwave signals. In addition, a wireless microwave signal can be characterized using the proposed devices through EO modulation with larger modulation index.

In the following sections, I will present the device structure, operational principle, analysis, fabrication, and measurement of optical modulator modulators using an EO crystal suspended to planar antennas on a low-*k* dielectric substrate. The proposed device advantages/ disadvantages and applications to wireless millimeter-wave to lightwave signal conversion are also discussed.

7.2 Antenna size

An antenna size for receiving a wireless millimeter-wave signal at an operational frequency of f_m can be calculated using Eq. (2-1) [40]. The size of the metal patch is inversely proportional to the square-root of the effective dielectric constant. By reducing the effective dielectric constant, the size of the antenna is increased. In order to reduce the effective dielectric constant of the antennas for the wireless millimeter-wave-lightwave signal conversion, a new device structure with low effective dielectric constant can be obtained by stacked/ suspended structure between a thin EO crystal and low-*k* dielectric material.

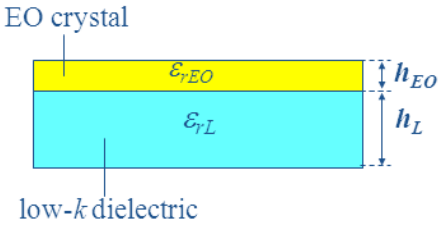

Figure 7-1 Configuration of suspended/ stacked structures.

The effective dielectric constant of the stacked/ suspended structures is expressed as [47]

$$\frac{1}{\varepsilon_{eff}} = \frac{\left(\frac{h_L}{\varepsilon_{rL}} + \frac{h_{EO}}{\varepsilon_{rEO}}\right)}{h_L + h_{EO}} \tag{7-1}$$

where ε_{rL} and h_L are the dielectric constant and thickness of the low-*k* dielectric substrate, respectively, and ε_{rEO} and h_{EO} are the dielectric constant and thickness of the EO crystal, respectively. By using a stacked/ suspended structure with a rather thin EO crystal (<100μm), the effective dielectric constant becomes low and it is almost close to the dielectric constant of the low-*k* dielectric substrate.

7.3 Device structure

The structure of the proposed optical modulators using an EO crystal suspended to gap-embedded patch antennas on a low-*k* dielectric material substrate is shown in Figure 7-2. An optical waveguide and patch antennas embedded with a narrow gap are fabricated on the bottom surface of a thin EO crystal (<100μm), like $LiNbO_3$ or $LiTaO_3$. The EO crystal is suspended to a low-*k* dielectric material. The metal patch length, *L*, and width, *W*, are set. The gap width, *G*, is on the order of a micrometer, and the gap itself is located at the center of the patch along the *y*-axis. An array of the gap-embedded patches is set with a distance of *D*. The optical waveguide is located on the one side of the gap edge, where the cross-sectional view of the proposed device is shown in Figure 7-2(b). A buffer layer is inserted between the metal patch and EO crystal. The EO crystal and low-*k* dielectric substrate are attached by use of an optical adhesive. The reverse side of the low-*k* dielectric material is covered by a ground metal.

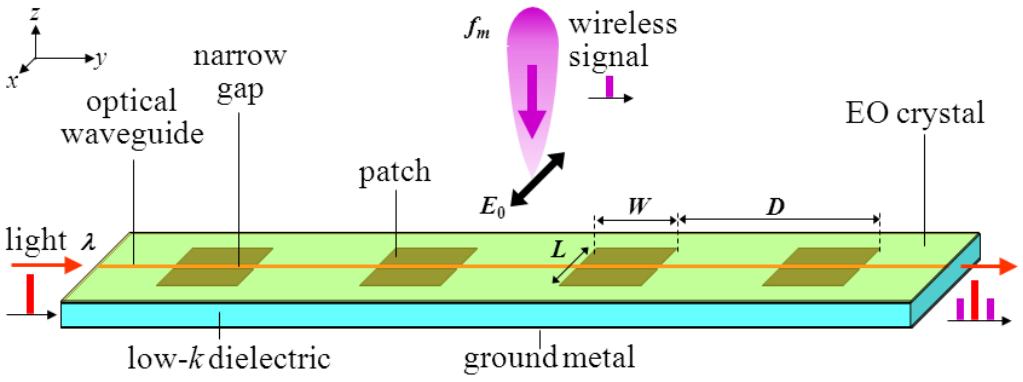

(a)

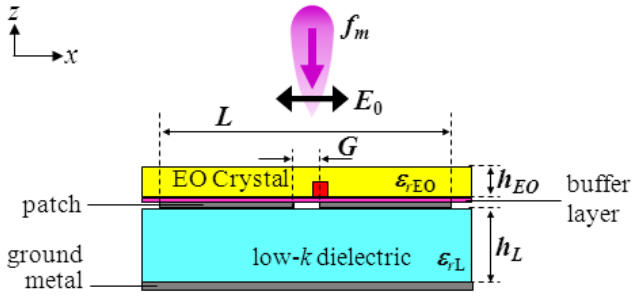

(b)

Figure 7-2 Device structure of optical modulators using an EO waveguide suspended to gap-embedded patch antennas on a low-*k* dielectric substrate.

The operational principles of the EO modulators using patch antennas embedded with a narrow gap were discussed in the Chapter 3. By utilizing displacement current and electric field across the gap, optical modulation can be obtained through the Pockels effects of an EO crystal. In this chapter, the proposed devices are fabricated on the suspended/ stacked structure between an EO crystal and low-*k*

dielectric substrate [83]. Low effective dielectric constant can be obtained for enlarging the antenna aperture size. Since the patch size is larger, millimeter-wave signal power received by the antennas is also larger. The electric field across the gap becomes stronger and the interaction length between the microwave and lightwave becomes longer than the EO modulators fabricated an EO crystal substrate. As a result, the modulation efficiency can be improved by using the proposed device.

7.4 Operational principle

7.4.1 Millimeter-wave electric field

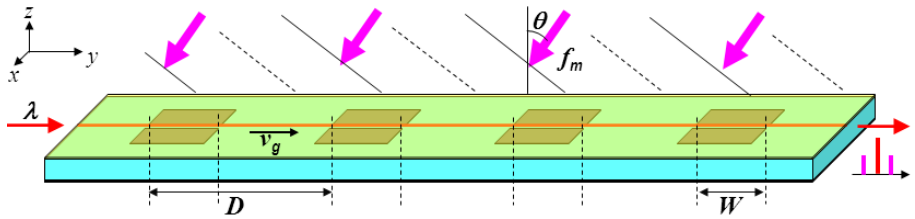

(a)

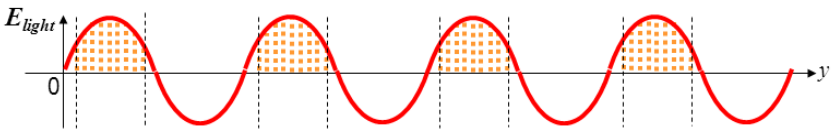

(b)

Figure 7-3 Operational principle of the proposed millimeter-wave optical modulator. (a) The proposed device under wireless irradiation angle of θ degrees. (b) The millimeter-wave electric field as would be observed by the lightwave. Conversion efficiency corresponds to sum of the shaded areas.

I have discussed operational principle of the EO modulators using an array of planar antennas in the Chapter 6. When the proposed optical modulators are irradiated with a wireless millimeter-wave signal, the millimeter-wave electric field in the free space above the proposed devices can be expressed as Eq. (6-1). Assuming that the position of the patch antenna is set at $z = 0$, and that the millimeter-wave electric field is not distorted by the patch antennas, the received millimeter-wave electric field by the h-th patch is shown in Eq. (6-2).

A millimeter-wave electric field is induced across the narrow gap in the h-th antenna. The induced millimeter-wave electric field across the gap is utilized for optical modulation through the Pockels effect. Therefore, millimeter-wave signals can be received and converted directly to lightwave signals.

7.4.2 Optical modulation

In the Chapter 6, optical modulation of the EO modulators using planar antennas was discussed. The modulation efficiency can be calculated by considering the interaction of the millimeter-wave and lightwave electric fields. In order to calculate the modulation index, the transit time effect must be considered since the millimeter-wave electric field across the gap changes its phase during the time for the lightwave propagation. Therefore, the millimeter-wave electric field as would be observed by the lightwave propagating in the optical waveguide, can be expressed by Eq. (6-4) with taking into account the transit-time of the lightwave. The millimeter-wave electric field as would be observed by the lightwave is shown by the sinusoidal-curve in Figure 7-3.

The modulation index can be calculated by the integration of the millimeter-wave electric field as would be observed by the lightwave along the gap-embedded patch antennas. It can be represented as Eq. (6-5). The overlap factor of the millimeter-wave and lightwave electric fields depends on the EO crystal orientation and optical field polarization. The modulation index of the proposed device corresponds to the sum of the shaded areas in Figure 7-3(b). Eq. (6-4) shows the modulation index as a function of the irradiation angle of the wireless millimeter-wave signal. The wireless irradiation angle for effective signal conversion is related to the distance between the antennas in the array structure. The effective irradiation angle can be adjusted also by changing the antenna distance or phase-inversed structures [60] [44].

7.5 Analysis

7.5.1 Millimeter-wave characteristics

The millimeter-wave characteristics of the proposed device were analyzed in detail using 3-D electromagnetic analysis software, HFSS. The device parameters for the millimeter-wave analysis are shown in Table 7-1.

In order to achieve effective operation, the EO crystal orientation, the distribution of the millimeter-wave electric field across the gap, and position of the waveguide must be taken into account. Since a *z*-cut $LiTaO_3$ crystal is used in the analysis, the optical waveguide should be set on one side of the gap edge, as shown in Figure 7-2(b). Therefore, the millimeter-wave electric field in the *z*-component, E_z, on one side of the gap edge is the dominant contribution for optical modulation using the Pockels effect.

The calculated distribution of the *z*-component of the millimeter-wave electric field is shown in Figure 7-4 for top and cross-sectional views, when the device is irradiated with the 60 GHz wireless millimeter-wave signal. We can see that the strong millimeter-wave electric field is induced on the gap edge.

Table 7-1 Device parameters for analyzing the suspended structure.

	Values
Low-*k* dielectric	
Dielectric constant, ε_{rL}	3.5
Thickness, h_L	130 μm
EO crystal (*z*-cut $LiTaO_3$)	
Dielectric constant, ε_{rEO}, (ε_x,ε_y, ε_z)	(43,43,41)
Thickness, h_{EO}	30–150 μm
Operational frequency, f_m	60 GHz
Gap-embedded patch antennas	
Antenna size, *L*x*W*	0.76 x 0.76 mm
Gap width, *G*	3–30 μm
Buffer layer	
Thickness	0.2 μm

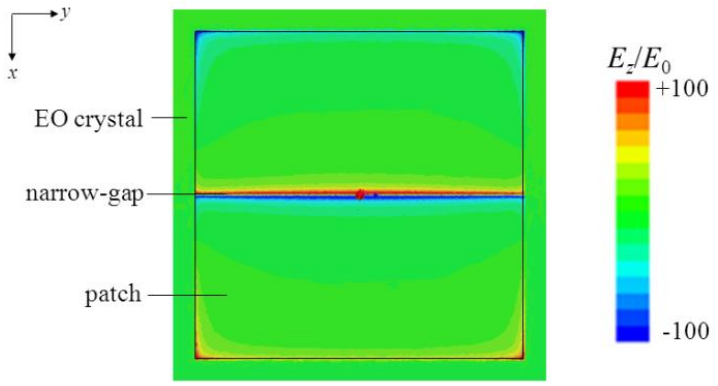

(a)

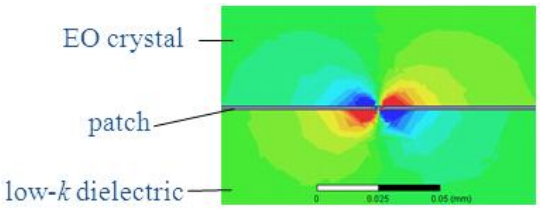

(b)

Figure 7-4 Calculated distribution of millimeter-wave electric field in the *z*-component: (a) top view and (b) cross-sectional view.

Calculated electric field magnitude and peak frequency of the millimeter-wave signal for several EO crystal thickness values are shown in Figure 7-5, when the gap width is set to 5 μm. We can see that the peak frequency becomes larger as the EO crystal becomes thinner, due to lowering of

the effective dielectric constant. The strong magnitude of the millimeter-wave electric field was obtained about 80 μm.

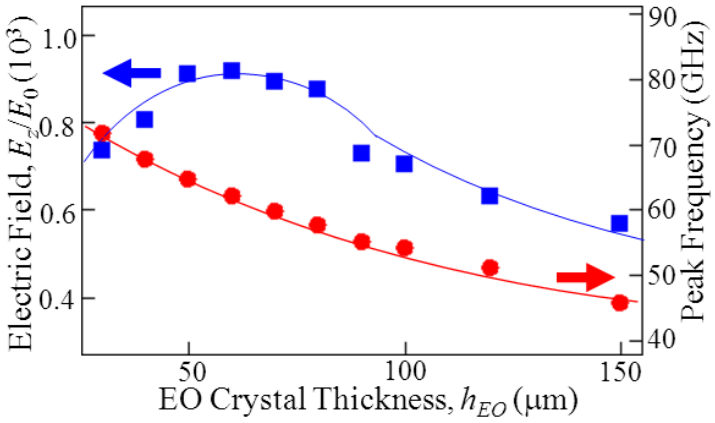

Figure 7-5 Calculated electric field magnitude and peak operational frequency of the millimeter-wave signal for several EO crystal thickness.

The calculated electric field magnitude and peak frequency of the millimeter-wave signal for several gap width values are shown in Figure 7-6, when the EO crystal thickness value is set to 80 μm. When the gap width is narrower, the operational frequency becomes lower due to large capacitance in the gap. The millimeter-wave electric field across the gap becomes strong for the narrower gap width.

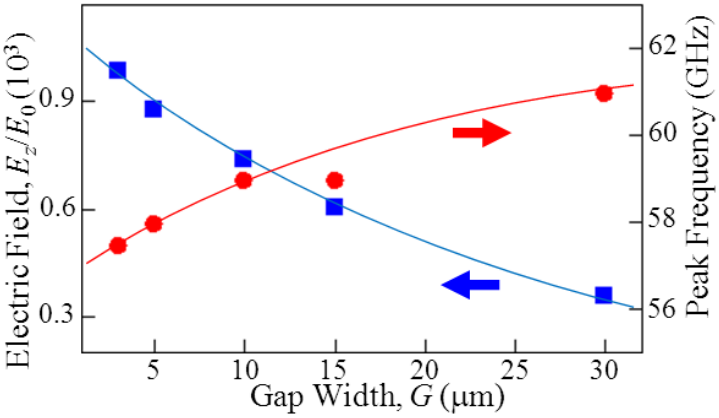

Figure 7-6 Calculated electric field magnitude and peak operational frequency of the millimeter-wave signal for several gap width values.

7.5.2 Modulation index

Based on the results of the millimeter-wave analysis and condition of the experimental device fabrication, the EO crystal thickness of 80 μm and the gap width of 5 μm were selected for a prototype device. The design parameters are shown in Table 7-2. Since the proposed device is phase

modulation with low modulation index below of unity, the modulation index can be expressed for the modulation efficiency from wireless millimeter-wave to lightwave signals. The modulation efficiency of the designed device can be calculated using Eq. (6-4).

Table 7-2 Parameters for design of the suspended device.

	Values
Low-*k* dielectric	
Dielectric constant, ε_{rL}	3.5
Thickness, h_L	130 μm
EO crystal (*z*-cut $LiTaO_3$)	
Dielectric constant, ε_{rEO}, (ε_x,ε_y, ε_z)	(43,43,41)
Thickness, h_{EO}	80 μm
Operational frequency, f_m	60 GHz
Gap-embedded patch antennas	
Antenna size, *L*x*W*	0.8 x 0.8 mm
Gap width, *G*	5 μm
Array structure	
Antenna number, *N*	9 elements
Antenna distance, *D*	2.4 mm
Buffer layer	
Thickness	0.2 μm
Optical waveguide	
Operational wavelength, λm	1.55 μm

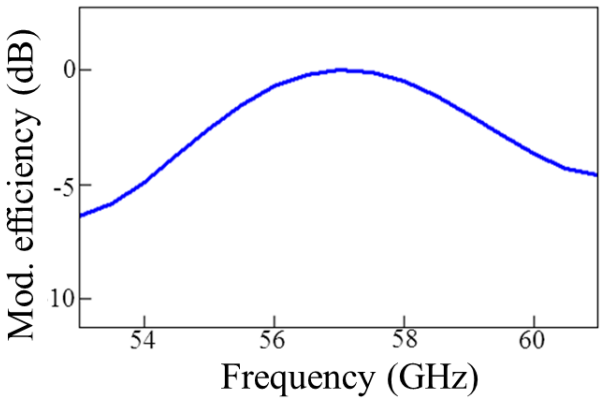

Figure 7-7 Calculated modulation efficiency as a function of operational frequency of wireless millimeter-wave signal.

The calculated modulation efficiency as a function of the operational frequency of the wireless millimeter-wave signal is shown Figure 7-7. It was obtained by considering the calculated magnitude of the millimeter-wave electric field across the gap. The designed device has effective millimeter-wave signal operational frequency of 58 GHz.

The calculated modulation efficiency as a function of the irradiation angle of the wireless millimeter-wave signal is shown in Figure 7-8. The effective modulation efficiency is obtained with the device irradiated by the wireless millimeter-wave signal normal to the surface (θ = 0 degree).

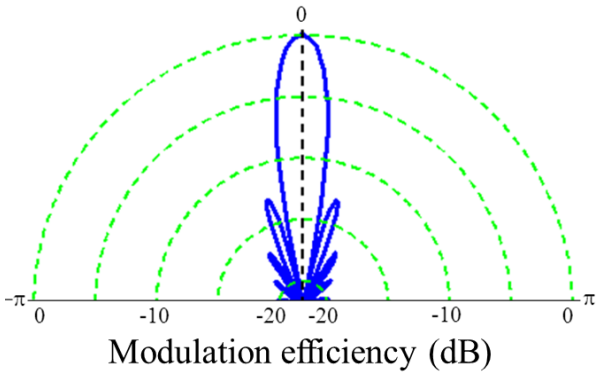

Figure 7-8 Calculated modulation efficiency as a function of irradiation angle of the wireless millimeter-wave signal.

7.6 Fabrication

The designed millimeter-wave-lightwave signal converter was fabricated. The fabrication process of the designed device is illustrated in Figure 7-9.

First, a *z*-cut $LiTaO_3$ EO crystal with a thickness of 250 μm was prepared. Then, a single-mode straight channel optical waveguide was fabricated on the EO crystal using an annealed proton exchange method [56]. A proton exchange process with benzoic acid at 240 ^{O}C for 12 hours and a thermal annealing process at 350 ^{O}C for 1 hour were done. After that, a 0.2 μm-thick SiO_2 buffer layer was deposited on the EO crystal. An array of patch antennas embedded with a narrow-gap was also fabricated on the EO crystal. The antennas were fabricated using a 1 μm-thick aluminum film on the EO crystal through thermal vapor deposition, standard photolithography, and a lift-off technique. The optical waveguide was aligned onto one side of the gap edge.

A ground metal was deposited to the bottom surface of a low-*k* dielectric material. Then, the top surface of a low-*k* dielectric material was covered with an optical adhesive in the bonding process.

In bonding process, the EO crystal was flipped with 180 degrees. So as the metal antennas become on the bottom side of the EO crystal surface. Then, the flipped EO crystal was bonded to the low-*k* dielectric material by exposing ultraviolet (UV) light to the UV-cured optical adhesive [84].

Finally, the 250μm-thick EO crystal was polished to the designed thickness of 80μm using a polishing machine with diamond slurry.

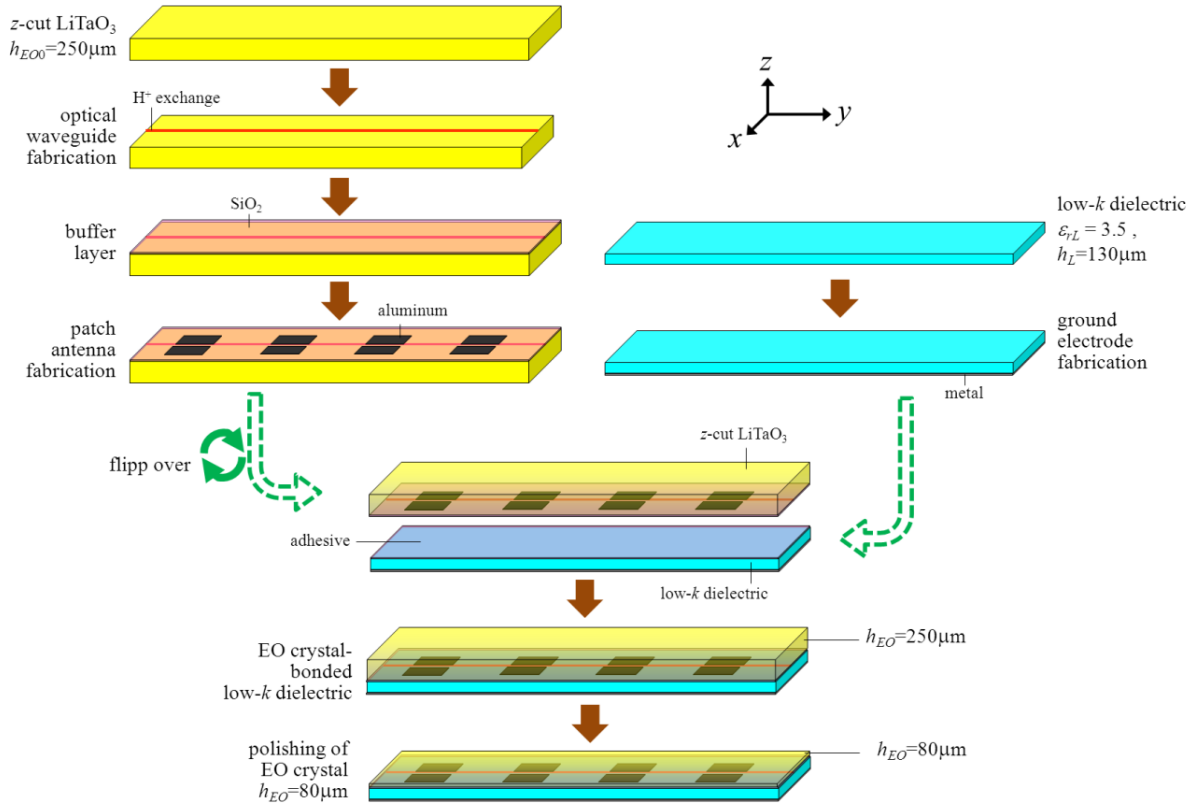

Figure 7-9 The fabrication process of the designed EO modulators for wireless millimeter-wave-lightwave signal conversion.

A photograph of the fabricated device is shown in Figure 7-10. I have fabricated the proposed device with 9 gap-embedded patch antennas. The total length of the fabricated device is about 20 mm.

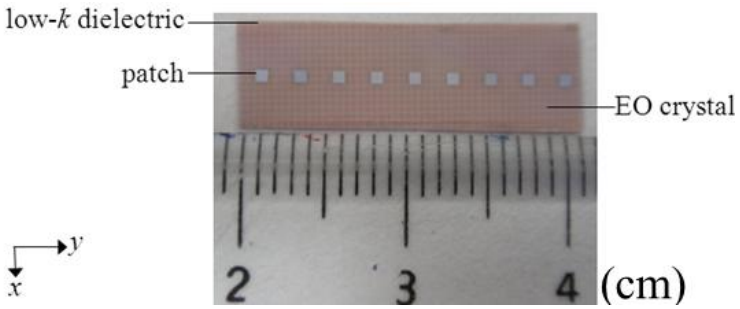

Figure 7-10 A photograph of the fabricated device of the suspended device.

7.7 Measurement

The performance of the fabricated device was measured experimentally with the measurement setup as shown in Figure 7-11. A lightwave of 1.55 μm wavelength from a laser was coupled to the fabricated device through an objective lens. A millimeter-wave signal in the 60 GHz band from a signal generator was amplified and irradiated to the fabricated device using a horn antenna with irradiation power of 20 mW. The output lightwave signal was measured using an optical spectrum analyzer.

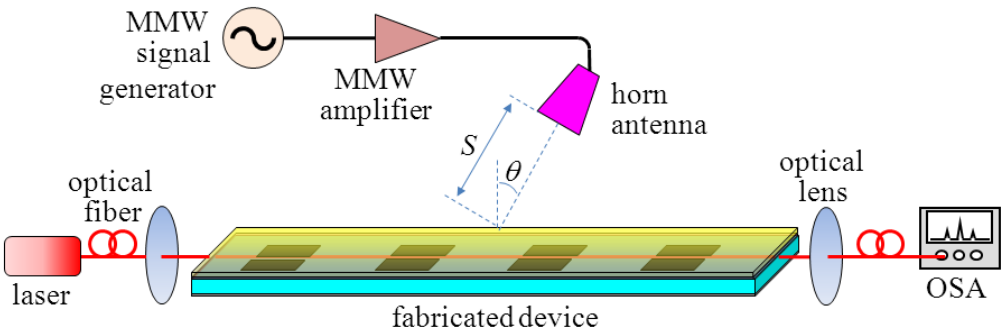

Figure 7-11 Experimental setup for measuring the performances of the suspended optical modulator.

The modulation index is calculated from the spectrum intensity ratio between the first sidebands and the optical carrier when the modulation index is smaller than unity. An example of the measured output light spectrum is shown in Figure 7-12, where a 58 GHz wireless millimeter-wave signal was irradiated at the device at a normal angle ($\theta = 0$ degree). The optical sidebands were observed clearly. The intensity ratio between the sidebands and optical carrier was 50 dB.

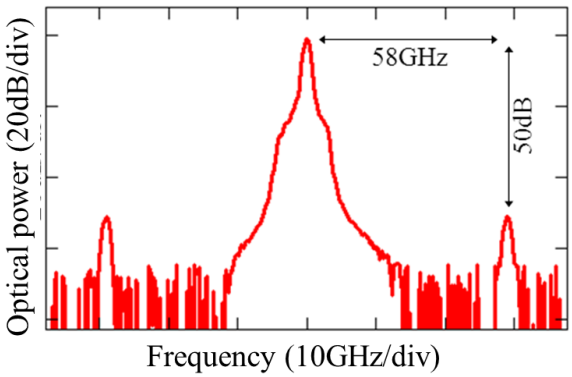

Figure 7-12 Measured output light spectrum by irradiating 58 GHz wireless millimeter-wave signal.

The measured modulation efficiency as a function of millimeter-wave frequency is shown by the dots in Figure 7-13, when the irradiation angle of the wireless millimeter-wave signal was set to be

normal to the device. The peak frequency of the fabricated device was about 58 GHz, which is almost coincided with the calculation result as shown by the solid line in Figure 7-13.

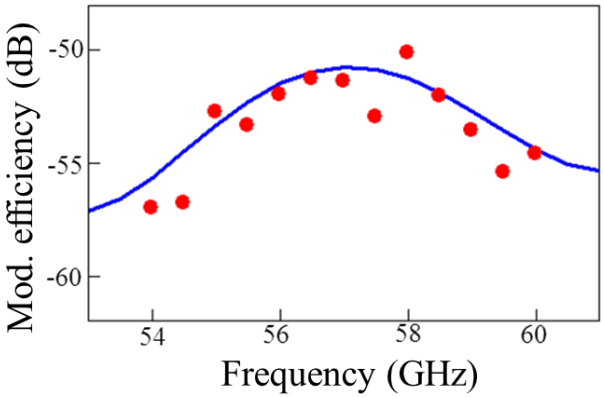

Figure 7-13 Measured modulation efficiency as a function of the operational frequency of the millimeter-wave signals.

Figure 7-14 shows the modulation efficiency as a function of wireless irradiation angle (directivity) in the *xy*-plane. The dots in Figure 7-14 shows the measured modulation efficiency, when the frequency of the wireless millimeter-wave signal was set at 58 GHz. The largest modulation efficiency was obtained with a normal irradiation angle. The measured directivity is in good agreement with the calculation results of the designed device as shown by the solid-line in Figure 7-14.

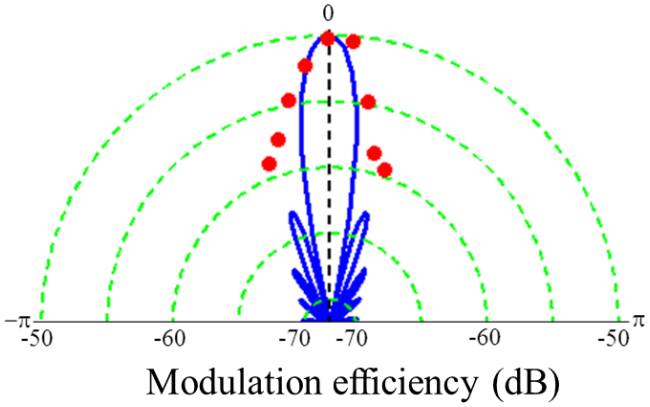

Figure 7-14 Measured modulation efficiency as a function of the irradiation angle of the wireless millimeter-wave signals.

Figure 7-15 shows the modulation efficiency as a function of separation between the horn antenna and the fabricated device, *S*. The dots in Figure 7-15 show the measured modulation efficiency, when the wireless millimeter-wave signal frequency was 58 GHz and the irradiation angle was set 0 degree. In the measurement, the optical side bands were observed clearly with the separation

of 200 mm. I believe that a wireless millimeter-wave signal with a few meters separation can be detected and converted to lightwave signal by increasing device performance and using photonic technology such as an optical amplifier and filter. By using optical filter, the lower sideband component can be eliminated and the optical carrier power can be reduced. As a result, the power ratio between the optical carrier and sideband becomes larger compared with no optical filter utilization.

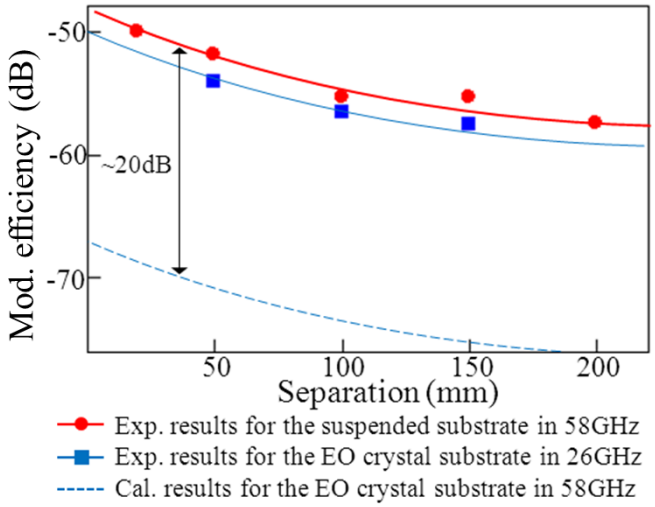

Figure 7-15 Measured modulation efficiency as a function of separation between the horn antenna and fabricated device.

Figure 7-15 shows also the modulation efficiency of the devices fabricated on an EO crystal substrate only as a function of horn antenna and device separation. The square in Figure 7-15 shows the measured modulation efficiency of the devices fabricated on EO crystal substrate only at operational frequency of 26 GHz, where the antenna aperture is relatively large than. Based on the measurement result, the modulation efficiency for 58 GHz operational frequency can be calculated as shown by the dashed-line in Figure 7-15. We can see that the modulation efficiency enhancement of about 20dB was obtained using the suspended structures than the device fabricated on the EO crystal substrate only.

7.8 *X*-cut $LiNbO_3$-based device

An optical modulator using an *x*-cut Ti:$LiNbO_3$ waveguide suspended on a low-*k* dielectric substrate was also proposed. The proposed device was designed for 60 GHz millimeter-wave signal with the parameters as shown in Table 7-3. The proposed device was successfully fabricated and then measured its performance for wireless millimeter-wave-lightwave signal conversion.

Table 7-3 Device parameters for analyzing the *x*-cut $LiNbO_3$-based suspended device.

	Values
Low-*k* dielectric	
Dielectric constant, ε_{rL}	3.5
Thickness, h_L	130 μm
EO crystal (*x*-cut $LiNbO_3$)	
Dielectric constant, ε_{rEO}, (ε_x,ε_y, ε_z)	(43,43,28)
Thickness, h_{EO}	80 μm
Operational frequency, f_m	58 GHz
Gap-embedded patch antennas	
Antenna size, *L*x*W*	0.84 x 0.84 mm
Gap width, *G*	5 μm

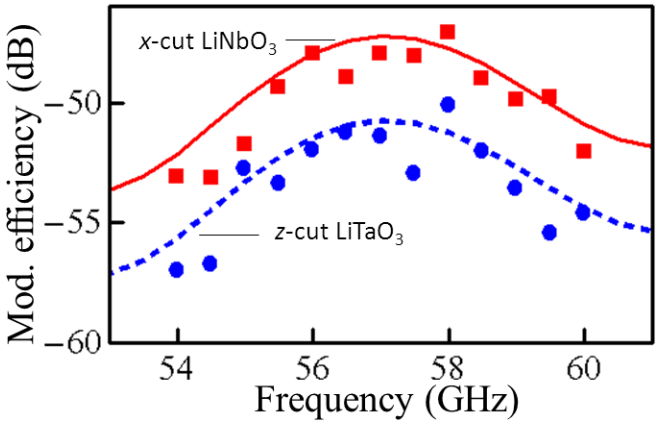

(a)

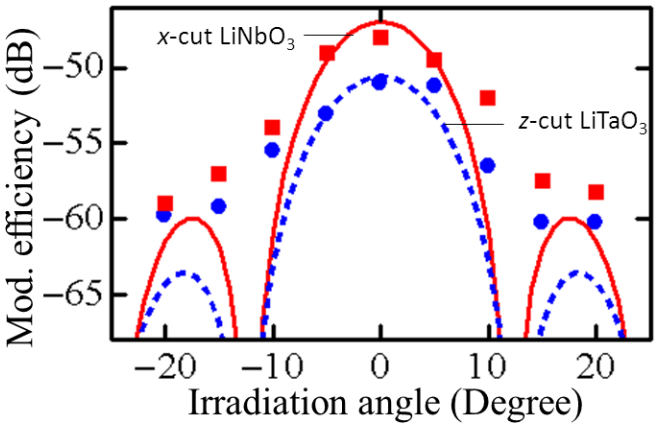

(b)

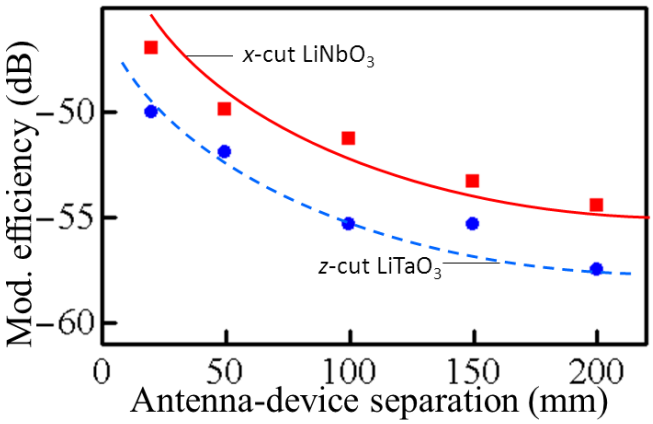

(c)

Figure 7-16 Measurement results of the fabricated optical modulator using a *x*-cut $LiNbO_3$ waveguide suspended to patch antennas embedded with a narrow gap on a low-*k* dielectric substrate. (a) frequency dependence, (b) wireless irradiation angle dependence, (c) antenna-device separation dependence.

The measurement results of the fabricated device are shown by the red dotted in Figure 7-16. The measured modulation efficiency as functions of the frequency dependence, wireless irradiation angle dependence, and dependence of separation between the device and antenna transmitter were reported. We can see that the *x*-cut $LiNbO_3$-based device has modulation efficiency about 3 dB larger than the *z*-cut $LiTaO_3$-based device. The modulation efficiency improvement might be due to lower effective dielectric constant and no buffer utilization in the *x*-cut $LiNbO_3$-based device.

7.9 Modulation efficiency improvement

The basic operation of the proposed optical modulator using an EO waveguides suspended to gap-embedded patch antennas on a low-*k* dielectric substrate was demonstrated experimentally for direct wireless millimeter-wave-lightwave signal conversion. The measured results in the experiment were in good agreement with the calculated results in the analysis.

Table 7-4 Comparison of the device fabricated on EO crystal only and on suspended with low-*k* dielectric substrate.

	EO crystal substrate	**EO crystal suspended to low-*k* substrate**
Effective dielectric constant, ε_{eff}	~42	~7
Operational frequency, f_m	58 GHz	58 GHz
Patch antenna length, *L*	~0.3 mm	~0.8 mm
Patch antenna length, *W*	~0.3 mm	~0.8 mm
Receiving power (ratio)	1	~4
Modulation index (ratio)	1	~10

In the proposed device, improvement of the modulation efficiency can be achieved, compared to the devices fabricated on an EO crystal substrate with a large dielectric constant as shown in Table 7-4. For comparison between the proposed devices and the devices fabricated on a high-*k* EO crystal substrate, the patch antenna length of the proposed devices is about two-times larger, and the antenna receiving power is over four-times greater. Based on that, the interaction length becomes about two-times since the antenna size corresponds to the millimeter-wave-lightwave interaction length in each antenna. The received power of the suspended structures is improved about four-times since the antenna aperture becomes four-times compered the device using a high-*k* EO crystal only as the substrate. Furthermore, the induced millimeter-wave electric field across the gap becomes also about five-times by considering dielectric constant value differences between the proposed device and the device fabricated on a high-*k* EO crystal. Therefore, modulation efficiency improvement of about ten times can be obtained owing to two-times interaction length and five-times induced electric field across the gap.

Further modulation efficiency improvement can be obtained by adopting quasi-phase-matching (QPM) array structures using polarization reversal structures [60]. The modulation efficiency can be improved by another +6 dB. In addition, effective millimeter-wave-lightwave signal conversion can be also further improved by utilizing photonic methods with an optical filter and amplifier [75]. I expect that the proposed device can be used for wireless millimeter-wave signals with power of 10 mW. In a radio-over-fiber (ROF) link, the converted lightwave signal can be detected by use of a high-speed photo-detector for conversion from lightwave to millimeter-wave signal.

As a further advantage of the proposed devices, since a thin EO crystal (<100 μm) is used, the substrate resonant modes in millimeter-wave bands can be eliminated. By using a thin EO crystal, cut-off frequencies of the substrate resonant modes become higher [85] [86]. Therefore, the proposed suspended structures are effective to operation in the millimeter-wave band for enhancing the modulation efficiency due to elimination of the substrate resonant modes.

7.10 Discussion and summary

New optical modulators using an EO crystal suspended to planar antennas on a low-*k* dielectric substrate were proposed for wireless millimeter-wave-lightwave signal conversion. The effective dielectric constant of the proposed devices becomes low compared to the devices fabricated on a high-*k* EO crystal substrate. Therefore, the antenna aperture size becomes large. Additionally, the substrate resonant modes can also be eliminated using a thin EO crystal (<100μm). As a result, modulation efficiency can be improved using the proposed devices compared to devices fabricated on a thick high-*k* EO crystal substrate.

A wireless millimeter-wave signal can be received and converted directly to a lightwave signal with the proposed device through EO modulation using the Pockels effect. The proposed devices were fabricated successfully. Basic performance of the proposed device for operation in the millimeter-wave band was demonstrated experimentally. The proposed devices have a compact structure and can be operated with a low millimeter-wave signal loss and no external electrical power supply.

The proposed millimeter-wave-lightwave signal converters can be used for a variety of ROF applications in communication, electromagnetic field measurements, radar, and so on. In communication, large volumes of data can be transferred at a high rate to the users through wireless millimeter-wave signals and to other access points through optical fiber links by the proposed millimeter-wave-lightwave signal converters [69]. Therefore, the proposed devices can be used for realize broadband mobile communication.

In electromagnetic field measurement, electromagnetic field characteristics such as magnitude, phase, and polarization can be measured and identified using the proposed devices with low millimeter-wave loss since no other microwave circuit is used in the measurement [73]. The proposed devices are operated passively with no external power supply. Therefore, no-inductance electromagnetic field measurements can be obtained through the ROF technology.

In a radar system, a microwave/ millimeter-wave signal is transmitted to and received from a certain direction by use of an antenna array with a beam-forming controller. By considering basic operations of the proposed device, a wireless microwave/ millimeter-wave signal with certain direction can be received using an array structure and phase-inversed structures [44] [60] [75]. Therefore, the proposed device can be used for optical beam-forming of the wireless microwave/ millimeter-wave signal in the radar applications with the ROF technology.

Chapter 8 Conclusion

8.1 General Conclusion

This dissertation described electro-optic (EO) modulators using planar antennas for wireless microwave-lightwave signal conversion in the radio-over-fiber (ROF) technology. New EO modulators using planar antennas were proposed with the fusion and integrated structures. Efforts for enhancing device functionality and improving device performances were also done using several device configurations with array and suspended structures.

In the Chapter 1, the backgrounds of this dissertation were presented relating on wireless communication trends, capacity enhancement using high frequency operation such as 60 GHz bands, ROF technology for coverage area expansion, and key devices in the ROF technology. The objectives and structure of this dissertation were also explained and shown.

In the Chapter 2, the fundamentals and characteristics of the planar antennas and EO modulators were discussed. Wireless microwave-lightwave signal conversion by combining the planar antennas and EO modulators were presented briefly with discrete, integrated, and new fusion structures with their features.

In the Chapter 3, new fusion EO modulators using a patch antenna embedded with a single narrow gap were proposed. Antenna characteristics of the proposed devices are the same as the standard patch antennas. Optical modulation can be obtained by utilization of a displacement current and electric field across the gap. Basic operations of the proposed devices for wireless microwave-lightwave signal conversion were verified experimentally.

In the Chapter 4, in order to improve functionality of the fusion devices, fusion EO modulators using a patch antenna embedded with double narrow gaps were presented with two device configurations. First, an EO modulator using a patch antenna embedded with two parallel gaps was suggested for application as a Mach-Zehnder interferometer. Second, an EO modulator using a patch antenna embedded with two orthogonal gaps was proposed for operation to wireless microwave signal with two orthogonal linear polarizations. The circular polarization of wireless microwave signals can be also received and converted to the lightwave signals using this proposed device.

In the Chapter 5, an integrated EO modulator using a planar Yagi antenna coupled to a resonant electrode was proposed. This device advantages are higher antenna gain, and longer interaction length. However, rather difficult precise tuning compared to the fusion EO modulators is the drawback.

Modulation efficiency improvement was achieved using this proposed device compared to the previous fusion structures.

In the Chapter 6, EO modulators using an array of planar antennas were proposed for improving modulation efficiency and enhancing device functionality. Modulation efficiency is proportional to antenna number, where transit time of the lightwave passing through each antenna is considered for effective modulation. Double modulation efficiency improvement was obtained by EO modulator using a new quasi-phase-matching (QPM) array of patch antennas embedded with a narrow gap. This device has twice antennas with the same device length compared to the conventional array device. A ROF link using this proposed device was demonstrated experimentally. Furthermore, an EO modulator using a 2-D array of patch antennas embedded with orthogonal meandering gaps was proposed. 1-D and 2-D beamforming receiving of wireless microwave signals were achieved through optical technology.

In the Chapter 7, optical modulators using thin EO waveguides suspended to planar antennas on a low-*k* dielectric substrate were proposed. A large antenna size and long interaction length was obtained using the proposed devices compared to the device fabricated on an only EO crystal substrate. Modulation efficiency was improved. Additionally, substrate resonant mode can be eliminated since a thin EO crystal is used. These structures are promising for high frequency operation such as in millimeter-wave bands.

8.2 Current research progress

In this dissertation, I have proposed EO modulators using planar antennas with fusion and integrated structures for wireless microwave-lightwave signal conversion. The operation of the proposed devices were verified and demonstrated experimentally. I proposed also several device configurations for improving device performance and enhancing device functionality. Currently, the modulation efficiency still remains low in several tens milli-radian per watt by irradiating a wireless microwave signal from the space. A ROF link using the proposed devices was also demonstrated firstly. The measured carrier-to-noise ratio (CNR) of the ROF link remains still low. In order to transfer the data in the ROF link, CNR enhancement is required by improving modulation efficiency of the proposed devices.

Research progress of the proposed EO modulators using planar antennas for wireless microwave-lightwave signal conversion is reported in Figure 8-1. The research roadmap of the EO modulators using planar antennas is illustrated in Figure 8-2. Several EO modulators using planar antennas were proposed and developed. Verification of basic operations of the proposed devices and efforts for improving modulation efficiency and enhancing device functionality were also reported and discussed.

As the current status, 60 GHz millimeter-wave optical modulators using EO waveguides suspended to planar antennas on a low-*k* dielectric substrate were proposed. I expect that the modulation efficiency improvement of about 20 dB can be obtained than the EO modulators using planar antennas fabricated on an only EO crystal as the substrate. As a result, the CNR of the ROF link using the suspended structure becomes larger. For more effective device performance, further modulation efficiency is still required as the suggested activities in the future.

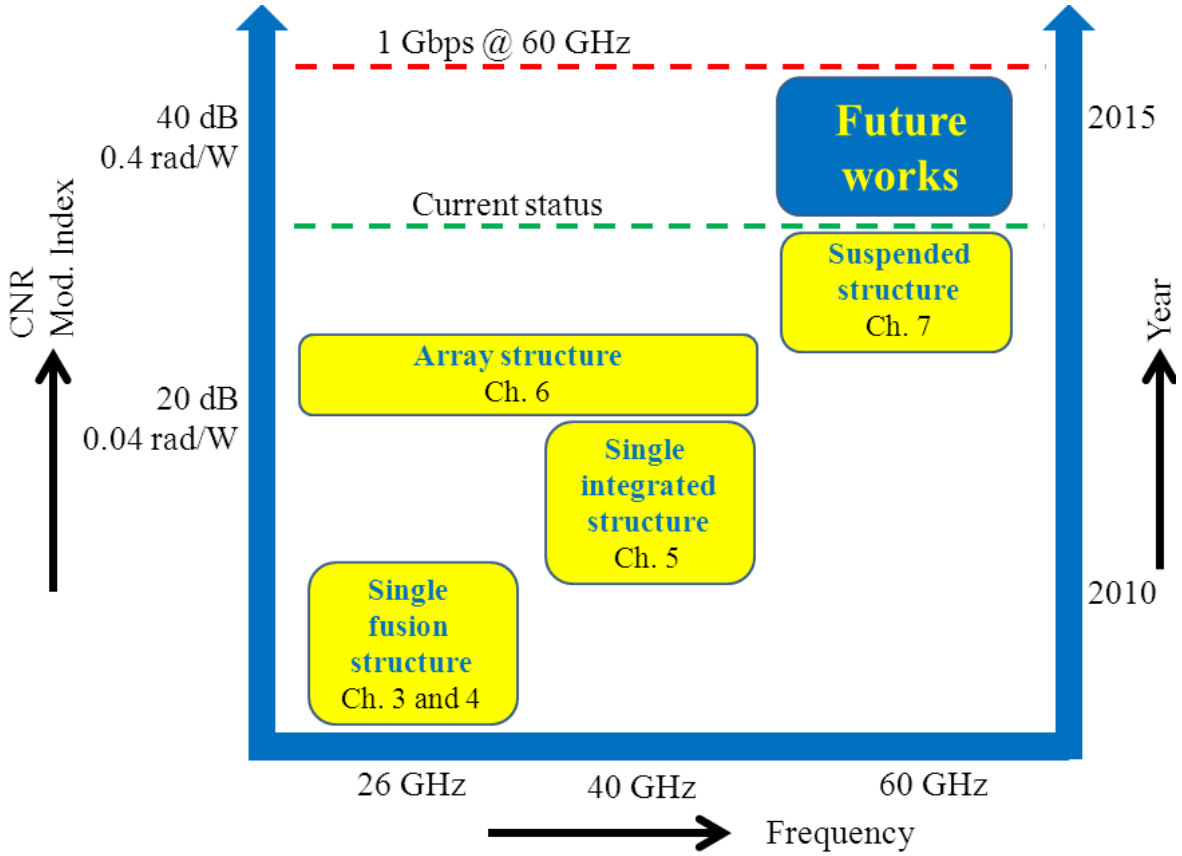

Figure 8-1 Research progress on the EO modulators using planar antennas for wireless microwave-lightwave signal conversion.

In order to achieve higher device performance, modulation efficiency should be improved furthermore. The modulation efficiency of about 0.4 rad/W might be enough for achieved 1 Gbps data rate since large bandwidth of about 100 MHz in the 60 GHz millimeter-wave bands is used. The modulation efficiency of the proposed devices can be improved in further using several techniques. First, by increasing antenna numbers in the array structures, the antenna performance becomes large [87]. In this technique, the modulation efficiency can be improved due to the antenna performance and interaction length of the microwave and lightwave electric fields. The modulation efficiency can be improved using over 30 antenna numbers in array structures. However, the array structures have narrow beam width as a drawback [88]. It can be solved using many devices with array structures for

several wireless irradiation angles [82]. The other technique for improving modulation efficiency is by using a microwave lens for collecting the microwave signal from the space to the proposed devices [89]. As a result, the microwave signal can be received effectively by use of the proposed device. The photonic technology using an optical amplifier and filter are also promising to improve the device performance [60]. One sideband will be cut by using the optical filter and the optical carrier will be cut also. As results, the single sideband optical spectrum can be obtained with larger sideband-carrier ratio of the optical power. Therefore, the device performance can be improved using the techniques for obtaining large modulation efficiency. I believe that the modulation efficiency of about 0.4 rad/ W can be obtained. By using the expected modulation efficiency, large CNR of about 40 dB can be achieved for data transfer through the ROF link using the proposed devices. Therefore, 1 Gbps data rate might be achieved since the 60 GHz millimeter-wave bands is used.

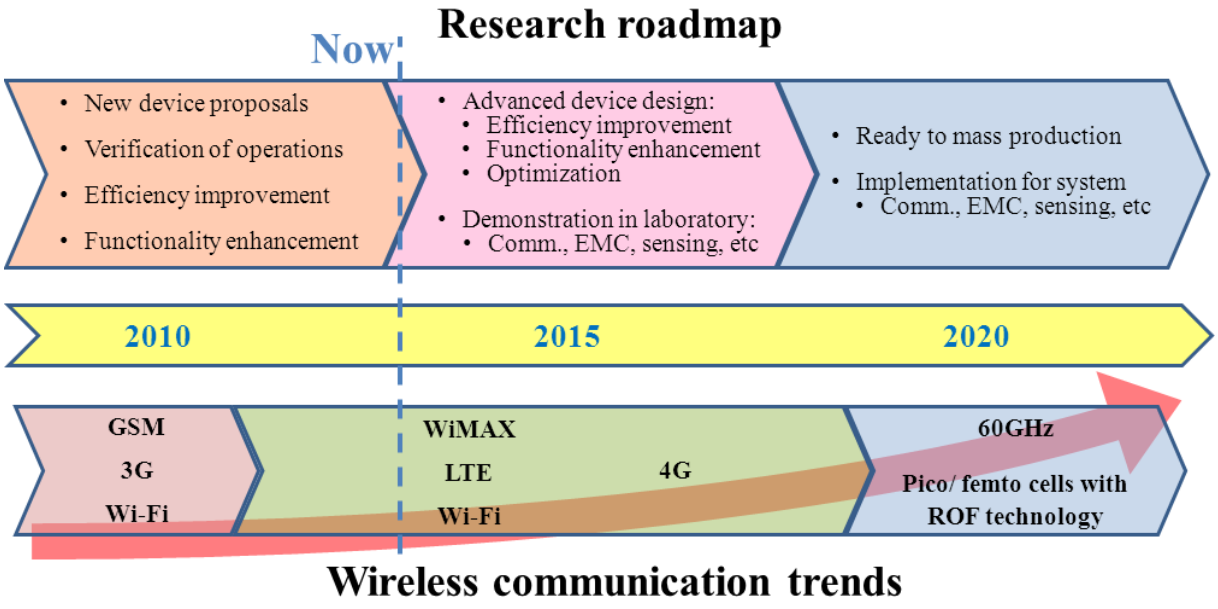

Figure 8-2 Roadmap of the research on EO modulators using planar antennas and the wireless communication trends.

8.3 Future research prospects

In this section I would like to discuss the future research prospect relating the EO modulators using planar antennas for wireless microwave-lightwave signal conversion in the ROF technology. The current remained issues were discussed in the previous section. In order to solve the issues, several techniques for improving modulation efficiency in further of the proposed devices can be adopted.

The research progress and roadmap of the EO modulators using planar antennas are shown in Figure 8-1 and Figure 8-2, respectively. The next issue is modulation efficiency improvement for

achieving high data rate in wireless communication through the ROF link. The techniques for improving the modulation efficiency were discussed in previous section. The suggested techniques are important activities in the future.

Advanced devices for improving modulation efficiency and enhancing functionality can be proposed in further. One attractive design is optical modulators using stacking planar antennas with stacking materials. The devices are composed of several thin EO waveguides on a low-*k* dielectric substrate. The planar antennas are inserted between them as the stacking structures. The stacking planar antennas are used as parasitic elements for improving the device performance such as antenna gain and directivity. As a result, modulation efficiency of the new proposed device can be improved. Additionally, several modulated lightwave signals can be also obtained since thin EO waveguides are used in the proposed device at each layer of the stacking structures. Based on this, new functionality of the new proposed device can be achieved also.

The proposed devices are promising for several attractive applications such as communication, electromagnetic compatibility, sensing, and so on. The device applications should be also demonstrated experimentally in the laboratory for verifying the device functionality. The activities are also the suggested for the next activities as shown by the research roadmap in Figure 8-2.

As the trends, the broadband wireless communication is required always for anticipating the bottleneck of the data traffic in the future, since the data traffic are always increased every years. The wireless communication trends are illustrated in Figure 8-2. The wireless communication with large bandwidth can be realized using 60 GHz millimeter-wave signal with ROF technology. Broadband wireless communication with about 1 Gbps data rate will be established soon by considering the demands to large capacity of the data traffic as predicted by the Cisco [6] [7]. I believe that the proposed devices can be used to implement in the broadband wireless communication with ROF technology for wireless microwave-lightwave signal conversion. The proposed devices are located on the base-station units for receiving wireless microwave signals from mobile devices and converting the microwave to lightwave signals directly. Then, the lightwave signals are transferred to others base-station units through optical fibers with low propagation loss. The optical fibers are used for enlarging the coverage areas using many base-stations with pico/ femto cells.

The other attractive applications of the proposed device are electromagnetic compatibility (EMC) measurement, automotive radar, remote sensing, and so on. By using the proposed devices through the ROF technology, no induction EMC measurement can be realized [68] [90] [91]. This technique is useful in the future since precise measurement in the high operational frequency with low losses is required. As a sensing application, automotive radar with millimeter-wave signal and short range detection can be also realized for improving the safety [92] [93].

References

[1] J.-W. Shi, C.-B. Huang and C.-L. Pan, "Millimeter-Wave Photonic Wireless Links for Very High Data Rate Communication," *NPG Asia Materials,* vol. 3, pp. 41-48, 2011.

[2] Z. Abichar, Y. Peng and J. Chang, "WiMAX: The Emergence of Wireless Broadband," *IEEE Computer Society,* Vols. July-August, pp. 44-48, 2006.

[3] F. Ohrtman, WiMAX Handbook: Building 802.16 Wireless Networks, McGraw-Hill, 2005.

[4] I. Akyildiz, G.-E. D.M. and E. Reyes, "The Evolution to 4G Cellular Systems: LTE-Advanced," *Physical Communication,* vol. 3, pp. 217-244, 2010.

[5] O. Bespalova, "Future of Multi-Gigabit Wireless Communications," in *International Conference Parallel and Distributed Computing Systems*, Kharkiv, 2013.

[6] "Cisco Visual Networking Index: Global Mobile Data Traffice Forecast Update, 2012 - 2017," Cisco, 2013.

[7] Z. Pi and F. Khan, "An Introduction to Millieter-Wave Mobile Broadband Systems," *IEEE Communications Magazine,* vol. June 2011, pp. 101-107, 2011.

[8] J. Howarth, A. Lauterbach, M. Boers, L. Davis, A. Parker, J. Harrison, J. Rathmell, M. Batty, W. Cowley, C. Burnet, L. Hall, D. Abbott and N. Weste, "60GHz Radios: Enabling Next-Generation Wireless Applications," in *TENCON 2005 2005 IEEE Region 10* , Melbourne, 2005.

[9] P. Adhikari, "Understanding Millimeter Wave Wireless Communication," Loea Corporation, San Diego, 2008.

[10] N. Guo, R. Qiu, S. Mo and K. Takahashi, "60-GHzMillimeter-Wave Radio: Principle, Technology, and New Results," *EURASIP Journal onWireless Communications and Networking,* vol. 2007, p. 68253, 2007.

[11] V. Chandrasekhar, J. Andrews and A. and Gatherer, "Femtocells Networks: A Survey," *IEEE Communication Magazine,* vol. 46, no. 9, pp. 59-67, 2008.

[12] T. Nakamura, S. Nagata, A. Benjebbor, Y. Krishiyama, T. Hai, S. Xiaodong, Y. Ning and L. Nan, "Trends in Small Cell Enhancements in LTE Advanced," *IEEE Communication Magazine,* vol. February, pp. 98-105, 2013.

[13] S. Ramanath, E. Altman, V. Kumar and M. Debbah, "Optimizing Cell Size in Pico-Cell Networks," in *RAWNET/WNC3*, Seoul, 2009.

[14] Electronic Warfare and Radar Systems Engineering Handbook, Washington DC: Avionics Department AIR-4.5, 1999.

[15] O. Tipmongkolship, S. Zaghloul and A. Jukan, "The Evoluation of Cellular Backhaul Technologies: Current Issues and Future Trends," *IEEE Communications Survey and Tutorial,* vol. 13, no. 1, pp. 97-113, 2011.

[16] D. Payne and W. Gambling, "New Silica Based Low-Loss Optical Fibre," *Electronics Letters,*

vol. 10, no. 15, 1974.

[17] D. Wake, A. Nkansah and N. J. Gomes, "Radio Over Fiber Link Design for Next Generation Wireless Systems," *Journal of Lightwave Technology*, vol. 28, no. 16, pp. 2456-2464, 2010.

[18] M. Larrode and A. Koonen, "Towards a Reliable RoF Infrastructure for Broadband Wireless Access," in *Symposium IEEE/LEOS Benelux Chapter*, Eindhoven, 2006.

[19] S. Iezekiel, Microwave Photonic : Device and Applications, Chichester: John Wiley & Sons, Ltd., 2009.

[20] J. Capmany and D. Novak, "Microwave Photonics Combines Two Worlds," *Nature Photonics*, vol. 1, pp. 319-330, 2007.

[21] A. J. Seeds, "Microwave Photonics," *IEEE Transactions on Microwave Theory and Techniques*, vol. 50, no. 3, pp. 877-887, 2002.

[22] J. Liu, Photonic Device, Cambridge: Cambridge University Press, 2005.

[23] B. Vidal, T. Nagatsuma, N. Gomes and T. Darcie, "Photonic Technologies for Millimeter- and Submillimeter-Wave Signals," *Advances in Optical Technologies*, vol. 2012, p. 925065, 2012.

[24] K. Kato, "Ultrawide-Band/High-Frequency Photodetectors," *IEEE Transactions on Microwave Theory and Techniques*, vol. 47, no. 7, pp. 1265-1281, 1999.

[25] A. Wakatsuki, Y. Muramoto and T. Ishibashi, "Development of Terahertz-wave Photomixer Module Using a Uni-traveling-carrier Photodiode," *NTT Technical Review*, vol. 10, no. 2, pp. 1-7, 2012.

[26] M. Tonouchi, "Cutting-Edge Terahertz Technology," *Nature Photonics*, vol. 1, pp. 97-105, 2007.

[27] H. Ito, T. Ito, Y. Muramoto, T. Furuta and T. Ishibashi, "F-Band (90-140 GHz) Uni-Traveling-Carrier Photodiode Module for a Photonic Local Oscillator," in *14th International Symposium on Space Terahert:- Technology*.

[28] T. Nagatsuma and H. Ito, "High-Power RF Uni-Traveling-Carrier Photodiodes and Their Applications," in *Advances in Photodiodes*, InTech, 2011, pp. 292-314.

[29] S. Ebihara, "Directional Borehole Radar with Dipole Antenna Array Using Optical Modulators," *IEEE Transaction on Geoscience and Remote Sensing*, vol. 42, no. 1, pp. 45-58, 2004.

[30] S. Shinada, T. Kawanishi, T. Sakamoto, M. Andachi, K. Nishikawa, S. Kurokawa and M. Izutsu, "A 10-GHz Resonant-Type $LiNbO_3$ Optical Modulator Array," *IEEE Photonics Technology Letters*, vol. 19, no. 10, pp. 735-737, 2007.

[31] T. Kawanishi, "High-Speed Optical Modulators and Photonic Sideband Management," *International Journal of Microwave and Optical technology*, vol. 1, no. 1, pp. 114-120, 2006.

[32] H. Pham, H. Murata and Y. Okamura, "Travelling-Wave Electro-Optic Modulators with Arbitrary Frequency Response Utilising Non-Periodic Polarization Reversal," *Electronics Letters*, vol. 43, no. 24, pp. 1379-1381, 2007.

[33] T. Kawanishi, S. Oikawa, K. Higuma, Y. Matsuo and M. Izutus, "Low-Driving-Voltage Band-Operation $LiNbO_3$ Modulator with Lightwave Reflection and Double-Stub Structure," *Electronics Letters*, vol. 38, no. 20, pp. 1204-1205, 2002.

[34] G. Agrawal, Lightwave Technology, New Jersey: John Wiley and Sons, 2004.

[35] E. L. Wooten, K. Kissa, A. Yi-Yan, E. Murphy, D. Lafaw, P. Hallemeier, D. Maack, D. Attanasio, D. Fritz and G. McBrien, "A Review of Lithium Niobate Modulators for Fiber-Optic Communications Systems," *IEEE Journal of Selected Topics in Quantum Electronics,* vol. 6, no. 1, pp. 69-82, 2000.

[36] R. B. Waterhouse and D. Novak, "Integrated Antenna/Electro-Optic Modulator for RF photonic Front-End," in *International Microwave Symposium*, Baltimore, 2011.

[37] R. Martin, C. Schuetz, T. Dillon, C. Chen, J. Samluk, E. L. Stein Jr., M. Mirotznik and D. Prather, "Design and Performance of a Distributed Aperture Millimeter-Wave Imaging System using Optical Upconversion," *Proc. Of SPIE,* vol. 7309, 2009.

[38] N. Kohmu, H. Murata and Y. Okamura, "Electro-Optic Modulators Using Double Antenna-Coupled Electrodes for Radio-over-Fiber Systems," *IEICE Transaction on Electronics,* Vols. E96-C, no. 2, pp. 204-211, 2013.

[39] C. Lee, Microwave Photonics, New York: CRC Press Taylor & Francis Group, 2007.

[40] R. Garg, P. Bartia, I. Bahl and A. Ittipiboon, Microstrip Antenna Design Handbook, Norwood: Artech House, Inc., 2001.

[41] D. G. Fang, Antenna Theory and Microstrip Antennas, Florida: CRC Press Taylor & Francis Group, 2010.

[42] A. Roger, Essentials of Photonics, North West: CRC Press Taylor and Francis Group, 2009.

[43] R. G. Hunsperger, Integrated Optics: Theory and Technology, New York: Springer, 2009.

[44] H. Murata, S. Matsunaga, A. Enikohara and Y. Okamura, "Resonant Electrode Guided-Wave Electro-Optic Phase Modulator Using Polarisation-Reversal Structures," *Electronics Letters,* vol. 41, no. 8, pp. 497-498, 2005.

[45] K. C. Gupta, R. Garg and I. Bahl, Microstrip Lines and Slotlines, Norwood: Arech House, Inc., 2001.

[46] I. Bahl and P. Bhartia, Microstrip Antennas, Dedham: Artech House, Inc., 1980.

[47] V. R. Gupta and N. Gupta, "Characteristics of a Compact Microstrip Antenna," *Microwave and Optical Technology Letters,* vol. 40, no. 2, pp. 158-160, 2004.

[48] K. F. Lee and K. M. Luk, Microstrip Patch Antennas, London: Imperial College Press, 2011.

[49] G. Lefort and T. Razban, "Microstrip Antennas Printed on Lithium Niobate Substrate," *Electronics Letters,* vol. 33, no. 9, pp. 726-727, 1997.

[50] K. Noguchi, "Ultra-high-speed $LiNbO_3$ modulators," in *Ultrahigh-Speed Optical Transmission Technology*, Springer, 2007, pp. 89-101.

[51] A. Chen and E. Murphy, Broadband Optical Modulators: Science, Technology, and Applications, North West: CRC Press: Taylor and Francis Group, 2012.

[52] M. E. Lines and A. Glass, Principles and Applications of Ferroelectrics and Related Materials, Oxford: Oxford University Press, 1996.

[53] S. Ramo, J. Whinnery and T. Van Duzer, Fields and Waves in Communication Elecctronics,

Canada: John Wiley & Sons, Inc., 1994.

[54] R. E. Newnham, Properties of Materials, New York: Oxford University Press Inc., 2005.

[55] K. Iizuka, Engineering Optics, New York: Springer, 2008.

[56] K. Tada, T. Murai, T. Nakabayashi, T. Iwashima and T. Ishikawa, "Fabrication of $LiTaO_3$ Optical Waveguide by H+ Exchange Method," *Japanese Journal of Applied Physics*, Vols. 26-1, no. 3, pp. 503-504, 1987.

[57] H. Murata and Y. Okamura, "Fabrication of Proton-ExchangeWaveguide Using Stoichiometric $LiTaO_3$ for Guided Wave Electrooptic Modulators with Polarization- Reversed Structure," *Advances in OptoElectronics*, vol. 2008, p. 654280, 2008.

[58] L. W. Stulz, "Titanium In-Diffused $LiNbO_3$ Optical Waveguide Fabrication," *Applied Optics*, vol. 18, no. 12, pp. 2041-2044, 1979.

[59] W. Bridges, F. Sheehy and J. Schaffner, "Wave-Coupled $LiNbO_3$ Modulator for Microwave and Millimeter-Wave Modulation," *IEEE Photonics Technology Letters*, vol. 3, no. 2, pp. 133-135, 1991.

[60] H. Murata, R. Miyanaka and Y. Okamura, "Wireless Space-Division-Multiplexed Signal Discrimination Device Using Electrooptic Modulator with Antenna-Coupled Electrodes and Polarization-Reversed Structures," *International Journal of Microwave and Wireless Technologies*, vol. 4, pp. 399-405, 2012.

[61] I. Watanabe, T. Nakata, M. Tsuji, K. Makita, T. Torikai, Taguchi and K., "High-Speed, High-Reliability Planar-Structure Superlattice Avalanche Photodiodes for 10-Gbps Optical Receivers," *Journal of Lightwave Technology*, vol. 18, no. 12, pp. 2200-2207, 2000.

[62] R. Krähenbühl, J. H. Cole, R. P. Moeller and M. M. Howerton, "High-Speed Optical Modulator in $LiNbO_3$ With Cascaded Resonant-Type Electrodes," *Journal of Lightwave Technology*, vol. 24, no. 5, pp. 2184-2189, 2006.

[63] F. T. Sheehy, W. B. Bridges and J. H. Schaffner, "60 GHz and 94 GHz Antenna-Coupled $LiNbO_3$ Electrooptic Modulators," *IEEE Photonics Technology Letters*, vol. 5, no. 3, pp. 307-310, 1993.

[64] Y. N. Wijayanto, H. Murata and Y. Okamura, "Novel Electro-Optic Microwave-Lightwave Converters Utilizing a Patch Antenna Embedded with a Narrow Gap," *IEICE Electronics Express*, vol. 8, no. 7, pp. 491-497, 2011.

[65] Y. N. Wijayanto, H. Murata, H. Shiomi and Y. Okamura, "A New Electro-Optic Microwave-Lightwave Converter Using a Square Patch Antenna Embedded with a Narrow Gap," in *2nd Global COE Student Conference on Innovative Electronic Topics (SCIENT)*, Osaka, 2010.

[66] R. Rodriguez-Berral, F. Mesa and D. R. Jackson, "Gap Discontinuity in Microstrip Lines: An Accurate Semianalytical Formulation," *IEEE Transactions on Microwave Theory and Techniques*, vol. 59, no. 6, pp. 1441-1453, 2011.

[67] A. Yariv, Quantum Electronics, 3rd ed., New York: Wiley, 1989.

[68] Y. N. Wijayanto, H. Murata and Y. Okamura, "Electro-Optic Microwave-Lightwave Converters Utilizing Patch Antennas with Orthogonal Gaps," *Journal of Nonlinear Optical Physics and Materials*, vol. 12, no. 1, p. 1250001, 2012.

[69] Y. N. Wijayanto, H. Murata, T. Kawanishi and Y. Okamura, "*X*-Cut $LiNbO_3$ Microwave-Lightwave Converters Using Patch-Antennas with a Narrow-Gap for Wireless-Over-Fiber Networks," in *IEEE Photonics Conference*, San Francisco, 2012.

[70] Y. N. Wijayanto, H. Murata, T. Kawanishi and Y. Okamura, "*X*-Cut $LiNbO_3$ Optical Modulators Using Gap-Embedded Patch-Antennas for Wireless-Over-Fiber Systems," *Advances in Optical Technologies*, vol. 2012, p. 383212, 2012.

[71] K. Wong, Properties of Lithium Niobate, London: INSPECT, The Institute of Electrical Engineering, 2002.

[72] K. Chang, RF and Microwave Wireless Systems, New York: John Wiley & Sons, Inc, 2000.

[73] Y. N. Wijayanto, H. Murata and Y. Okamura, "Discrimination of Wireless Electromagnetic Signals by Electro-Optic Modulators Using an Array of Patch Antennas Embedded with Orthogonal Gaps," *Journal of Physics: Conference Series*, vol. 2012, no. 1, p. 379, 2012.

[74] R. Fitzpatrick, Maxwell's Equation and the Principles of Electromagnetism, Hingham: Infinity Science Press, 2008.

[75] Y. N. Wijayanto, H. Murata and Y. Okamura, "Wireless Microwave-Optical Signal Conversion in Quasi-Phase-Matching Electro-Optic Modulators Using Gap-Embedded Patch-Antennas," *IEICE Transaction on Electronics*, Vols. E96-C, no. 2, pp. 212-219, 2013.

[76] Y. N. Wijayanto, H. Murata and Y. Okamura, "Novel Electro-Optic Modulators Suspended to Low-*k* Dielectric Substrates Using Narrow-Gap-Embedded Patch-Antennas," in *Photonic Global Conference*, Singapore, 2012.

[77] Y. N. Wijayanto, H. Murata and Y. Okamura, "Electro-Optic Wireless Millimeter-Wave-Lightwave Signal Converters Using Planar Yagi-Uda Array Antennas Coupled to Resonant Electrodes," in *OptoEelectronics and Communications Conference*, Busan, 2012.

[78] H. H. K. Kan, R. Waterhouse, A. Abbosh and M. Bialkowski, "Simple Broadband Planar CPW-Fed Quasi-Yagi Antenna," *IEEE Antennas and Wireless Propagation Letters*, vol. 6, pp. 18-20, 2007.

[79] J. Yao, "A Tutorial on Microwave Photonics," *IEEE Photonics Society Newletter*, vol. June, pp. 5-12, 2012.

[80] Y. Wijayanto, H. Murata and Y. Okamura, "Electro-Optic Modulators with Gap-Embedded Patch Antenna Array for Wireless-Fiber Links," in *2012 Asia-Pacific Microwave Photonics Conference*, Kyoto, 2012.

[81] Y. N. Wijayanto, H. Murata and Y. Okamura, "Electro-Optic Microwave-Lightwave Converters for Dual-Polarized Wireless Signals Using Patch Antennas Embedded with Orthogonal Gaps," in *8th International Symposium on Modern Optics and its Applications*, Bandung, 2011.

[82] Y. Wijayanto, H. Murata and Y. Okamura, "Electro-Optic Beamforming Device Using a Two-Dimensional Array of Patch-Antennas Embedded with Orthogonal-Gaps for Millimeter-Wave Signals," in *IEEE Photonic Conference*, Washington, 2013.

[83] W. W. R. Rowe, "Efficient Wideband Printed Antennas on Lithium Niobate for OEICs," *IEEE Transactions on Antennas and Propagation*, vol. 51, no. 6, pp. 1413-1415, 2003.

[84] M. Udin, H. Chan, T. Tsun and Y. Chan, "Uneven Curing Induced Interfacial Delamination of

UV Adhesive-Bonded Fiber Array V-Groove for Photonic Packaging," *Journal of Lightwave Technology*, vol. 24, no. 3, pp. 1342-1349, 2006.

[85] T. Zhi and A. Mitchell, "Investigation of Substrate Modes in High Speed $LiNbO_3$ Electro-Optic Modulators," in *Conference on Optical Internet Australian Conference on Optical Fiber Technology*, Melborne, 2007.

[86] W. Kim, W. Yang and H. Lee, "Effect of Parasitic Modes in High-Speed Optical Modulators," *Optical Express*, vol. 12, no. 12, pp. 2568-2573, 2004.

[87] T. N. Chang and J.-H. Jiang, "Enhance Gain and Bandwidth of Circularly Polarized Microstrip Patch Antenna Using Gap-Coupled Method," *Progress In Electromagnetics Research*, vol. PIER 96, pp. 127-139, 2009.

[88] T.-C. Tang, Y.-R. Chuang and K.-H. Lin, "A Narrow Beamwidth Array Antenna Design for Indoor Non-Contact Vital Sign Sensor," in *IEEE Antennas and Propagation Society International Symposium (APSURSI)*, Chicago, 2012.

[89] C. Fernandes and J. Fernandes, "Performance of Lens Antennas in Wireless Indoor Millimeter-Wave Applications," *IEEE Transaction on Microwave Theory and Technique*, vol. 47, no. 6, pp. 732-737, 1999.

[90] S. Kingsley, B. Tian and S. Sriram, "Analog Fiber Optic Links for EMC Emission Testing," SRICO inc, 1999.

[91] M. Tsuchiya and T. Shiozawa, "Photonics Makes Microwaves Visible," *IEEE Photonics Society Newletters*, vol. December, pp. 9-17, 2012.

[92] S. Honma and N. Uehara, "Millimeter-Wave Radar Technology for Automotive Application," Mitsubishi Electric ADVANCE, 2001.

[93] T. Yamawaki and S. Yamano, "60-GHz Millimeter-Wave Automotive Radar," Fujitsu Ten Tecnhnology, 1998.

[94] D. Wake, A. Nkansah and N. Gomes, "Radio Over Fiber Link Design for Next Generation Wireless Systems," *Journal of Lightwave Technology*, vol. 28, no. 16, pp. 2456-2464, 2010.

Acknowledgments

In the name of Allah (subhana wa taala), the Most Gracious and Most Merciful. Alhamdulillah, all praises to Allah by His blessing to me with health, patience, and knowledge to complete this dissertation.

This work has been done at the Optics and Microwave Engineering Laboratory (Okamura Laboratory), Department of Systems Innovation, Graduate School of Engineering Science, Osaka University, Japan. This dissertation is by far the most significant accomplishment in my life and it would be impossible without peoples who supported me and believed in me.

First, I would like to express the sincerest gratitude to Prof. Yasuyuki Okamura, who is my supervisor, advisor and guarantor during my study and live in Japan. His kindness, guidance, encouragement, and patience were important during my study and research activities at his laboratory. I greatly appreciate his patience in reviewing this dissertation.

I would like to express my gratitude and indebtedness to Prof. Hiroshi Murata, for his unlimited patience and kindness in teaching and guiding me. Without his discussion, valuable comments, insightful suggestions, kind support in the analysis and experiments, this work would not run smoothly. Furthermore, his patience during our joint review of the published papers and this dissertation was also an invaluable contribution.

I am really grateful to Prof. Shinji Urabe and Prof. Tadao Nagatsuma in the Graduate School of Engineering Science, Osaka University for their review and evaluation of this dissertation through constructive comments and suggestions for improvement.

I deeply appreciate their kind attention that Prof. Hideo Itozaki, Prof. Masahiro Kitagawa, Prof. Mikio Takai, Prof. Akira Sakai, Prof. Hiroaki Okamoto, Prof. Masashi Shiraishi, and others, from the Graduate School of Engineering Science, Osaka University displayed through their comments to my research activities.

I would like to express my appreciation to Dr. Hidehisa Shiomi and Dr. Kazuhiro Kitatani, from the Graduate School of Engineering Science, Osaka University and to Dr. Tetsuya Kawanishi from National Institute of Information, Communications Technology (NICT) Japan, for their valuable comments, suggestions, support during the discussion and experiments.

I would like to thank all members of the Okamura Laboratory, Department of System Innovation, Graduate School of Engineering Science, Osaka University during period from 2008 to 2013. Especially, Dr. Q. H. Ngo, Mr. Y. Ohmura, Mr. R. Miyanaka, Mr. K. Furusho, Mr. K. Jitsuhara,

Mr. J. Ozaki, Mr. J. Nishioka, Y. Maejima, Mr. N. Kohmu, Mr. Y. Takashima, Mr. S. Klink, Mr. T Mitsubo, and others for their help in research activities and social life during the time I have spent.

I am thankful to my colleagues in the Research Center for Electronics and Telecommunication, Indonesian Institute of Sciences (LIPI), who shouldered my duties while I have been absent from work to study in Japan.

I would also like to thank my friends from Indonesia who are studying in Osaka University for being my side. With them, living and studying in Osaka University, Japan feels more comfortable and happy.

I would like to acknowledge the Ministry of Education, Culture, Sports, Science and Technology (MEXT) of Japan for the financial support they provided in form of scholarships during my study at the Graduate School Engineering Science, Osaka University from 2008 to 2013.

My deepest love and gratitude is reserved for my family, my beloved wife Dwi Hastuti, my beloved sons Naufal Zaky Yudhinta and Mifzal Asfa Yudhinta, and my beloved parents and all family members. Thanks for your love, prayers, support, understanding, and patience. May the blessings and goodness of the Allah come to us always with happiness in this world and hereafter.

Last but not least I would like to thank all people who were involved directly or indirectly in successful completion of this dissertation.

List of Publications

- **Peer-reviewed papers**:

1. Y. N. Wijayanto, H. Murata, and Y. Okamura, "Electro-Optic Millimeter-Wave-Lightwave Signal Converters Suspended to Gap-Embedded Patch Antennas on Low-*k* Dielectric Materials," *IEEE Journal of Selected Topics in Quantum Electronics*., vol.19, no.6, November/ December 2013. (accepted for publication)
2. Y. N. Wijayanto, H. Murata, and Y. Okamura, "Wireless Microwave-Optical Signal Conversion in Quasi-Phase-Matching Electro-Optic Modulators Using Gap-Embedded Patch-Antennas," *IEICE Transaction on Electronics*, vol.E96-C, no.2, pp.212-219, Feb. 2013.
3. Y. N. Wijayanto, H. Murata, T. Kawanishi, and Y. Okamura, "*X*-Cut $LiNbO_3$ Optical Modulators Using Gap-Embedded Patch-Antennas for Wireless-Over-Fiber Systems," *Advances in Optical Technologies*, vol. 2012, Article ID 383212, 8 pages, 2012. doi:10.1155/2012/383212.
4. Y. N. Wijayanto, H. Murata, and Y. Okamura, "Discrimination of Wireless Electromagnetic Signals by Electro-Optic Modulators Using an Array of Patch Antennas Embedded with Orthogonal Gaps," *Journal of Physics: Conference Series*, 379 (2012) 012017 (10 pages) DOI:10.1088/1742-6596/379/1/012017.
5. Y. N. Wijayanto, H. Murata, and Y. Okamura, "Electro-Optic Microwave-Lightwave Converters Utilizing Patch Antennas with Orthogonal Gaps," *Journal of Nonlinear Optical Physics and Material*, vol. 21, no. 1 (2012) 1250001 (12 pages) DOI: 10.1142/S0218863512500014.
6. Y. N. Wijayanto, H. Murata, and Y. Okamura, "Electro-Optic Microwave-Lightwave Converters Utilizing a Quasi-Phase-Matching Array of Patch Antennas with a Gap," *Electronics Letters*, vol. 48, no. 1, pp. 36-38, January 2012.
7. Y. N. Wijayanto, H. Murata, and Y. Okamura, "Novel Electro-Optic Microwave-Lightwave Converters Utilizing a Patch Antenna Embedded with a Narrow Gap," *IEICE Electronics Express*, vol. 8, no. 7, pp.491-497, April 2011.

- **Presentations in International Conferences:**

1. Y. N. Wijayanto, H. Murata, and Y. Okamura, "Electro-Optic Beamforming Device Using a Two-Dimensional Array of Patch-Antennas Embedded with Orthogonal-Gaps for Millimeter-

Wave Signals," in *IEEE Photonics Conference 2013*, San Francisco, California – USA, 23 – 27 September 2013. (accepted for presentation)

2. Y. N. Wijayanto, H. Murata, and Y. Okamura, "60GHz Electro-Optic Modulator Suspended to Patch-Antennas Embedded with a Gap on Low-*k* Dielectric Material," in *2013 Conference on Laser and Electro-Optics Pacific Ring and OptoElectronics and Communications Conference/ Photonics in Switching*, ThL2-5, Kyoto, Japan, 30 June – 4 July 2013.
3. Y. N. Wijayanto, H. Murata, T. Kawanishi, and Y. Okamura, "*X*-Cut Ti:$LiNbO_3$ Optical Modulator Suspended to Gap-Embedded Patch Antennas on Low-*k* Dielectric Substrate," in *8th International Symposium on Modern Optics and its Applications*, pp. 95–97, Institut Teknologi Bandung, Bandung – Indonesia, June 2013.
4. Y. N. Wijayanto, H. Murata, and Y. Okamura, "Millimeter-Wave Electro-Optic Modulators Suspended to Patch-Antennas Embedded with a Narrow-Gap on Low-*k* Dielectric Substrates," in *2013 Asia-Pacific Microwave Photonics*, PA-5, Gwangju – Korea, 22 – 24 April 2013.
5. Y. N. Wijayanto, H. Murata, and Y. Okamura, "Novel Electro-Optic Modulators Suspended to Low-*k* Dielectric Substrates Using Narrow-Gap-Embedded Patch-Antennas," in *Photonic Global Conference 2012*, 1-4F-5, Singapore, 13 – 16 December 2012.
6. Y. N. Wijayanto, H. Murata, and Y. Okamura, "Electro-Optic Modulators Utilising Gap-Embedded Patch-Antennas for ROF Communication and Measurement Systems," in *2nd PostGraduate Student Global Conference 2012*, Singapore, 16 December 2012.
7. Y. N. Wijayanto, H. Murata, T. Kawanishi, and Y. Okamura, "*X*-Cut $LiNbO_3$ Microwave-Lightwave Converters Using Patch-Antennas with a Narrow-Gap for Wireless-Over-Fiber Networks," in *IEEE Photonics Conference 2012*, WS-4, San Francisco, California – USA, 23 – 27 September 2012.
8. Y. N. Wijayanto, H. Murata, and Y. Okamura, "Electro-Optic Wireless Millimeter-Wave-Lightwave Signal Converters Using Planar Yagi-Uda Array Antennas Coupled to Resonant Electrodes," in *17-th Opto-Electronic Communications Conference*, 5E1-2, Busan – Korea, 2-6 July 2012.
9. Y. N. Wijayanto, H. Murata, and Y. Okamura, "Electro-Optic Modulators with Gap-Embedded Patch Antenna Array for Wireless-Fiber Links," in *2012 Asia-Pacific Microwave Photonics*, WD01, Co-op Inn Hotel, Kyoto – Japan, April 2012.
10. Y. N. Wijayanto, H. Murata, and Y. Okamura, "Passive Electromagnetic Field Sensors Using Electro-Optic Crystals with Metal Planar Antennas and Narrow Gaps," in *International Symposium on Materials Science and Innovation for Sustainable Society: Eco-Materials and Eco-Innovation for Global Sustainability*, PT 7-13, Hotel Hankyu Expo Park, Osaka – Japan, November 2011.

11. Y. N. Wijayanto, H. Murata, and Y. Okamura, "Electro-Optic Microwave-Lightwave Converters for Dual-Polarized Wireless Signals Using Patch Antennas Embedded with Orthogonal Gaps," in *8th International Symposium on Modern Optics and its Applications*, Bandung Institute of Technologies, CP-8, Institut Teknologi Bandung, Bandung – Indonesia, July 2011.
12. Y. N. Wijayanto, H. Murata, H. Shiomi, and Y. Okamura, "Electro-Optic Microwave-Lightwave Converter Using Patch Antenna Embedded with a Narrow Gap for Optical Modulation," in *Conference of Lasers and Electro-Optics 2011*, JWA122, Baltimore Convention Center, Baltimore – USA, May 2011.
13. Y. N. Wijayanto, H. Murata, H. Shiomi, and Y. Okamura, "A New Electro-Optic Microwave-Lightwave Converter Using a Square Patch Antenna Embedded with a Narrow Gap," in *2nd Global COE Student Conference on Innovative Electronic Topics 2010*, pp. 86 (PO-37), Osaka University, Osaka - Japan, July 2010.

- **Presentations in Domestic Conferences:**

1. Y. N. Wijayanto, H. Murata, T. Kawanishi, and Y. Okamura, "Millimeter-wave-Lightwave Converters Using *X*-Cut Ti:$LiNbO_3$ Waveguide Suspended to Patch Antennas Embedded with a Gap on Low-*k* Dielectric Substrate," in *JSAP–OSA Joint Symposia in the 74th JSAP Autumn Meeting 2013*, Doshisha University, Kyoto, September 2013. (to be presented)
2. Y. N. Wijayanto, H. Murata, and Y. Okamura, "Millimeter-Wave Optical Modulator Using Electro-Optic Waveguide Suspended to Gap-Embedded Patch Antennas on Low-*k* Dielectric Substrate," in *the 74th JSAP Autumn Meeting 2013*, Doshisha University, Kyoto, September 2013. (to be presented)
3. Y. N. Wijayanto, H. Murata, and Y. Okamura, "Analysis of Millimeter-Wave Electro-Optic Modulator Suspended to Gap-Embedded Patch-Antenna on Low-*k* Substrate," in *the 60nd JSAP Spring Meeting 2013*, 29a-B3-6, Kanagawa Institute of Technology, Kanagawa, March 2013.
4. Y. N. Wijayanto, H. Murata, and Y. Okamura, "Electro-Optic Millimeter-Wave-Lightwave Converter Suspended to Gap-Embedded Patch-Antenna Array on Low-*k* Substrate for Broadband Mobile Communications," in *IEICE Spring General Conference 2013*, C-14-1, Gifu University, Gifu, March 2013.
5. Y. N. Wijayanto, H. Murata, T. Kawanishi, and Y. Okamura, "Electro-Optic Modulators Based on *X*-Cut $LiNbO_3$ Crystals Using Patch-Antenna Embedded a Narrow-Gap," *IEICE Technical Reports*, vol. 112, no. 259, OPE2012-113, pp. 109-114, October 2012.

6. Y. N. Wijayanto, H. Murata, and Y. Okamura, "Wireless Microwave-Optical Signal Converters Using Optical Modulation in Gap-Embedded Patch-Antennas on Ferroelectric Optical Crystals," in *JSAP–OSA Joint Symposia in the 73rd JSAP Autumn Meeting 2012*, 13p-G1-9, Ehime University, Ehime, September 2012.
7. Y. N. Wijayanto, H. Murata, and Y. Okamura, "*X*-Cut Optical Modulators Using Patch Antennas with a Gap for Microwave-Lightwave Conversion," in *IEICE Spring General Conference 2012*, C-14-1, Okayama University, Okayama, March 2012.
8. Y. N. Wijayanto, H. Murata, and Y. Okamura, "High-Speed Guided-Wave Electro-Optic Modulators Using an Array of Gap-Embedded Patch Antennas with Phase Reversal," *IEICE Technical Reports*, vol. 111, no. 416, MWP2011-72 (EMT-12-030), pp. 133-138, January 2012.
9. Y. N. Wijayanto, H. Murata, and Y. Okamura, "Electro-Optic Microwave-Lightwave Converters Using Quasi-Phase-Matched Patch Antennas Embedded with a Gap," in *IEICE Fall General Conference 2011*, C-14-4, Hokaido University, Hokaido, September 2011.
10. Y. N. Wijayanto, H. Murata, and Y. Okamura, "Electro-Optic Modulators using Patch Antennas with Orthogonal Gaps for Microwave Polarization Discrimination," in *the 72nd JSAP Fall Meeting 2011*, 1a-ZN-11, Yamagata University, Yamagata, August 2011.
11. Y. N. Wijayanto, H. Murata, and Y. Okamura, "New Electro-Optic Microwave-Lightwave Converters Using Channel Optical Waveguides and Microstrip-Patch-Antennas with Narrow-Gaps," *IEICE Technical Reports*, vol. 111, no. 22, MWP2011-2, pp. 7-12, April 2011.
12. Y. N. Wijayanto, H. Murata, and Y. Okamura, "Proposal of New Electro-Optic Modulators using a Patch Antenna Embedded with an Orthogonal Narrow Gap," in *the 58th JSAP Spring Meeting 2011*, 26a-KB-10, Kanagawa Institute of Technology, Kanagawa, March 2011.
13. Y. N. Wijayanto, H. Murata, and Y. Okamura, "Electro-Optic Modulators utilizing Patch Antenna Embedded with a Narrow Gap for Radio-Over-Fiber Systems," in *IEICE Spring General Conference 2011*, C- 14-17, Tokyo City University, Tokyo, March 2011.
14. Y. N. Wijayanto, H. Murata, and Y. Okamura, "New Electro-Optic Modulator Using Square Patch Antenna Embedded with a Narrow Gap for Optical Modulation," in *the 71st JSAP Fall Meeting 2010*, 16a-G-1, Nagasaki University, Nagasaki, September 2010.

- **Special feature in Electronics Letters:**

1. "Wireless Sees the Light," *Electronics Letters*, vol. 48, no. 1, p. 3, January 2012.

List of Awards

- JSAP Young Scientist Oral Presentation Award for the paper entitled "Analysis of Millimeter-Wave Electro-Optic Modulator Suspended to Gap-Embedded Patch-Antenna on Low-*k* Substrate", in *the 60st JSAP Spring Meeting 2013*, 29a-B3-6, Kanagawa Institute of Technology, Japan, March 2013.

- IEEE Photonics Society Japan Young Scientist Award for the paper entitled "Electro-Optic Modulators with Gap-Embedded Patch Antenna Array for Wireless-Fiber Links," in *7th Asia-Pacific Microwave Photonics*, WD-01, CO-OP Inn Hotel, Kyoto, Japan, April 2012.

- ECO-MATES 2011 Promotion Award for the paper entitled "Passive Electromagnetic Field Sensors Using Electro-Optic Crystals with Metal Planar Antennas and Narrow Gaps," in *International Symposium on Materials Science and Innovation for Sustainable Society: Eco-Materials and Eco-Innovation for Global Sustainability*, PT 7-13, Hotel Hankyu Expo Park, Osaka, Japan, November 2011.